Swine immune response to Salmonella enterica serovar Typhimurium. A functional genomics approach

Rodrigo Prado Martins

Swine immune response to *Salmonella enterica* serovar Typhimurium. A functional genomics approach

RODRIGO PRADO MARTINS

TITULO: *Swine inmune response to Samonella enterica serovar Typhirumium. A functional genomics approach*

AUTOR: *RODRIGO PRADO MARTINS*

Swine immune response to *Salmonella enterica* serovar Typhimurium. A functional genomics approach

Tesis doctoral

Presentada por:
Rodrigo Prado Martins

Dirigida por:
Prof. Dr. Juan José Garrido Pavón

Córdoba - Julio de 2013

Dr. Juan José Garrido Pavón, Profesor Titular de Universidad del Departamento de Genética de la Universidad de Córdoba

CERTIFICA QUE:

El trabajo de investigación presentado por D. Rodrigo Prado Martins titulado "**Swine immune response to *Salmonella enterica* serovar Typhimurium. A functional genomics approach**" ha sido realizado bajo su supervisión y dirección y reúne los requisitos de originalidad y calidad científica necesarios para constituir una Tesis Doctoral y optar al Grado de Doctor por la Universidad de Córdoba.

Y para que así conste y a efectos oportunos, firma el presente informe.

VºBº del director del trabajo

Prof. Dr. Juan José Garrido Pavón

Córdoba, 24 de junio de 2011

TÍTULO DE LA TESIS: Swine immune response to *Salmonella enterica* serovar Typhimurium. A functional genomics approach.

DOCTORANDO: Rodrigo Prado Martins

INFORME RAZONADO DEL DIRECTOR DE LA TESIS
(se hará mención a la evolución y desarrollo de la tesis, así como a trabajos y publicaciones derivados de la misma).

La idea directriz del trabajo de tesis de D. Rodrigo Prado Martins ha sido la caracterización a nivel molecular de la respuesta del hospedador porcino a la infección por *Salmonella typhimurium*, utilizando para ello una aproximación integrada de técnicas inmunogenómicas y proteómicas. Los resultados obtenidos se ajustan a los objetivos inicialmente previstos y deberán ser de gran interés para un mejor conocimiento de los mecanismos inmunológicos de defensa contra la infección en la especie porcina. La producción científica derivada de esta tesis es la siguiente:

Martins RP, Collado-Romero M, Martínez-Gomáriz M, Carvajal A, Gil C, Lucena C, Moreno A, Garrido JJ. Proteomic analysis of porcine mesenteric lymph-nodes after *Salmonella typhimurium* infection. Journal of Proteomics. 2012; 75:4457-4470.

Martins RP, Collado-Romero M, Arce C, Lucena C, Carvajal A, Garrido JJ. Exploring the immune response of porcine mesenteric lymph nodes to *Salmonella enterica* serovar Typhimurium: an analysis of transcriptional changes, morphological alterations and pathogen burden. Comparative Immunology, Microbiology and Infectious Diseases. 2013; 36:149-160.

Martins RP, Lorenzi V, Arce C, Lucena C, Carvajal A, Garrido JJ. Innate and adaptive immune mechanisms are effectively induced in ileal Peyer's patches of *Salmonella typhimurium* infected pigs. Developmental and Comparative Immunology. 2013; 41:100-104.

Por todo ello, se autoriza la presentación de la tesis doctoral.

Córdoba, 24 de junio de 2013

Firma del director

Fdo.: Prof. Dr. Juán José Garrido Pavón

A todos mis profesores, en especial dos de ellos: mis padres.

A todos meus professores, em especial dois deles: meus pais.

No entiendo. Esto es tan vasto que supera cualquier entender. Entender es siempre limitado. Pero no entender puede no tener fronteras. Siento que soy mucho más completa cuando no entiendo. No entender, del modo en que lo digo, es un don. No entender, pero no como un simple estado de ánimo. Lo bueno es ser inteligente y no entender. Es una bendición extraña, como tener locura sin ser loco. Es un manso desinterés, es una dulzura de estupidez. Sólo que de vez en cuando viene la inquietud: quiero entender un poco. No demasiado: pero por lo menos entender que no entiendo.

Clarice Lispector

Não entendo. Isso é tão vasto que ultrapassa qualquer entender. Entender é sempre limitado. Mas não entender pode não ter fronteiras. Sinto que sou muito mais completa quando não entendo. Não entender, do modo como falo, é um dom. Não entender, mas não como um simples estado de espírito. O bom é ser inteligente e não entender. É uma benção estranha, como ter loucura sem ser doida. É um desinteresse manso, é uma doçura de burrice. Só que de vez em quando vem a inquietação: quero entender um pouco. Não demais: mas pelo menos entender que não entendo.

Clarice Lispector

Abstract

Genetic improvement of the resistance to infectious diseases represents an essential step for the development of sustainable and economically viable animal production systems. Control of salmonellosis in swine herds generates increased production costs and public health issues due to the risk of dispersal of antibiotic resistant strains. Therefore, the breeding of resistant animals, in combination with good hygiene practices offers a promising strategy to fight against *Salmonella* in pigs. Recently, functional genomics approaches combining the power of gene mapping technologies, gene expression studies and modern bioinformatics tools have begun to contribute to a better understanding of the host response to microbial diseases. In light of this, this thesis aimed to identify and describe the molecular pathways and interactions involved in the porcine intestinal immune response to *Salmonella enterica* serovar Typhimurium (*S.* Typhimurium).

The first, second and third studies that constitute this thesis aimed to explore the molecular mechanisms occurring in porcine mesenteric lymph-nodes (MLN) at 1, 2 and 6 days post-infection (dpi) with *S.* Typhimurium. Firstly, the differential expression of immune-related genes was analysed in correlation with changes in tissue morphology and pathogen burden. Results revealed that infection resulted in a substantial infiltration of phagocytes and up-regulation of pro-inflammatory genes. Of note, host defence mechanisms led to a relevant reduction of *S.* Typhimurium load in tissue, but pathogen was found to maintain itself in MLN at 6 dpi. Subsequently, DIGE-based proteomics was carried out, uncovering that infection caused changes in abundance of proteins involved in diverse host cellular functions, leading to the induction of processes such as phagocyte infiltration, cytoskeleton remodelling, pyroptosis and antigen presentation in infected MLN. Finally, host response to infection was accessed by microarrays analysis and then complemented with gene expression data from pathogen found in tissue. The conjunctive analysis of both parties involved in infection revealed that although *S.* Typhimurium was able to express virulence factors in porcine MLN, host succeeded in counteracting pathogen strategies by modulating infected cell death and inducing an early cytotoxic response.

The forth and fifth studies reported in this thesis were focused on the role of porcine Peyer's Patches (PP) upon *S.* Typhimurium infection. Initially, laser microdissection coupled to qPCR technology uncovered that both innate and adaptive immunity mechanisms are effectively triggered in PP follicles during infection. Afterwards, microarray analysis was carried out to better-explain results from this preliminary approach. It could be confirmed that the bacterial challenge provoked a remarkable inflammatory response and the establishment of multiple

levels of adaptive response against *S.* Typhimurium in PP follicles. Interestingly, several evidences of cross-presentation triggering were observed in follicles, besides the induction of humoral responses.

As conclusions, this thesis highlights that in spite of the sophisticated strategies evolved by pathogen to cause disease, swine appear to induce pyroptosis and inhibit apoptosis of infected cells in MLN to promote clearance of bacteria in the extracellular milieu during *S.* Typhimurium infections. This mechanism might enable MLN to act as a firewall to prevent pathogen spread beyond intestinal tract. Simultaneously, host might mediate an early cytotoxic response against *Salmonella* by cross-presentation of bacterial antigens in these organs, coordinating both arms of immunity in order to control infection. Additionally, it could be observed that besides eliciting B-cell-mediated immune responses, PP follicles mediate the generation of effector and memory CD8 T cells during infections by S. Typhimurium, which could represent a novel function for this PP area during *Salmonella* infections.

Resumen

La mejora de la resistencia genética a las enfermedades infecciosas representa una etapa fundamental para el desarrollo de sistemas de producción animal económicamente viables y sostenibles. El control de la salmonelosis porcina genera elevados costes de producción y supone un riesgo para la salud pública por la posibilidad de desarrollo y dispersión de cepas resistentes a antibióticos. Por lo tanto, la cría de animales resistentes, asociada a buenas prácticas de higiene durante la producción, representa una estrategia prometedora para la lucha contra infecciones por *Salmonella* en cerdos. Recientemente, la genómica funcional, al combinar la potencia de las tecnologías de mapeo genético, los estudios de expresión génica y las modernas herramientas bioinformáticas empieza a contribuir a una mejor comprensión de la respuesta del hospedador a las infecciones microbianas. Debido a esto, en esta tesis doctoral se planteó como objetivo identificar y describir las rutas e interacciones moleculares involucradas en la respuesta a la infección con *Salmonella enterica* serovar Typhimurium (*S.* Typhimurium) en la especie porcina.

Los tres primeros estudios que componen esta tesis doctoral tuvieron como objetivos explorar los mecanismos moleculares que ocurren en los nódulos linfáticos mesentéricos (NLM) porcinos tras 1, 2 y 6 días post-infección (dpi) con *S.* Typhimurium. Inicialmente, la expresión diferencial de genes relacionados con la respuesta inmunitaria fue analizada y correlacionada con cambios en la morfología tisular y carga de patógeno. Los resultados revelaron que la infección resultó en una abundante infiltración de fagocitos y sobre-expresión de genes pro-inflamatorios. Notablemente, una significativa reducción de la presencia de la bacteria en el tejido fue observada, en asociación con la activación de los mecanismos de defensa del hospedador. A pesar de ello, el patógeno logró mantenerse en los NLM, siendo detectado a los 6 dpi. A continuación, un análisis proteómico mediante DIGE fue llevado a cabo, poniendo de manifiesto que la infección resultó en cambios en la abundancia de proteínas involucradas en distintas funciones celulares del hospedador, promoviendo en los NLM infectados la inducción de procesos como la infiltración de fagocitos, remodelación del citoesqueleto, piroptosis y presentación antigénica. Finalmente, la respuesta del hospedador a la infección fue evaluada mediante análisis de micromatrices y los resultados obtenidos fueron complementados con datos de expresión génica procedentes del patógeno presente en tejido. En conjunto, el estudio reveló que, aunque *S.* Typhimurium expresa factores de virulencia en NLM porcinos, el hospedador contrarresta de forma efectiva las estrategias de virulencia del patógeno, mediante la modulación de la muerte celular de células infectadas y la inducción de una respuesta citotóxica temprana.

Los estudios cuarto y quinto reportados en esta tesis doctoral estuvieron centrados en el estudio de la función de las placas de Peyer (PP) porcinas durante la infección con *S.* Typhimurium. Inicialmente, la técnica de microdisección laser, asociada a ensayos de PCR cuantitativa, reveló que mecanismos de respuesta inmune innata y adaptativa son efectivamente inducidos en los folículos de las PP durante la infección. Dichos resultados fueron confirmados y ampliados mediante un análisis de micromatrices que permitió observar que la infección con *S.* Typhimurium provocó una notable respuesta inflamatoria en los folículos de las PP, resultando al mismo tiempo estimulada la respuesta adaptativa a diferentes niveles. Interesantemente, evidencias de la inducción de *cross-presentation* y desarrollo de respuesta humoral fueron también observadas.

Como conclusiones, esta tesis doctoral pone de manifiesto que, pese a las sofisticadas estrategias desarrolladas por *S.* Typhimurium para causar enfermedad, en los NLM porcinos se inducen de manera coordinada mecanismos innatos y específicos de defensa que tienen como objetivo el control de la infección. Entre estos mecanismos, la inducción de piroptosis y la inhibición de la apoptosis de las células infectadas podrían jugar un papel crítico en la función de los NLM porcinos como una barrera para prevenir la dispersión del patógeno más allá del tracto intestinal. A la vez, la infección determinó la activación de una respuesta citotóxica temprana contra *Salmonella,* mediante la *cross-presentation* de los antígenos bacterianos. Por otro lado, además de la estimulación de la respuesta mediada por células B, los folículos de las PP promueven la producción de células T CD8 efectoras y de memoria, lo que representa una función no observada hasta el momento en este tejido en su papel como órgano de respuesta frente a la infección con *Salmonella.*

Contents

1. General introduction

1.1 The biology of *Salmonella*

Salmonella are Gram-negative bacilli belonging to the *Enterobacteriaceae* family, considered a major cause of disease in cold-blooded and warm-blooded animals (Jacobsen et al., 2011). According to the contemporary nomenclature, the genus *Salmonella* contains only two species: *Salmonella enterica* and *Salmonella bongori*. *S. enterica* subdivides into the subspecies *enterica*, *salamae*, *arizonae*, *diarizonae*, *houtenae* and *indica*, while *S. bongori* has no subspecies (Sánchez-Vargas et al., 2011). To date more than 2,500 different *Salmonella* serovars/serotypes have been characterized, being most of them classified as part of the *Salmonella* subsp. *enterica* (Andrews-Polymenis et al., 2010). The characterization of *Salmonella* serovars is based on their surface antigens: the O (somatic) antigens, which consist in a part of the variable long chain lipopolysaccharide, and the two H (flagellar) antigens (Jacobsen et al., 2011). Besides, *Salmonella* serotypes can be divided into host restricted, host specific, and generalist serotypes. Host restricted serotypes are predominantly associated with one species, but are able to infect other species as well (ex. *S. enterica* subsp. *enterica* ser. Dublin). Host specific only cause disease in one host (ex. *S. enterica* subsp. *enterica* ser. Typhi) and host generalist serotypes commonly cause disease in a broad range of hosts (ex. *S. enterica* subsp. *enterica* ser. Typhimurium) (Hoelzer et al., 2011).

1.2 Human infections by foodborne *Salmonella*

Disease caused by *Salmonella* in humans ranges from gastroenteritis to systemic infections (Monack, 2012). Depending on the clinical syndromes caused in this host, strains can be classified into two groups: typhoid *Salmonella* and non-typhoid *Salmonella.* The former group comprises the causative agents of

enteric fever (*S. enterica* subsp. *enterica* ser. Typhi and *S. enterica* subsp. *enterica* ser. Paratyphi), whereas the latter one includes the remaining serovars (Sánchez-Vargas et al., 2011).

Gastroenteritis by *Salmonella* is a major concern in developed and developing countries. Majowicz et al. (2010) estimates that each year, non-typhoid *Salmonella* causes 93.8 million illnesses, of which 80.3 million are foodborne, and 155,000 deaths worldwide. Additionally, these authors highlight that *Salmonella* infections represent approximately 3% of diarrhoeal illnesses occurring at global scale. In the United States, it is reported that *Salmonella* alone causes approximately 1 million foodborne infections and costs $365 million in direct medical expenditures annually (CDC, 2010). Similarly, the European Food Safety Authority (EFSA) state that *Salmonella* was the most frequently reported cause of foodborne outbreaks in 2011 (EFSA, 2013).

A screening by the World Health Organization Global Foodborne Infections Network revealed that *S.* Enterica and *S.* Typhimurium are respectively the most common and second most common *Salmonella* serovars isolated from human infections worldwide, except for North America and Oceania, where the highest prevalence is observed for *S.* Typhimurium (Hendriksen et al., 2011). *S.* Typhimurium has a broad host range, causing disease in a variety of animals. In humans, infections by this serovar generally results in a self-limiting gastroenteritis. However, multidrug resistant strains of this pathogen have been reported to cause recurrent systemic infections in humans (Monack, 2012).

1.3 Porcine salmonellosis and public health

Salmonella prevalence estimates for pig farms seem to differ considerably by production and management type. In the USA, average between-herd estimates equals 53%, exceeding 80% for some farrow-to-finish production

systems, while within-herd estimates range from 3.5 to 28% (Foley et al., 2008). At EU level, 28.7% of breeding holdings are *Salmonella* positive but among the Member States a wide variation (0–64%) exists (De Busser et al., 2013).

Salmonella serovars commonly associated with swine are a major public health concern, being *S.* Typhimurium is the most frequently reported serovar in pigs and pork in European countries (EFSA, 2013). Infections of pigs with *S.* Typhimurium may result in long-term asymptomatic carriage of these organisms (Boyen et al., 2008a). Thus, carrier animals can act as reservoirs of pathogen and produce the cross-contamination of carcasses during slaughterhouse operations (Methner et al., 2011). In fact, human infections by this pathogen are mostly associated with the consumption of contaminated pig and meat thereof (EFSA, 2013). The risk of *Salmonella* infection from consumption of contaminated pork depends on factors that include the level of infection in the pig herd, hygiene during carcass processing in the slaughterhouse, meat storage and distribution conditions and finally the handling of undercooked pork by the consumer (Boyen et al., 2008a).

Pork meat is the most widely consumed meat in Europe and its consumption has grown steadily during the last years (Resano et al., 2011). Since pigs are relevant reservoirs of *Salmonella*, this tendency increases the potential of exposure to this pathogen (Foley et al., 2008). Curiously, data from the EFSA Panel on Biological Hazards indicate that the contribution of pigs to the prevalence of human infection by *Salmonella* is currently higher than that of laying hens and eggs. Around 56.8% of the human salmonellosis cases could be attributable to pigs, while the contributions of total reservoirs associated with laying hens, broilers and turkeys are estimated to be 17%, 10.6% and 2.6%, respectively (EFSA, 2013).

1.4 Epidemiology, control and economic impact of *S.* Typhimurium infections in swine

S. Typhimurium can cause infection without disease and persist in the host with intermittent faecal shedding. These asymptomatic carriers are difficult to be detected by bacteriological or serological methods (Boyle et al., 2008) and represent the most important source of *Salmonella* introduction onto pig farms (Hoelzer et al., 2011). However, contact with people, contaminated slurry or sharing contaminated equipment was also proven to be risk factors for the transmission of *Salmonella* between pig herds and from cattle to pig herds. Additionally, *Salmonella* infected rodents have been identified as a source of bacteria in pig herds (Wilhelm et al., 2012).

Contaminated feed is recognized as a source of *Salmonella* for both livestock and poultry. Nevertheless, Doyle and Erickson (2012) state that feed should play only a minor role in the swine industry. Indeed, influence of feed in the prevalence of pig salmonellosis is related to the provision of wet or dry feed in farms. It is reported that dry feed enhances the risk of *Salmonella* shedding compared to wet feed (Farzan et al. 2006).

Salmonella transmission to pigs occurs mostly via the faeco-oral route, but oro-pharyngeal secretions can also be contaminated so allowing nose-to-nose spread of disease (De Busser et al., 2013). Although all age groups are susceptible to *Salmonella* infection, disease is most commonly observed among weaned pigs more than eight weeks of age (Hoelzer et al., 2011). It is inferred that the increase in *Salmonella* shedding by piglets at this stage of production is a consequence of feed transition and a decrease in sow colostral antibodies (Fosse et al., 2009).

Studies highlight the implication of infection status of sows on *Salmonella* infections in fattening pigs. A high level of seropositivity in sows was observed to

be related to a progressive increase of seropositivity in pigs during farrowing, post-weaning and fattening periods (Lurette et al., 2008). Environmental contamination may also play an important role in maintaining endemic infections. A previous work demonstrated that *Salmonella* free finishing herds can be produced from endemically infected herds if pigs are strategically moved to clean stalls as they move through the farrow-to-finish system (Hoelzer et al., 2011). In line with this, hygiene measures in farrowing rooms were uncovered to exert a great impact on *Salmonella* occurrence among all factors explaining *Salmonella* status in pig herds. Moreover, other factors as mixing pig batches along production, antibiotic treatment during the fattening period or a high number of animals per herd seem to increase the risk of transmission of *Salmonella* (Correia-Gomes et al., 2013).

Effective food safety interventions to reduce or control foodborne pathogens are needed throughout the food continuum, from the farm to the end user (Methner et al., 2011). Thus, the development of on-farm practices aiming to reduce the number of *Salmonella*-contaminated animals arriving at the processing plants might contribute significantly toward a reduction of *Salmonella* contamination of pork (Foley et al., 2008). In order to effectively accomplish this aim, attention should be paid to pig feed, cleaning and disinfection procedures at farms and purchase of animals (Wilhelm et al., 2012). Significant reductions of *Salmonella* in finisher swine can be further achieved by the use of vaccines that, despite of showing disadvantages of limited protection are able to reduce the length of infectious period and consequently reduce the risk of pathogen dispersal (De Ridder et al., 2013; Doyle and Erickson, 2012).

According to De Busser et al. (2013), interventions at slaughterhouse level are, at present, more likely to produce larger reductions of human illness than actions at the level of primary production. Nevertheless, reducing the prevalence of *Salmonella* in herds is particularly important because prevalence at

slaughter tends to be considerably higher than on farm. Stress during transport may enhance shedding of *Salmonella* by non-apparent carriers and subsequently, cause the infection of trucks or interinfection of pigs during lairage, increasing the risk of carcass contamination along the slaughter line. Thus, fasting procedures before slaughter, animal handling during loading and transport and lairage conditions should be critically evaluated to protect food supply from *Salmonella* (Fosse et al., 2009). Besides, carcass decontamination in addition to hygiene, cleaning and disinfection measures at the slaughter stage as well as education and training are essential to achieve this goal (Botteldoorn et al., 2003).

Efficient improvement of food safety also involves economic considerations. Using a model based on data from Danish programs, Baptista et al. (2011) assert that a substantial cost reduction of about € 400,000 per year for the finisher pig sector would be obtained if no herd surveillance activities were carried out to reduce the prevalence of *Salmonella* in carcass. Besides, these authors observed that interventions at slaughtering are less cost-effective in small and medium-sized abattoirs compared to large ones. Another study also carried out in Denmark uncovered that costs of pig carcass decontamination ranged from €4 to €5.4 million per year, depending on the decontamination method employed (Lawson et al., 2009). Although measures aiming to control *Salmonella* represent relevant economic efforts to porcine production system, their importance is unquestionable. Failures at controlling *Salmonella* in the primary production could lead to the spread of bacteria to other species and the environment, resulting in an increased public health risk via direct transmission and contamination of vegetables (Baptista et al., 2011). Additionally, initiatives during slaughterhouse operations are essential to mitigate the risk of *Salmonella* in pork (Goldbach et al., 2006).

1.5 Structural and functional aspects of mesenteric lymph-nodes and Peyer's Patches

In vertebrates, the immune system is subdivided into the innate and adaptive arms of immunity. The innate immune system is composed of anatomic, physiologic, phagocytic and inflammatory barriers that consist in the first line of defence against infectious disease. At the same time, innate immune components also interact extensively with adaptive components to help them to generate specific humoral response and immunologic memory (Burkey et al. 2009). The integration of the complex cellular interactions that trigger immune responses takes place most efficiently within the organized architecture of secondary lymphoid organs, which include the spleen, lymph nodes, Peyer Patches (PP), tonsils and adenoids (Matsuno et al., 2010). These organs are similarly organized, although differences in their vasculature, mode of antigen entrance, local environment and the stimuli they are subjected may differ. All of them exhibit a compartmentalized T and B areas, antigen presenting cells (APC), lymphoid chemokines, high endothelial venules (HEV), lymphatic vessels and in some cases M cells (Ruddle et al., 2009).

Thus, in addition to the physical barrier provided by epithelia, the intestinal mucosa immune system also uses the gut-associated lymphoid tissues (GALT) to protect the organism and to mediate subsequent innate and adaptive immune responses (Burkey et al., 2009). Traditionally, GALT comprises four distinct lymphoid compartments: the Peyer's patches (PP) and other lymphoid follicles associated with the follicle associated epithelium (FAE); the lamina propria; intraepithelial lymphocytes (IELs); and mesenteric lymph nodes (MLN) (Acheson and Luccioli, 2004).

1.5.1 Mesenteric lymph-nodes

Mesenteric lymph-nodes (MLN), as other lymph-nodes consist of the outer/superficial cortex, inner/deep cortex, medullary cord and marginal, cortical and medullary lymphatic sinuses (Figure 1). The cortical region is composed of primary follicles of densely packed naïve B cells and follicular dendritic cells (FDC), surrounded by the interfollicular area (Matsuno et al., 2010). Upon antigenic stimulus, antigen-activated B cells proliferate giving rise to secondary follicles and germinal centers (Elmore et al., 2006). The inner cortex is the T cell area with DC and HEV. The medullary cord is the plasma cell area with some B cells, while the lymphatic sinuses are populated by macrophages (Newberry and Lorenz, 2005). The collected lymph and cell contents enter the lymph-node via afferent lymphatic vessels and filter the node through the lymphatic sinuses in the medulla or move via the subcapsular sinus to leave through efferent lymphatic vessels. Cells and antigens also enter the lymph-node via an arteriole, which branches into a capillary bed (Ruddle et al., 2009).

In swine, lymph-nodes show some peculiarities when compared to other animals. Both peripheral and mucosa-associated lymph-nodes have a specific structure that is called inverted and are mostly composed of cortex and paracortex, lacking a larger medullary area (Scharek et al., 2007). Besides, lymphocyte trafficking in porcine also differs from that in other animals. As usual, the immigration of lymphocytes into the lymph-node takes place either by afferent lymph vessels or HEV (Rothkotter, 2009). However, in pigs very few lymphocytes leave lymph-nodes in the lymph, since they emigrate via paracortical post-capilary venules and not via efferent lymph vassels (Scharek et al., 2007).
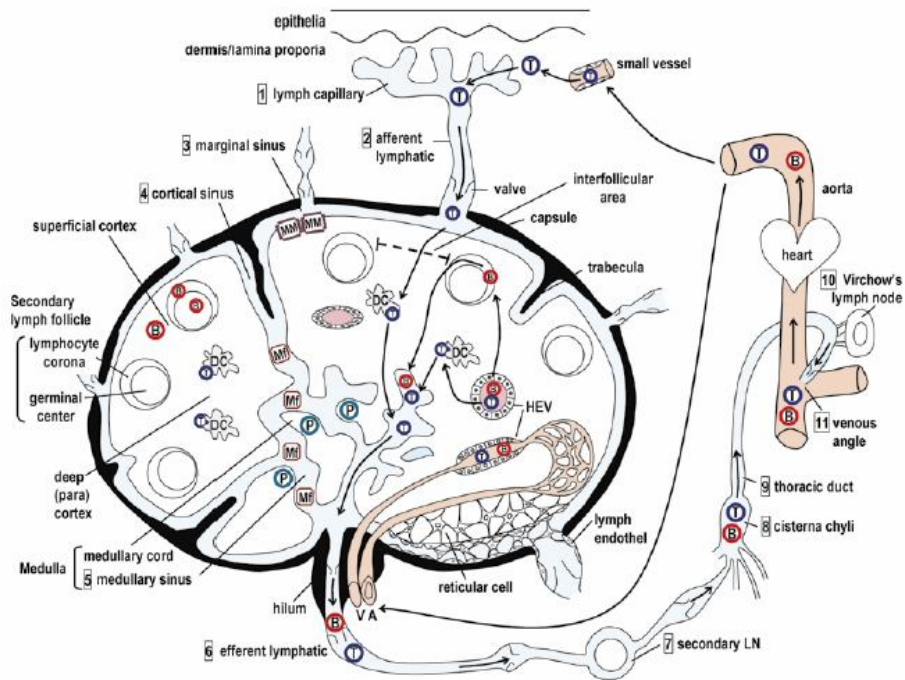
Figure 1 – Schematic drawing of the structure of the lymph-node and trafficking routes for T cells (T) and B cells (B). Numbers in the square indicate the direction of the lymph flow from the initial lymphatic capillary in peripheral organs to the draining lymph-node and then to the blood circulation via the central thoracic duct. A: artery, DC: interdigitating dendritic cell, HEV: high endothelial venule, Mf: sinus macrophage, MM: marginal macrophage, P: plasma cell, V: vein (Matsuno et al., 2000).

1.5.2 Peyer's Patches

PP are islands of organized lymphoid tissue located in the small intestine. In human and swine, PP are predominantly found in the ileum show a prenatal development (Makala et al., 2002). As other secondary lymphoid organs, PP contain areas populated by B and T lymphocytes (Figure 2). Follicles are pear shaped zones composed of B-cells and FDC, which are separated by the interfollicular area (T-cell area) (Matsuno et al., 2010). These structures are overlaid with the FAE, which harbours specialized antigen-sampling M cells

interdigitated within the epithelium (Burkey et al., 2009). The PP region between the follicles and the FAE is called the dome and contains mainly T cells, plasma cells, interdigitating DC and macrophages (Makala et al., 2002).

PP are strategically integrated to intestinal surface as a forward defensive system, acting as sites of antigen sampling and induction of mucosal immune responses (Newberry and Lorenz, 2005). Gut antigens enter this organ via uptake by M cells located in the specialized FAE (Rothkotter, 2009). Subsequently, antigens encounter numerous professional APC in the dome that prime naïve T and B cells. These lymphocytes become memory or effector cells and migrate from PP to MLN via efferent lymph and then via the thoracic duct to peripheral blood for subsequent extravasation at mucosal effector sites (Brandtzaeg, 2009).
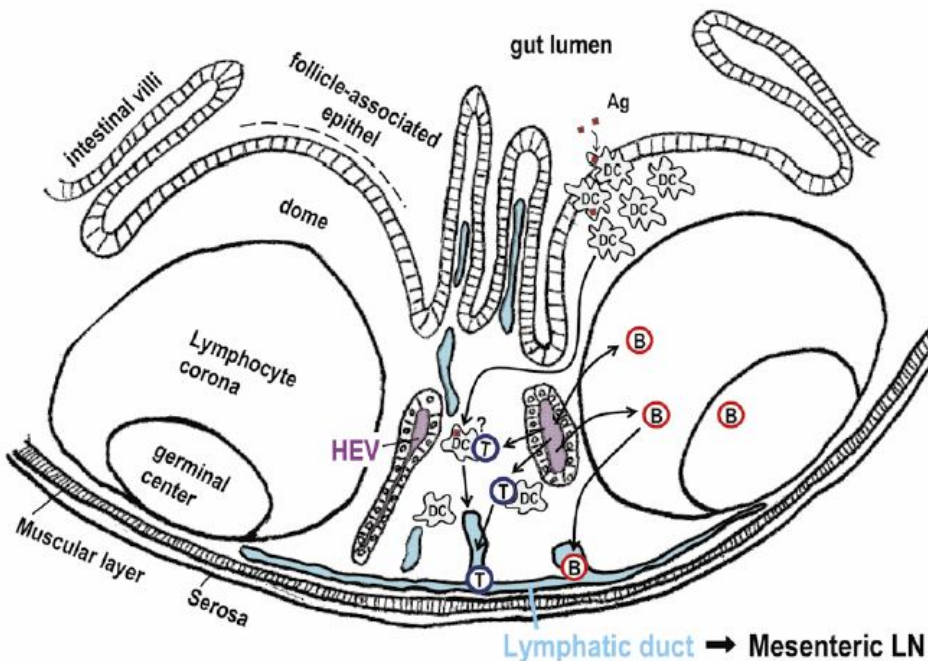
Figure 2 – Schematic drawing of the structure of Peyer's patches and trafficking route of T cells (T), B cells (B). HEV: high endothelial venule (Matsuno et al., 2010).

1.6 The biology of *Salmonella* Typhimurium infections

1.6.1 The murine model

Murine infections by *S.* Typhimurium have been largely exploited as a model for the study of typhoid and general salmonellosis. *S.* Typhimurium causes in mice a systemic disease with a pathogenesis resembling typhoid fever in humans (Wick, 2010). *S.* Typhimurium is a food- and water-borne pathogen. Thus, following ingestion, a proportion of inoculum that succeeds in tolerating the low pH environment of the stomach enters the small intestine to establish infection (Álvarez-Ordóñez et al., 2011). At this point, *S.* Typhimurium must adhere itself to epithelial cells in the gut by several adhesins and fimbriae and subsequently cross the intestinal epithelium (Broz et al., 2012). As depicted in the Figure 3, multiple traversal routes are involved in *Salmonella* penetration of host mucosa (Tam et al., 2008).

The host-*Salmonella* interaction is dominated by the broad array of sophisticated weaponry used by bacteria to overcome host defences (Andrews-Polymenis et al., 2010). *S.* Typhimurium preferentially targets the M cells located in the PP follicle-associated epithelium, manipulates their function and moves through them, accessing lymphoid cells of GALT (Martinoli et al., 2007). However, this pathogen can also induce its internalization in enterocytes through its virulence-associated type III secretion system (TTSS) encoded by *Salmonella* pathogenicity Island 1 (SPI-1) (Ly and Casanova, 2007). TTSS encode needle-like complexes that inject bacterial effector proteins that are able to hijack host cell functions, including those associated with cytoskeleton remodelling and immunomodulatory activity (Garai et al. 2012). Invasion also has been proposed to occur by paracellular pathways following disruption of epithelia tight junctions and via DC intercalated between epithelial cells. However, the importance of

these invasion-independent alternative pathways remains to be determined (Broz et al., 2012).
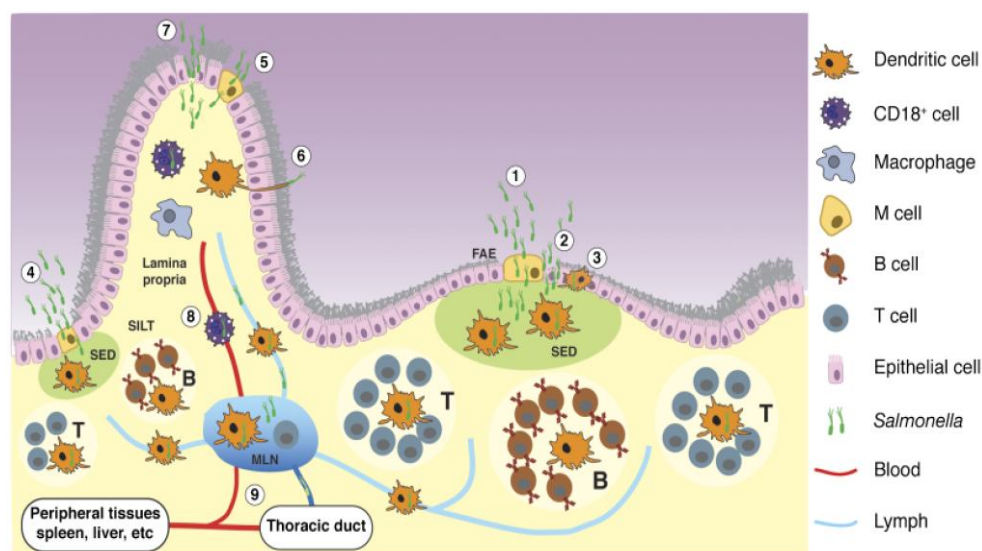
Figure 3 – Entry and capture of orally acquired *Salmonella*. *Salmonella* can cross the intestinal epithelium and enter the host at different sites, mostly at the distal ileum. Two of these sites are organized lymphoid structures, Peyer's patches (PP) and solitary intestinal lymphoid tissue (SILT). The third site is the intestinal villus. *Salmonella* can also invade using different mechanisms, which are indicated with numbers. Within PP, *Salmonella* can traverse the intestinal barrier through: (1) M cells in the follicle-associated epithelium (FAE); (2) epithelial cells forming the FAE, in particular after bacteria compromise M cells and the intestinal barrier; (3) DCs located in the FAE, could capture *Salmonella*. Once bacteria cross the FAE they can be captured by DCs located in the subepithelial dome (SED). DCs containing *Salmonella* can then initiate an adaptive immune response by stimulating T cells in the PP (marked T in the figure) or migrate to the mesenteric lymph node (MLN) to initiate adaptive immunity. In addition, *Salmonella* can cross the intestinal barrier through SILT, probably in a similar manner as in PP, as represented in (4). At villi, *Salmonella* can enter in different ways: (5) through M cells; (6) captured by DCs extending dendrites; or (7) passing through or between compromised epithelial cells. After the bacteria reach the lamina propria, they can access the MLN within migrating DCs, which are abundant in the lamina propria. Finally, the bacteria may be able to reach the blood stream, presumably transported by CD18+ phagocytes, as shown in (8). In addition to being transported to the MLN via lymph within DCs, it remains possible that free bacteria could be transported in lymph. (9) Bacteria can exit the MLN as free bacteria or possibly associated with cells and seed other tissues in the body (Tam et al., 2008).

After crossing the epithelium, *Salmonella* is taken by phagocytes located in the PP dome that work to remove invading microbes by phagocytosis and alert other immune cells of the infection, either directly or by releasing pro-inflammatory cytokines (Tam et al., 2008). Indeed, a rapid recruitment of neutrophils to infected tissue is the pathological hallmark of gastroenteritis caused by non-typhoidal *Salmonella* serovars (Andrews-Polymenis et al., 2010). For initiation of responses against microbes, macrophages and dendritic cells express multiple pathogen recognition receptors, including the cytosolic nucleotide-binding and oligomerization domain (NOD)-like receptors (NLR) and the Toll-like receptors (TLR) located on the cell surface or within a vacuolar compartment (Wick, 2011). Furthermore, a subset of NLR induces the assembly of a large multiprotein signaling complex called the inflammasome, which in cooperation with the adaptor protein ASC and activated caspase-1 (CASP1), leads to production and secretion of mature interleukin-1β and IL18 (Figure 4). CASP1 activation also initiates a proinflammatory cell-death called pyroptosis (Miao and Rajan, 2011).

Although pyroptosis and apoptosis are both programmed forms of cell death, pyroptosis is not considered immunulogically silent, since it causes the release of cellular contents and proinflamatory cytokines (Duprez et al., 2009). Of note, induction of pyroptosis was proved to be a mechanism that benefits host during *Salmonella* infections by eliminating the intracellular niche of the pathogen and re-exposing it to extracellular immune defenses, mainly clearance by neutrophils (Miao et al., 2010). Indeed, this evidence justifies the crucial role of neutrophils to prevent the dissemination of bacteria from the gut during salmonellosis, despite the fact that this *S.* Typhimurium is mainly considered an intracellular pathogen (Broz et al., 2012).
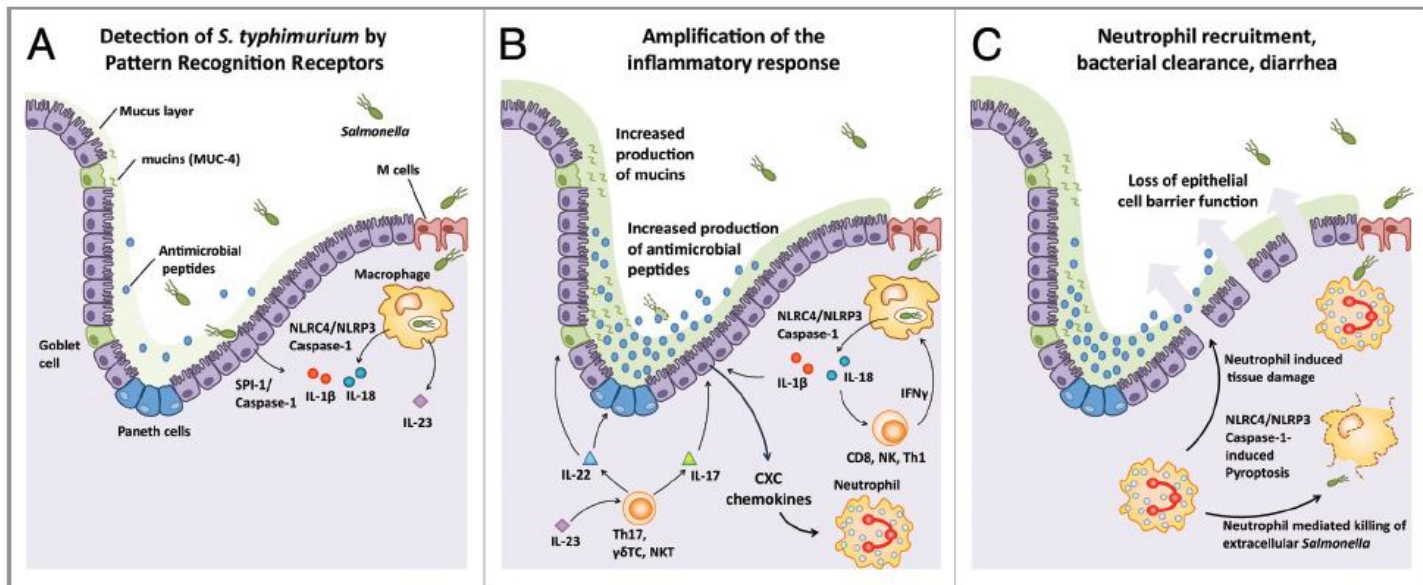
Figure 4 - The intestinal innate immune response to *Salmonella*. (A) Following the invasion of the mucosa, the presence of *Salmonella* is detected by pattern recognition receptors. Extracellular *Salmonella* are detected by Toll-like receptors inducing a transcriptional response leading to the expression of proinflammatory cytokines such as IL-23. Intracellular *Salmonella* activate NOD-like receptors that can induce IL-23 expression, as well as the assembly of NLRC4/NLRP3 inflammasomes that activate Caspase-1, promoting the secretion of mature IL-1β and IL-18. (B) IL-18 and IL-23 amplify the inflammatory response by paracrine signaling. IL-18 induces the release of IFNγ from T cells, while IL-23 induces the release of IL-22 and IL-17. These cytokines induce the increased production of mucins and antimicrobial peptides, and promote the release of CXC chemokines leading to an influx of neutrophils into the mucosa. (C) Infiltrating neutrophils are crucial for the killing of extracellular *Salmonella*. Although considered an intracellular pathogen, *Salmonella* can be found extracellularly following transcytosis through M cells or after pyroptosis induced host cell lysis. Besides clearing the pathogen, neutrophil influx can also lead to damage to intestinal tissue, resulting in the loss of epithelial cell barrier function and promoting diarrhea (Broz et al., 2012).

Despite innate mechanisms are triggered by host to fight against infection, *Salmonella* is able to maintain itself in an intracellular compartment named the *Salmonella* containing vacuole (SCV) following phagocytosis. To establish this niche, pathogen expresses its SPI-2-efectors that act stabilizing the vacuolar membrane, modulating endocytic trafficking and inducing delayed host cell death (Garai et al., 2012). The SPI-2 TTSS plays an essential role in preventing rapid pathogen clearance by promoting its survival within mononuclear phagocytes (Srikanth et al., 2011).

From intestine, *Salmonella* can reach the MLN via the draining lymph as free extracellular bacteria or be transported by cells, presumably DC, from the lamina propria and/or Peyer's patches. At this stage of an orally acquired infection, pathogen is still confined to intestine and associated lymphoid tissue. However, in mice infections virulent *Salmonella* disseminate and reach other tissues such as the liver, spleen and bone marrow. To cause this systemic dissemination, *Salmonella* reach bloodstream via lymph that empties into the blood in the thoracic duct or possibly via CD18^{+} phagocytes infected in the gut (Tam et al., 2008).

Continuous spread of the bacteria from infected cells to new infection foci is one of the key features of murine systemic *Salmonella* infections. This spread avoids high intracellular bacterial densities within the phagosomal compartment, a situation that would render the bacteria either nutritionally or spatially constricted. Moreover, bacterial spread from established foci to new infection foci at immunologically unprimed sites is also likely to be a mechanism that allows *Salmonella* to stay one step ahead of the progressive local activation of the inflammatory response (Haimovich and Venkatesan, 2006). *S.* Typhimurium can be recovered from systemic sites up to one year after infection from asymptomatic mice. Although persisting bacteria sequestered within macrophages appear to enter a dormant-like state, *S.* Typhimurium survival and

replication in hemophagocytic macrophages may play a key role in the establishment of persistent infections (Monack, 2012).

Effective control and eventual eradication of bacteria during the late phases of a primary infection and the generation of protective immunity against subsequent infections require the development and active recruitment of adaptive immunity mediators (Dougan et al., 2011). However, accumulation evidences have shown that *Salmonella* is able to inhibit T-cell activation by interfering with the presentation of antigens on the DC surface (Bueno et al., 2012). Since DC are important APC linking innate and adaptive immunity, interfering with their capacity to stimulate naïve T cells may allow pathogens evading adaptive immunity. Such interference would promote pathogen survival and dissemination, both crucial events in *Salmonella* pathogenesis (Swart and Hensel, 2012).

1.6.2 Differences between infections in mouse and other hosts

When considering host response to salmonellosis, it is important to stress that most of available knowledge was accessed by the study of mouse model, as this has been worked on most extensively. Nevertheless, observations from this approach do not always correlate with human (Tsolis, 2011) and farm animals infections (Bearson and Bearson, 2011). In different hosts, the outcome of infection differs in terms of local versus systemic spread, influence of infecting isolate properties and specific breed responses to pathogen (Dougan et al., 2011). While septicemic episodes have been reported for *Salmonella* in mice, colonization by *S.* Typhimurium in food-producing animals is usually limited to the gastrointestinal tract (Hoelzer et al., 2011).

Natural or experimental infection of calves with serotype Typhimurium results in an enteric disease with clinical and pathological features that parallel

the disease in man. The intestinal pathology and the predominant influx of PMN leucocytes observed in infected calves are strikingly similar to that of *S.* Typhimurium-induced enteritis in humans. In both species, PMN leukocytes are proposed to play a decisive role in the pathogenesis of serotype Typhimurium-induced diarrhoea (Santos et al., 2001). Pig infections with *S.* Typhimurium are also clinically similar to those observed in human. However, besides some evidences indicating the influx of PMN cells to the porcine gut during *S.* Typhimurium infections, information on processes behind the induction of diarrhoea is still scarce (Boyen et al., 2008a).

Existing data from the mouse model support that the Peyer's patch route predominates in traversal of *Salmonella*. Nevertheless, little is known about how *Salmonella* penetrates the mucosa in man and other species (Dougan et al., 2011). According to Costa et al. (2012), *S.* Typhimurium induces ruffling of the plasma membrane at the apical side of intestinal epithelial cells during bovine infections, invading M cells and absorptive enterocytes. Similarly, it has been shown that *Salmonella* can invade porcine absorptive enterocytes, M-cells and even goblet cells (Boyen et al., 2008a). In a study by scanning and transmission electron microscopy, Meyerholz et al. (2002) demonstrate a preferential adherence of *S.* Typhimurium to M cells within 5 minutes post infection of swine ileum. In addition, these authors demonstrated that this pathogen may use sites of cell extrusion as an additional mechanism for early invasion. Moreover, in accordance to evidences from murine infections, Boyen et al. (2006) asserted that SPI-1 is necessary to promote the invasion of porcine intestinal epithelial cells by *S.* Typhimurium, thereby contributing to the efficient short-term colonization of the porcine gut and to the induction of influx of neutrophils into the intestinal lumen.

S. Typhimurium triggers the up-regulation of pro-inflammatory genes and a Th1 oriented immune response in porcine jejunal gut loops (Meurens et al.,

2009). Moreover, swine jejunum, ileum and colon respond differently to *in vivo* infections with *S. typhimurium.* In spite of the up-regulation of genes coding for innate immunity mediators, ileum showed a down-regulation of IL12 and CASP1, both relevant molecules in the response of host to *Salmonella.* This result could represent an advantage to pathogen during pig infections and was inferred to be related to the preference of *S.* Typhimurium for invading intestinal mucosa through ileum (Collado-Romero et al., 2010).

In pigs, S. Typhimurium is sporadically present in liver and spleen shortly after experimental inoculation but does not seem to replicate and is cleared from these organs a few days after inoculation. However, bacteria are able to persist in the gut and gut-associated lymph nodes (Boyen et al., 2008a). Gut-associated lymph-nodes are considered important niches for *S.* Typhimurium during swine infections. In fact, *Salmonella* prevalence in lymph-nodes of slaughter pigs from EU countries ranges from 0% to 29% (Baptista et al., 2011). Basing on data from mouse infections, it could be inferred that *S.* Typhimurium reach MLN via intestinal lymph, being shuttled by infected phagocytes or as extracellular bacteria. Nevertheless, this issue has never been addressed to date by any available report. Uthe et al. (2007) observed that *S.* Typhimurium could be isolated from pig MLN at 8 hours post oral infection and verified that pathogen was able to maintain itself in these organs at least 21 days post infection. Macrophages located in mesenteric lymph nodes are considered to be important players in the induction of long-term persistence of *S.* Typhimurium in infected pigs (Boyen et al. 2008a). Epidemiological analysis has established that *Salmonella* persistent carriers are crucial targets for disease control, because they shed the pathogen in high enough numbers to transmit disease (Gopinath et al., 2012). Indeed, asymptomatic carriers represent the most important source of *Salmonella* introduction onto pig farms (Hoelzer et al., 2011). For this reason, a comprehensive view of the processes involved in the maintenance of pathogen in

host lymphoid organs and the conversion of infected pigs to carriers consist in an essential step for controlling salmonellosis.

As previously discussed, SPI-2 effector are indispensable for systemic infection of mice, since they support the intracellular survival of *Salmonella* inside host cell, especially macrophages (Garai et al. 2012). Curiously, *S.* Typhimurium strains mutants for SPI-2 were found to be fully capable of colonizing the intestines of pigs and to establish a long-term intestinal persistent infection after oral inoculation (Boyen et al., 2008b), suggesting that *S.* Typhimurium might employ different strategies to promote the carrier state during mouse and pig infections. Therefore, this divergence highlights the need of models other than murine infections to elucidate the mechanisms involved in the induction of persistent infections by *Salmonella* and reinforces the notion that the extrapolation of data from murine model to other species should be done with prudence.

1.7 Swine as a model for the study of *Salmonella* Typhimurium infections

Animal models are valuable tools for a better understanding of pathogenesis mechanisms behind human diseases. To date, mouse has been widely used to provide novel knowledge in distinct fields of biology and medicine. However, mouse disease models often do not faithfully mimic the relevant human conditions, bringing to light the need of better animal models (Luney, 2007).

Swine are increasingly appreciated for their potential to model human disease and this tendency was further reinforced by the recent advances in pig genomics and proteomics (Prather, 2013; Bendixen et al., 2010). Besides, pigs and humans are remarkably similar in terms of physiology. Interestingly, the

porcine immune system shows a higher level of similarity to human one than murine. Genomic comparisons between human, murine and porcine sequences also demonstrate more resemblances between human and porcine than human and murine sequences (Luney, 2007).

The swine model has been used to study as a model for many human infectious diseases and represent a valuable intermediate species to validate the applicability of knowledge obtained using rodent models to human (Meurens et al., 2012). However, although former reports of experimental infections of pig with *Salmonella* can be found in the literature (Williams et al. 1978, Baskerville et al. 1972), it was the 1990s when the use of this species for the study of salmonellosis became more current.

Advances in mammalian models of *Salmonella* infection are expected to result in new understanding of salmonellosis pathogenesis, contributing to the control and cure of human cases (Gopinath et al., 2012). Upon infection with *S.* Typhimurium, swine undergo a self-limiting enterocolitis which parallels the clinical manifestation observed in man (Sanchez-Vargas et al. 2011; Boyen et al., 2008a). In light of this and the potential of swine as models of human disease, pigs can be stressed as an ideal model for investigating the pathogenesis of human non-typhoidal salmonellosis.

1.8 Use of functional genomics to identify target molecules and mechanisms for the improvement of resistance to infectious diseases in animals

Resistance and tolerance to infectious pathogens are important characteristics of livestock to counteract the potential detrimental impact of pathogens on animal health and production (Doeschl-Wilson et al., 2012a).

Strong evidence has accumulated that livestock species from birds to mammals, harbour genes that control protective responses to the various classes of pathogen from viruses to nematodes. However, there remains a gap for traits linked to disease resistance and tolerance because the main polymorphisms that underpin these traits have not been identified. This is partly because host-pathogen interactions are highly complex, involving many different molecules and cell types which interact together over time (Glass, 2012).

Disease traits have been difficult to target by traditional selection, but recent developments in high throughput genomics provide opportunities to dissect host responses to infectious pathogens and to increase the accuracy of selection (Doeschl-Wilson et al., 2012b). Knowledge obtained from the complete genome sequencing of many species has enabled discovery of new aspects of the host–pathogen interaction. Moreover, the development of genomics, transcriptomics, proteomics and computational biology has resulted in the systematic study of the host–pathogen interaction. Thus, functional genomics approaches have enabled the integration of experimental data from the diverse high-throughput methods to create a global picture of host–pathogen interplay in space and time (Hartlova et al., 2011).

In order to gain access to the host environment, a pathogen must cross the mucosal surfaces of the gut, respiratory tract, mammary gland and genital tract. After invading, these organisms should be able to tolerate and overcome host immunity. Thus, genetic variance in molecules taking part in the distinct partners of host defence against invaders might play an important role in the development of resistance or tolerance to infections. Strikingly, some examples have been described in veterinary. Recently, genetic variants in bovine CD46 have been shown to influence cell permissiveness for bovine viral diarrhoea virus and thus carriers of CD46 alleles might vary in resistance to this pathogen. Besides, the gut receptor for *E. coli* F18 encoded by the FUT1 gene in pigs was found to

confer complete resistance to *E. coli* (Glass, 2012). Another report, exploring the genetic resistance of bovine to the tick-borne protozoan *Theileria annulata*, demonstrated that an up-regulation of SIRPβ and TGFβ2, both mediators of inflammatory response, is associated to greater virulence and also higher propensity for invasion observed Holstein cows compared to the *Bos indicus* cattle breed Sahiwal (Chauessepied et al., 2010).

In the case of *S.* Typhimurium infections, genetic resistance to systemic disease in mice has been linked to many factors including the major histocompatibility complex (MHC), Toll-like receptor 4 and the natural resistance associated macrophage protein (NRAMP1). NRAMP1 is the most studied of all these factors and exerts effects on macrophage activation including MHC expression, release of pro-inflammatory cytokines and the production of antimicrobial effectors such as nitric oxide and oxidative burst. Mutations in this gene result in mice susceptible to *S.* Typhimurium and other intracellular pathogens such as *Leishmania* and *Mycobacterium* (Wigley, 2004). In fowl, comparisons of different models have successfully identified the genomic regions carrying the genes TLR4, NRAMP1 and the QTL SAL1 as having roles in phenotypic variations related to *Salmonella* resistance (Calenge et al., 2010).

Control of salmonellosis in swine herds generates increased production costs and public health issues in the use of prophylactic antibiotic potentially leading to development of antibiotic resistant strains. Therefore, the breeding of resistant animals, in combination with good hygiene practices offers a promising low risk strategy to fight against *Salmonella* in this species. In pigs, NRAMP1 is strongly expressed on macrophages and neutrophils following stimulation with LPS, but any role for this gene in *Salmonella* infection is yet to be described (Wigley, 2004). On the other hand, other authors have demonstrated the influence of genetic variance in the outcome of *S.* Typhimurium infections in porcine. Uthe et al. (2009) asserted a positive association between genetic

polymorphisms in the CCT7 gene with *Salmonella* shedding in swine. Besides, another report by Tuggle et al (2010) detected transcriptional changes in blood of persistent *Salmonella* shedder pigs which resulted in increased levels of intracellular-oriented responses compared to low shedder animals.

In spite of the association between genetic variation and resistance to salmonellosis in swine, selective breeding for resistance traits aiming to control the disease or the carriage of *Salmonella* in this species is still not feasible. In fact, targeting of the key host molecules and mechanisms involved in bacterial pathogenesis is indispensable to address this issue and a robust analysis of *S.* Typhimurium–pig interactions by integrative approaches represent a necessary step towards this aim.

References

1. Acheson DW, Luccioli S. Microbial-gut interactions in health and disease. Mucosal immune responses. Best Pract Res Clin Gastroenterol. 2004; 18:387-404.

2. Andrews-Polymenis HL, Bäumler AJ, McCormick BA, Fang FC. Taming the elephant: *Salmonella* biology, pathogenesis, and prevention. Infect Immun. 2010; 78:2356-69.

3. Baptista FM, Halasa T, Alban L, Nielsen LR. Modelling food safety and economic consequences of surveillance and control strategies for *Salmonella* in pigs and pork. Epidemiol Infect. 2011; 139:754-64.

4. Baskerville A, Dow C, Curran WL, Hanna J. Ultrastructure of phagocytosis of *Salmonella* cholerae-suis by pulmonary macrophages *in vivo*. Br J Exp Pathol. 1972; 53:641-7.

5. Bearson BL, Bearson SM. Host specific differences alter the requirement for certain *Salmonella* genes during swine colonization. Vet Microbiol. 2011;150:215-9.

6. Bendixen E, Danielsen M, Larsen K, Bendixen C. Advances in porcine genomics and proteomics--a toolbox for developing the pig as a model organism for molecular biomedical research. Brief Funct Genomics. 2010; 9:208-19.

7. Botteldoorn N, Heyndrickx M, Rijpens N, Grijspeerdt K, Herman L. *Salmonella* on pig carcasses: positive pigs and cross contamination in the slaughterhouse. J Appl Microbiol. 2003; 95:891-903.

8. Boyen F, Haesebrouck F, Maes D, Van Immerseel F, Ducatelle R, Pasmans F. Non-typhoidal *Salmonella* infections in pigs: a closer look at epidemiology, pathogenesis and control. Vet Microbiol. 2008a; 130:1-19.

9. Boyen F, Pasmans F, Van Immerseel F, Morgan E, Botteldoorn N, Heyndrickx M, Volf J, Favoreel H, Hernalsteens JP, Ducatelle R, Haesebrouck F. A limited role for SsrA/B in persistent *Salmonella* Typhimurium infections in pigs. Vet Microbiol. 2008b;128:364-73.

10. Boyen F, Pasmans F, Van Immerseel F, Morgan E, Adriaensen C, Hernalsteens JP, Decostere A, Ducatelle R, Haesebrouck F. *Salmonella* Typhimurium SPI-1 genes promote intestinal but not tonsillar colonization in pigs. Microbes Infect. 2006; 8:2899-907.

11. Brandtzaeg P. Mucosal immunity: induction, dissemination, and effector functions. Scand J Immunol. 2009; 70:505-15.

12. Broz P, Ohlson MB, Monack DM. Innate immune response to *Salmonella* typhimurium, a model enteric pathogen. Gut Microbes. 2012; 3:62-70.

13. Bueno SM, Riquelme S, Riedel CA, Kalergis AM. Mechanisms used by virulent *Salmonella* to impair dendritic cell function and evade adaptive immunity. Immunology. 2012; 137:28-36.

14. Burkey TE, Skjolaas KA, Minton JE. Board-invited review: porcine mucosal immunity of the gastrointestinal tract. J Anim Sci. 2009; 87:1493-501.

15. Calenge F, Kaiser P, Vignal A, Beaumont C. Genetic control of resistance to salmonellosis and to *Salmonella* carrier-state in fowl: a review. Genet Sel Evol. 2010; 42:11.

16. Centers for Disease Control and Prevention (CDC). Vital signs: incidence and trends of infection with pathogens transmitted commonly through food--foodborne diseases active surveillance network, 10 U.S. sites, 1996-2010. MMWR Morb Mortal Wkly Rep. 2011; 60:749-55.

17. Chaussepied M, Janski N, Baumgartner M, Lizundia R, Jensen K, Weir W, Shiels BR, Weitzman JB, Glass EJ, Werling D, Langsley G. TGF-b2 induction regulates invasiveness of Theileria-transformed leukocytes and disease susceptibility. PLoS Pathog. 2010; 6:e1001197.

18. Collado-Romero M, Arce C, Ramírez-Boo M, Carvajal A, Garrido JJ. Quantitative analysis of the immune response upon *Salmonella* typhimurium infection along the porcine intestinal gut. Vet Res. 2010; 41:23.

19. Correia-Gomes C, Mendonça D, Vieira-Pinto M, Niza-Ribeiro J. Risk factors for *Salmonella* spp in Portuguese breeding pigs using a multilevel analysis. Prev Vet Med. 2013;108:159-66.

20. Costa LF, Paixão TA, Tsolis RM, Bäumler AJ, Santos RL. Salmonellosis in cattle: advantages of being an experimental model. Res Vet Sci. 2012; 93:1-6.

21. De Busser EV, De Zutter L, Dewulf J, Houf K, Maes D. *Salmonella* control in live pigs and at slaughter. Vet J. 2013; 196:20-7.

22. De Ridder L, Maes D, Dewulf J, Pasmans F, Boyen F, Haesebrouck F, Méroc E, Butaye P, Van der Stede Y. Evaluation of three intervention strategies to reduce the transmission of *Salmonella* Typhimurium in pigs. Vet J. 2013; pii: S1090-0233(13)00144-5.

23. Doeschl-Wilson AB, Bishop SC, Kyriazakis I, Villanueva B. Novel methods for quantifying individual host response to infectious pathogens for genetic analyses. Front Genet. 2012; 3:266.

24. Doeschl-Wilson AB, Villanueva B, Kyriazakis I. The first step toward genetic selection for host tolerance to infectious pathogens: obtaining the tolerance phenotype through group estimates. Front Genet. 2012; 3:265.

25. Dougan G, John V, Palmer S, Mastroeni P. Immunity to salmonellosis. Immunol Rev. 2011; 240:196-210.

26. Duprez L, Wirawan E, Vanden Berghe T, Vandenabeele P. Major cell death pathways at a glance. Microbes Infect. 2009; 11:1050-62.

27. Elmore SA. Histopathology of the lymph nodes. Toxicol Pathol. 2006; 34:425-54.

28. European Food Safety Authority (EFSA). The European Union summary report on trends and sources of zoonoses, zoonotic agents and food-borne outbreaks in 2011. Euro Surveill. 2013; 18:20449.

29. Farzan A, Friendship RM, Dewey CE, Warriner K, Poppe C, Klotins K. Prevalence of *Salmonella* spp. on Canadian pig farms using liquid or dry-feeding. Prev Vet Med. 2006; 73:241-54.

30. Foley SL, Lynne AM, Nayak R. *Salmonella* challenges: prevalence in swine and poultry and potential pathogenicity of such isolates. J Anim Sci. 2008; 86:E149-62.

31. Garai P, Gnanadhas DP, Chakravortty D. *Salmonella enterica* serovars Typhimurium and Typhi as model organisms: revealing paradigm of host-pathogen interactions. Virulence. 2012; 3:377-88.

32. Glass EJ. The molecular pathways underlying host resistance and tolerance to pathogens. Front Genet. 2012; 3:263.

33. Goldbach SG, Alban L. A cost-benefit analysis of *Salmonella*-control strategies in Danish pork production. Prev Vet Med. 2006; 77:1-14.

34. Gopinath S, Carden S, Monack D. Shedding light on *Salmonella* carriers. Trends Microbiol. 2012; 20:320-7.

35. Hartlova A, Krocova Z, Cerveny L, Stulik J. A proteomic view of the host-pathogen interaction: The host perspective. Proteomics. 2011;11:3212-20.

36. Hendriksen RS, Vieira AR, Karlsmose S, Lo Fo Wong DM, Jensen AB, Wegener HC, Aarestrup FM. Global monitoring of *Salmonella* serovar distribution from the World Health Organization Global Foodborne Infections Network Country Data Bank: results of quality assured laboratories from 2001 to 2007. Foodborne Pathog Dis. 2011; 8:887-900.

37. Hoelzer K, Moreno Switt AI, Wiedmann M. Animal contact as a source of human non-typhoidal salmonellosis. Vet Res. 2011; 42:34.

38. Jacobsen A, Hendriksen RS, Aaresturp FM, Ussery DW, Friis C. The *Salmonella enterica* pan-genome. Microb Ecol. 2011; 62:487-504.

39. Lawson LG, Jensen JD, Christiansen P, Lund M. Cost-effectiveness of *Salmonella* reduction in Danish abattoirs. Int J Food Microbiol. 2009; 134:126-32.

40. Lunney JK. Advances in swine biomedical model genomics. Int J Biol Sci. 2007; 3:179-84.

41. Ly KT, Casanova JE. Mechanisms of *Salmonella* entry into host cells. Cell Microbiol. 2007; 9:2103-11.

42. Majowicz SE, Musto J, Scallan E, Angulo FJ, Kirk M, O'Brien SJ, Jones TF, Fazil A, Hoekstra RM; International Collaboration on Enteric Disease 'Burden of Illness' Studies. The global burden of nontyphoidal *Salmonella* gastroenteritis. Clin Infect Dis. 2010; 50:882-9.

43. Makala LH, Suzuki N, Nagasawa H. Peyer's patches: organized lymphoid structures for the induction of mucosal immune responses in the intestine. Pathobiology. 2002-2003; 70:55-68.

44. Matsuno K, Ueta H, Shu Z, Xue-Dong X, Sawanobori Y, Kitazawa Y, Bin Y, Yamashita M, Shi C. The microstructure of secondary lymphoid organs that support immune cell trafficking. Arch Histol Cytol. 2010; 73:1-21.

45. Methner U, Rammler N, Fehlhaber K, Rösler U. *Salmonella* status of pigs at slaughter--bacteriological and serological analysis. Int J Food Microbiol. 2011; 151:15-20.

46. Meurens F, Berri M, Auray G, Melo S, Levast B, Virlogeux-Payant I, Chevaleyre C, Gerdts V, Salmon H. Early immune response following *Salmonella enterica* subspecies *enterica* serovar Typhimurium infection in porcine jejunal gut loops. Vet Res. 2009; 40:5.

47. Meurens F, Summerfield A, Nauwynck H, Saif L, Gerdts V. The pig: a model for human infectious diseases. Trends Microbiol. 2012; 20:50-7.

48. Meyerholz DK, Stabel TJ, Ackermann MR, Carlson SA, Jones BD, Pohlenz J. Early epithelial invasion by *Salmonella enterica* serovar Typhimurium DT104 in the swine ileum. Vet Pathol. 2002; 39:712-20.

49. Miao EA, Leaf IA, Treuting PM, Mao DP, Dors M, Sarkar A, Warren SE, Wewers MD, Aderem A. Caspase-1-induced pyroptosis is an innate immune effector mechanism against intracellular bacteria. Nat Immunol. 2010; 11:1136-42.

50. Monack DM. *Salmonella* persistence and transmission strategies. Curr Opin Microbiol. 2012;15:100-7.

51. Newberry RD, Lorenz RG. Organizing a mucosal defense. Immunol Rev. 2005; 206:6-21.

52. Prather RS. Pig genomics for biomedicine. Nat Biotechnol. 2013;31:122-4

53. Resano H, Perez-Cueto FJ, de Barcellos MD, Veflen-Olsen N, Grunert KG, Verbeke W. Consumer satisfaction with pork meat and derived products in five European countries. Appetite. 2011; 56:167-70.

54. Rothkötter HJ. Anatomical particularities of the porcine immune system--a physician's view. Dev Comp Immunol. 2009; 33:267-72.

55. Ruddle NH, Akirav EM. Secondary lymphoid organs: responding to genetic and environmental cues in ontogeny and the immune response. J Immunol. 2009; 183:2205-12.

56.Sánchez-Vargas FM, Abu-El-Haija MA, Gómez-Duarte OG. *Salmonella* infections: an update on epidemiology, management, and prevention. Travel Med Infect Dis. 2011; 9:263-77.

57. Santos RL, Zhang S, Tsolis RM, Kingsley RA, Adams LG, Bäumler AJ. Animal models of *Salmonella* infections: enteritis versus typhoid fever. Microbes Infect. 2001; 3:1335-44.

58. Scharek L, Tedin K. The porcine immune system--differences compared to man and mouse and possible consequences for infections by *Salmonella* serovars. Berl Munch Tierarztl Wochenschr. 2007; 120:347-54.

59. Swart AL, Hensel M. Interactions of *Salmonella enterica* with dendritic cells. Virulence. 2012; 3:660-7.

60. Tam MA, Rydström A, Sundquist M, Wick MJ. Early cellular responses to *Salmonella* infection: dendritic cells, monocytes, and more. Immunol Rev. 2008; 225:140-62.

61. Tsolis RM, Xavier MN, Santos RL, Bäumler AJ. How to become a top model: impact of animal experimentation on human *Salmonella* disease research. Infect Immun. 2011; 79:1806-14.

62. Tuggle CK, Bearson SM, Uthe JJ, Huang TH, Couture OP, Wang YF, Kuhar D, Lunney JK, Honavar V. Methods for transcriptomic analyses of the porcine host immune response: application to *Salmonella* infection using microarrays. Vet Immunol Immunopathol. 2010; 138:280-91.

63. Uthe JJ, Royaee A, Lunney JK, Stabel TJ, Zhao SH, Tuggle CK, Bearson SM. Porcine differential gene expression in response to *Salmonella enterica* serovars Choleraesuis and Typhimurium. Mol Immunol. 2007; 44:2900-14.

64. Uthe JJ, Wang Y, Qu L, Nettleton D, Tuggle CK, Bearson SM. Correlating blood immune parameters and a CCT7 genetic variant with the shedding of *Salmonella enterica* serovar Typhimurium in swine. Vet Microbiol. 2009; 135:384-8.

65. Wick MJ. Innate immune control of *Salmonella enterica* serovar Typhimurium: mechanisms contributing to combating systemic Salmonella infection. J Innate Immun. 2011; 3:543-9.

66. Wigley P. Genetic resistance to *Salmonella* infection in domestic animals. Res Vet Sci. 2004; 76:165-9.

67. Wilhelm B, Rajić A, Parker S, Waddell L, Sanchez J, Fazil A, Wilkins W, McEwen SA. Assessment of the efficacy and quality of evidence for five on-farm interventions for *Salmonella* reduction in grow-finish swine: a systematic review and meta-analysis. Prev Vet Med. 2012; 107:1-20.

68. Williams RD, Rollins LD, Pocurull DW, Selwyn M, Mercer HD. Effect of feeding chlortetracycline on the reservoir of *Salmonella* typhimurium in experimentally infected swine. Antimicrob Agents Chemother. 1978; 14:710-9.

2. Objectives

Genetic improvement of the resistance to infectious diseases represents an essential step for the development of sustainable and economically viable animal production systems. This issue is of particular importance in the case of zoonotic diseases, since a safe food supply largely depends on controlling the infection in livestock hosts. Functional genomics approaches combining the power of gene mapping technologies, gene expression studies and modern bioinformatics tools have begun to contribute very recently to a better understanding of the host response to microbial diseases. The knowledge provided may reveal new tools, therapeutics, and improved strategies for the establishment of future programs to develop disease-resistant livestock breeds, which should be aimed at improving health and welfare of animals, and as a result, improved quality and food safety.

The **overall objective** of this thesis is to identify and describe molecular pathways and the interactions involved in the porcine intestinal immune response to *Salmonella enterica* serovar Typhimurium. To achieve this objective, an *in vivo* experimental infection model was established and the following **five specific objectives** were set up:

1. Evaluate the differential expression of immune-related genes in the MLN of *S.* Typhimurium infected pigs, in correlation with changes in tissue cellularity and pathogen burden (Martins et al. Comp Immunol Microbiol Infect Dis. 2013. 36:149-160);

2. Explore the proteomic response of porcine MLN to *S.* Typhimurium infection (Martins et al. J Proteomics. 2012. 75:4457-4470);

3. Generate a comprehensive view of the mechanisms underlying host-pathogen interactions in MLN during pig infections with *S.*

Typhimurium, integrating gene expression data from host and pathogen (Martins et al. Vet Res. Under review);

4. Use laser microdissection coupled to qPCR technology and bioinformatic analysis to provide a preliminary understanding of the immune response processes engendered in swine PP follicles during *S.* Typhimurium infections (Martins et al. Dev Com Immunol. 2013. 41:100-104);

5. Dissect the global transcriptional response of swine PP follicles to *S.* Typhimurium infection by microarray analysis coupled to bioinformatic data mining (Martins et al. J Infect Dis. Manuscript in preparation).

3. Experimental studies

3.1 Exploring the immune response of porcine mesenteric lymph nodes to *Salmonella enterica* serovar Typhimurium: an analysis of transcriptional changes, morphological alterations and pathogen burden

Rodrigo Prado Martins[a], Melania Collado-Romero[a], Cristina Arce[a], Concepción Lucena [a], Ana Carvajal[b], Juan J. Garrido[a]*

[a] Grupo de Genómica y Mejora Animal, Departamento de Genética, Universidad de Córdoba, Campus de Rabanales, Edificio Gregor Mendel C5, 14071 Córdoba, Spain

[b] Departamento de Sanidad Animal, Facultad de Veterinaria, Universidad de León, 24071 León, Spain

Abstract

Infections caused by *Salmonella enterica* serovar Typhimurium (*S. typhimurium*) cause important economic problems in the swine industry and threaten the integrity of a safe and healthy food supply. Controlling the prevalence of *Salmonella* in pig production requires a thorough knowledge of the response processes that occurs in the gut associated immune tissues. To explore the *in vivo* porcine response to *S. typhimurium*, MLN samples from four control pigs and twelve infected animals at 1, 2 and 6 days post infection (dpi) were collected to quantify the mRNA expression of gene coding for 42 innate immune-related molecules. In addition, the presence of *S. typhimurium* in MLN was examined and its effect on tissue micro-anatomy. Higher *S. typhimurium* loads were observed at 2 dpi, triggering an innate immune response, marked by a substantial infiltration of phagocytes and up-regulation of pro-inflammatory genes. Such response resulted in a significant decrease in pathogen burden in MLN at 6 dpi, although *Salmonella* could not be completely eliminated from tissue. Furthermore, our results suggest that in porcine infections, *S. typhimurium* might interfere with dendritic cell–T cell interactions and this strategy could be involved in the conversion of *Salmonella* infected pigs to a carrier state.

Keywords: Pig, Mesenteric lymph-node, Immune response, *Salmonella enterica* serovar Typhimurium

3.1.1 Introduction

Salmonella is one of the most frequent causes of food-borne outbreaks in Europe, with 108,614 confirmed cases of human salmonellosis in 2009 [1]. Worldwide, *Salmonella* causes 94 million cases of acute gastroenteritis, including 155,000 that are fatal, with children in particular falling victim to the disease [2]. Among more than 2500 serovariants, the host-generalist *Salmonella enterica* serovar Typhimurium (herein *S. typhimurium*) is reported as the serovar most frequently associated with human illness, with *S. typhimurium* cases mostly associated with the consumption of contaminated pig and poultry meat [3].

Infections by *S. typhimurium* in pigs lead to a localized enterocolitis and, in general, infected swine evolve into healthy carriers in which bacteria are able to persist without triggering clinical signs [3]. The existence of asymptomatic carriers is a major threat to public health given that such animals cannot be detected easily and thus serves as source of contamination in food industry [4]. In addition to its importance as zoonotic disease, salmonellosis has an important impact in porcine health and negative implications in the efficiency and economy of the porcine production systems [5].

As a result of food poisoning, *Salmonella* enters the body through the gastrointestinal tract. After location in intestinal lumen and attachment in epithelial cells, *Salmonella* actively invade intestinal cells, colonize the lamina propria and Peyer's patches and rapidly invade host cells, especially macrophages, but also dendritic cells and neutrophils [6]. Consequently, these innate immune cells produce and release chemoattractant cytokines to recruit additional inflammatory cells into the site of invasion and initiate a T helper 1 (Th1) response [7]. From intestine, *Salmonella* reaches mesenteric lymph nodes (MLN), can enter the bloodstream and spread to internal organs [8]. To prevent

systemic infection, MLN form a life-saving firewall that protects the host from rapid pathogen dissemination beyond the intestine to others organs, such as liver and spleen [9].

One way to learn about the molecular interactions during *Salmonella* infection is to analyze the host response. To this end, infection experiments using isolated primary cells or cell lines have been carried out to generate most of the knowledge currently available on the molecular events during *Salmonella*–host interaction [10–12]. However, although these in vitro models can provide valuable information, it is clear that this approach does not enable the interaction of pathogens with a multitude of different interacting cells involved in the invasion process *in vivo* [13]. Moreover, in mammals, studies on the host mechanisms against *Salmonella* have been largely focused on mice infection models [14,15], although accumulating evidences suggest differences in virulence mechanisms, pathogen colonization and disease susceptibility in food-producing animals infections compared to the murine model of systemic disease [16]. Thus, while in mice *S. typhimurium* moves into the mesenteric lymph nodes, and from there bacteria spread via the efferent lymph to the circulatory system, causing a systemic disease [17], in pigs usually causes a self-limiting intestinal disease enterocolitis which is similar to gastroenteritis in humans [6]. Factors that could cause these differences have not been sufficiently clarified, but make the pig an ideal model for investigating enteric salmonellosis in humans.

In swine, in vitro and *in vivo* studies have generated valuable insight in the crosstalk between *Salmonella* and porcine tissues and cells [18–20]. Nevertheless, few studies have addressed the requirements for the gut-associated lymph nodes in the development of immune responses, their effect on the protective immunity against *Salmonella* infection and the relationship between changes in MLN transcriptome, tissue cellularity and level of pathogen invasion. In order to contribute to improved knowledge on the role of porcine

MLN on *S.* typhimurium infection, in the current study we use a model of *in vivo* experimental challenge to evaluate changes in gene expression and tissue morphological alterations that occur in these organs following infection.

3.1.2 Materials and methods

3.1.2.1. Experimental infection

The experimental infection design was described elsewhere [19]. Briefly, sixteen weaned piglets of approximately 4 weeks of age and fecal-negative for *Salmonella* were penned in an environmentally controlled isolation facility at 25°C with ad libitum access to feed and water. All the animals were randomly allocated to control group (4 piglets) or infected group (12 piglets). The four noninfected pigs were necropsied 2 h before the experimental infection. The animals belonging to the infected group were orally challenged with 108 CFU of *S. typhimurium* phagetype DT104. Afterwards, four infected pigs were randomly sampled and necropsied at 1, 2 and 6 days post infection (dpi). Fecal samples from the infected group were cultured for *Salmonella* to ensure the effectiveness of the experimental challenge. Furthermore, rectal temperature and clinical signs were daily recorded for each animal to observe the evolution of the infection. All procedures involving animals were performed in accordance with the European regulations regarding the protection of animals used for experimental and other scientific purposes.

3.1.2.2. Histopathology and immunohistochemistry

Samples of MLN from all experimental animals were fixed in 10% neutral buffered formalin for 24 h and embedded in paraffin-wax for histological processing. Afterwards, 5 μm tissue sections were routinely processed as

previously described [21], and stained with hematoxylin and eosin (H&E). Presence of bacteria in the tissue samples was demonstrated by using an anti-*Salmonella* polyclonal antibody raised by immunization of a New Zealand rabbit with a formalin fixed bacterial suspension. Quantification of tissue infiltration of macrophages was carried out by using a monoclonal antibody specific for porcine macrophages (clone 4E9/11) [22]. Immunohistochemical staining of formalin-fixed, paraffin-embedded sections of porcine MLN samples, subjected to heat-mediated antigen retrieval in 0.01 M citric acid, with *Salmonella* antiserum and 4E9 monoclonal antibody was performed by using the immunoperoxidase method as has been described elsewhere [21]. Neutrophils identify by morphology and immunolabeled macrophages were counted in 50 randomly selected high magnification fields (400×) in sections of two different MLN samples from each infected and control animal. Results were expressed as the mean number of cells per field.

3.1.2.3. Nucleic acids purification

Samples of MLN from control and infected animals were aseptically collected after necropsies and immediately frozen in liquid nitrogen for DNA and RNA isolation. Then, after treatment with RNAlater-ICE (Ambion), a volume of 0.6 ml of RLT buffer (Qiagen) was added per 30 mg of tissue followed by disruption in a rotor–stator homogenizer. DNA and RNA were isolated by using the AllPrep DNA/RNA/Protein Mini Kit (Qiagen) and eluted RNA was treated with RNase-Free DNase Set (Qiagen) according to manufacturer instructions. Afterwards, purified RNA and DNA were routinely precipitated with ethanol. RNA and DNA quality was checked by agarose gel electrophoresis before being quantified using a Nanodrop ND-1000 spectrophotometer (Thermo Scientific).

3.1.2.4. Quantitative real-time PCR

Real-time quantitative PCR (qPCR) technology was used to determine the relative expression of 42 immune-related genes along the time course of infection (1, 2 and 6 dpi). Total RNA (1.5 µg) from infected and control animals was reverse transcribed to cDNA using the iScript cDNA Synthesis kit (Biorad) in a total volume of 30 µl. cDNA solutions were diluted by adding 70 µl of UHQ water and stored at -20 °C. The qPCR assays were performed on an iQ5 Thermo Cycler (BioRad) using 96 well PCR plates. All samples were amplified in duplicate in the same PCR plate and plates were repeated at least twice. Twenty microliters qPCR reactions were prepared using 2 µl of cDNA as template and iQ SYBR® Green Supermix (BioRad) according to manufacturer's instructions. Final concentration of the primers in the PCR reactions was 0.4 µM. Primers (Table 1) were designed using Beacon Designer (Biosoft International) as previously described [19]. The qPCR conditions were as follows: 95 °C for 5 min, 35 cycles of 94 °C for 30 s, 57 °C for 30 s and 72 °C for 45 s. After amplification, a melting program was run to ensure correct amplification of the expected amplicons.

Table 1 - List of genes and primer sequences for quantitative PCR analysis.

Gene Name	Foward Primer (5' → 3')	Reverse Primer (5' → 3')	Accesion number
βActin	CAGGTCATCACCATCGGCAACG	GACAGCACCGTGTTGGCGTAGAGGT	U07786
CASP1	CTCTCCACAGGTTCACAATC	GAAGACGCAGGCTTAACTGG	NM_214162
CCL2	ACCAGCAGCAAGTGTCCTAAAG	GTCAGGCTTCAAGGCTTCGG	NM_214214
CCL3	TCTCGCCATCCTCCTCTG	TGGCTGCTGGTCTCAAAATA	AY643423
CCL4	CAGCACCAATGGGCTCAGA	TTCCGCACGGTGTATGTGA	EF107667
CCL5	CCAGCAGCAAGTGCTCCAT	ACACCTGGCGGTTCTTTCTG	NM_001129946.1
CCL28	AACATCACAGCAAGAGGAACAG	TGGCACAAAGGAACATTCACC	NM_001024695
CD11b	GCGAGGACTCCCACGGAACTC	GAAGATGGGGTGGTTTATGC	Y11618.1
CD14	ACCACCCTCAGACTCCGTAATG	TTGCGCCACTTTCAGTACCTT	EF051626
CD40	TGGTTTCCAGAGTCGGATGAG	ACAGGATCCCCAGCGTGAT	NM_214194.1
CD40L	CAACACCCACAGTTCCTCCAA	AGACTCCGCCCAAGTGAATG	AB040443.1

Table 1 – *Continued*

Gene Name	Foward Primer (5′ → 3′)	Reverse Primer (5′ → 3′)	Accesion number
CD209	CTGACTTGGCCCCTCCTTCT	GAGACTGGTGGATCCTGGAAAC	NM_001129972.1
CXCL2	GGATAGCACGCTGTACCATC	ACTGTCTCAATAAATAACAACCGAC	AY578786
CXCL8	TTCGATGCCAGTGCATAAATA	CTGTACAACCTTCTGCACCCA	M86923
Cyclophilin-A	CCTGAAGCATACGGGTCCT	AACTGGGAACCGTTTGTGTTG	AY266299
DEFB1	ACCGCCTCCTCCTTGTATTC	GGTGCCGATCTGTTTCATCT	NM_213838
DEFB2	CTGTCTGCCTCCTCTCTTCC	CAGGTCCCTTCAATCCTGTT	NM_214442
IFNγ	CAAAGCCATCAGTGAACTCATCA	TCTCTGGCCTTGGAACATAGTCT	X53085
IL1β	GGCCGCCAAGATATAACTGA	GGACCTCTGGGTATGGCTTTC	NM_214055
IL4	TTGCTGCCCCAGAGAAC	TGTCAAGTCCGCTCAGG	AY294020
IL5	TGGTGGCAGAGACCTTGACA	CCATCGCCTATCAGCAGAGTT	NM_214205.1
IL6	TGGCTACTGCCTTCCCTACC	CAGAGATTTTGCCGAGGATG	NM_214399
IL10	CAGATGGGCGACTTGTTG	ACAGGGCAGAAATTGATGAC	L20001
IL12p40	GGAGTATAAGAAGTACAGAGTGG	GATGTCCCTGATGAAGAAGC	U08317
IL13	AAGTGGCCCAGTTCGTAAAAGA	ACCCGTGGCGAAAAATCA	NM_213803.1
IL18	AGGGACATCAAGCCGTGTTT	CGGTCTGAGGTGCATTATCTGA	EU118362.1
IL23p19	GCTTGCAAAGGATCCACCAA	GGCTCCCCTGTGAAAATGTC	NM_001130236.1
MyD88	TGGTGGTGGTTGTCTCTGATGA	TGGAGAGAGGCTGAGTGCAA	NM_002468
NFκB1	CTCGCACAAGGAGACATGAA	ACTCAGCCGGAAGGCATTAT	DQ834921
NOD1	ACCGATCCAGTGAGCAGATA	AAGTCCACCAGCTCCATGAT	AB187219
NOD2	CCTTTTGAAGATGCTGCCTG	GATTCTCTGCCCCATCGTAG	NM_001105295
SELL	CGCTTCCCTTCAGTCGTAG	CCACACAGTCCTCCTTAGTC	NM_001112678
SLC11A1	CCAAAGCAGAGCAGAAC	GGTCCAGGTAAGCAATG	AF132037
TLR1	TGCTGGATGCTAACGGATGTC	AAGTGGTTTCAATGTTGTTCAAAGTC	AB219564
TLR2	TCACTTGTCTAACTTATCATCCTCTTG	TCAGCGAAGGTGTCATTATTGC	AB085935
TLR3	AGTAAATGAATCACCCTGCCTAGCA	GCCGTTGACAAAACACATAAGGACT	DQ266435
TLR4	GCCATCGCTGCTAACATCATC	CTCATACTCAAAGATACACCATCGG	AB188301
TLR5	CAGCGACCAAAACAGATTGA	TGCTCACCAGACAGACAACC	NM_001123202
TLR6	AACCTACTGTCATAAGCCTTCATTC	GTCTACCACAAATTCACTTTCTTCAG	AB085936
TLR7	TCAGTCAACCGCAAGTTCTG	GATGGATCTGTAGGGGAGCA	NM_001097434
TLR8	AAGACCACCACCAACTTAGCC	GACCCTCAGATTCTCATCCATCC	AB092975
TLR9	CACGACAGCCGAATAGCAC	GGGAACAGGGAGCAGAGC	AY859728
TLR10	CCTGTCCAACTGCCTCATTTG	CTAAGTGTTCTAAGGATGTGTTTCTG	AB219565
TNFα	CCTCTTCTCCTTCCTCCTG	CCTCGGCTTTGACATTGG	NM_214022

3.1.2.5. *Salmonella* quantification assay

TaqMan qPCR assays were used for quantifying the *S. typhimurium* load in MLN samples, following the method previously described by Park et al. [23]. DNA from the *Salmonella* strain employed in the experimental infection was extracted using DNeasy Blood & Tissue Kit (Qiagen) and subsequently diluted to final concentrations of $1.0x10^4$, $5.0x10^3$, $1.0x10^3$, $5.0x10^2$, $2.5x10^2$, $1.0x10^2$, $5.0x10^1$ and 0 genome equivalents (GE) per 1 µl. One genome equivalent of *S. typhimurium* corresponded to 5.46904 fg of DNA [23]. A 19-mer forward primer (5'GCGCACCTCAACATCTTTC-3'), a 22-mer reverse primer (5'-GGTCAAATAACCCACGTTCA-3') and a fluorogenic probe (FAM ATCATCGTCGACATGC MGB/NFQ) were used in the quantification assays. Each 25 µl PCR reaction contained 12.5 µl IQ Supermix 2X (Biorad), 0.4 µm of each primer, 0.2 µM probe, 1 µM MgCl2, 1µl DNA (at 800 ng/µl for porcine samples) and 10 µl UHQ water. PCR amplifications were performed on an iQ5 Thermo Cycler (Biorad) under the following conditions: 95 °C for 10 min and 35 cycles of 95 °C for 15 s and 60 °C for 1 min. Each MLN sample was tested by triplicate in three independent assays. Number of genome equivalents was deduced from the standard curve employing the quantification cycle (Cq) obtained for each sample. Results were shown as the number of genome equivalents of S. typhimurium per 800 ng of MLN DNA (GE/800 ng DNA).

3.1.2.6. Isolation of *S. typhimurium* from MLN samples

In order to verify the presence of live *S. typhimurium* in MLN samples, 1 g of tissue was drenched in 9 ml of buffered peptone water (Oxoid) and disrupted with sterile mortars and pestles. Tissue suspensions were transferred to sterile tubes and incubated at 37 °C with shaking at 200 rpm for 12 h. Afterwards, 10 µl of the resulting culture was streaked on XLD agar (Oxoid) plates and incubated at

37 °C for 24 h. The identification of the suspected colonies was confirmed by PCR assays. For this, 20 colonies with typical *Salmonella* morphology were collected from each plate, mixed in 300 µl of UHQ water and their DNA extracted by boiling. PCR was carried out in a final volume of 20 µl, containing 2 µl of DNA template, 400 nM of each primer, 200 nM of each dNTP, 2 mM MgCl2, 2 µl of 10X reaction buffer and 0.75 U Tth DNA polymerase (Biotools). Primers employed in this assay were the same used in the procedure of *S. typhimurium* quantification by TaqMan qPCR. PCR cycling protocol consisted of a denaturing step at 94 °C for 5 min, followed by 35 cycles of 94 °C for 30 s, 60 °C for 30 s, 72 °C for 30 s, and a final step of 6 min at 72 °C.

3.1.2.7. Data analysis

The relative gene expression was assessed by the $2^{-\Delta\Delta Cq}$ method [24] as previously described [19]. Afterwards, fold change values ($2^{-\Delta\Delta Cq}$) were standardized by a series of sequential corrections proposed by Willems et al. [25], which included log transformation, mean centering and autoscaling. A fold change of 1 denoted no change in gene expression. Values lower than 1 and higher than 1 denoted up and down-regulation, respectively. Standardized data were analyzed using the software SPSS 15.0 for Windows® (SPSS, Inc). Data were tested for normality and variance homogeneity by Shapiro–Wilk and Levene's tests, respectively. Those data assumed to be from a normal distribution and which within-group variances were constant across groups were analyzed by one-way ANOVA and Duncan post hoc test. Remaining data were analyzed by Kruskal–Wallis and Mann–Whitney tests. Differences in the rectal temperature among groups were assessed by ANOVA and Duncan post hoc test. Data from S. typhimurium quantification as well as neutrophil and macrophage count were analyzed by Kruskal–Wallis and Mann–Whitney tests. Spearman's rank

correlation test was used to examine the association among *S. typhimurium* load, neutrophil and macrophage count and gene expression. A p-value below 0.05 was considered statistically significant.

3.1.3. Results

3.1.3.1. Experimental infection

Animals experimentally infected were observed daily for development of clinical disease. The analysis of *S. typhimurium* fecal carriage revealed that all animals were positive after the bacterial challenge. In addition, infected pigs manifested clinical signs characterized as lethargy, weight loss and diarrhea. Rectal temperature changed significantly among groups (p = 0.000), fever began at 1 dpi (40.58±0.17) and peaked at 2 dpi (40.88±0.46 ∘C). However, at 6 dpi the rectal temperature declined to normal values (39.15±0.35 ∘C), not significantly different from those observed in control animals.

3.1.3.2. Histopathology and immunohistochemistry

Lymphadenitis, marked by a strong infiltration of inflammatory cells was observed at 2 dpi (Fig. 1A). Similar pathological alterations were observed at 1 and 6 dpi, although to a lesser extent than those seen at 2 dpi. Significant changes in neutrophil count were observed along the time course of the infection (p = 0.005). Thus, the number of neutrophils peaked at 2 dpi (Fig. 1C) and a broad infiltration of these cells around trabeculae was uncovered at this time point. Immunohistochemistry revealed that the presence of macrophages in MLN also changed significantly after *S. typhimurium* infection (p = 0.036). As shown in Fig. 1D, macrophages count peaked at 2 dpi, being predominantly found in lymph nodes capsule and within the T-cell area near trabeculae (Fig. 1B).

Immunohistochemistry was also carried out to verify the level of tissue invasion by *S. typhimurium*.
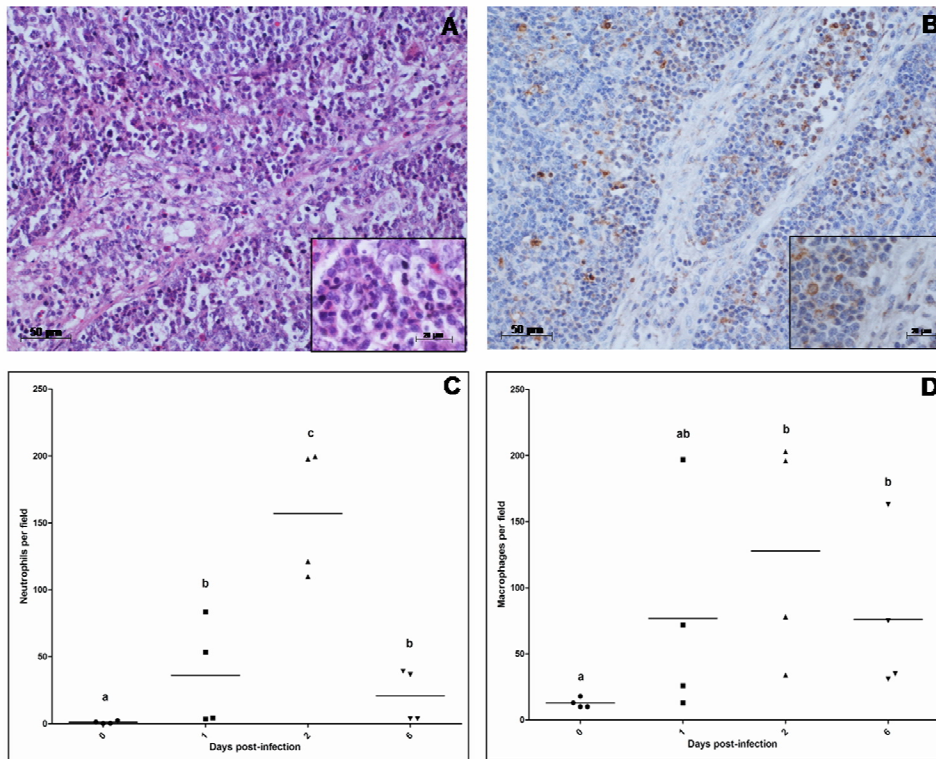
Figure 1. Histological analysis of MLN from *S. typhimurium* infected pigs. (A) Tissue-infiltrating phagocytes were visualized around trabeculae by H&E staining at 2 dpi. (B) 4E9/11 labeling shows the presence of macrophages within the lymph nodes T-cell area at 2 dpi. (C and D) Quantification of neutrophils and macrophages in tissue, respectively. Data are shown as the number of neutrophils or macrophages per microscope field. Different letters mean significant difference among groups ($p < 0.05$).

As shown in Fig. 2A–C, bacterial labeling was observed in the cytoplasm of mononuclear cells. In addition, infiltrated neutrophils were located in the diffuse lymphatic tissue around trabeculae. Again, our results demonstrated that labeled cells were more prevalent in lymph nodes at 2 dpi than in groups of animals infected at 1 and 6 dpi.
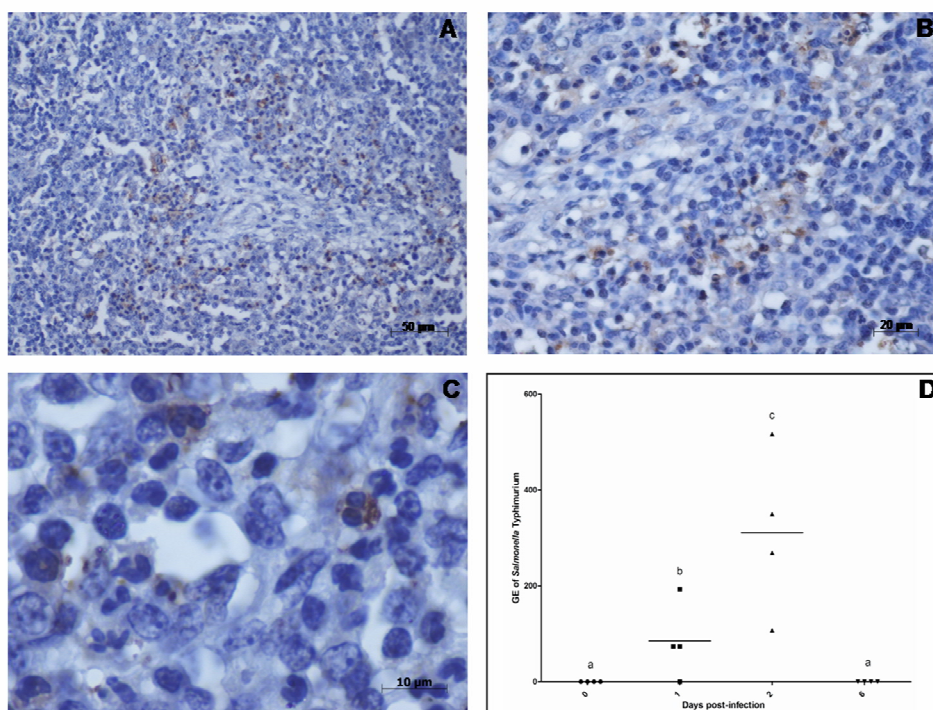
Figure 2. *S. typhimurium* labeling in MLN of infected pigs. (A) 100×, (B) 400× and (C) 1000×. (D) Quantification of *S. typhimurium* by TaqMan real-time PCR assay. Data are shown as the number of genome equivalents (GE) of *S. typhimurium* per 800 ng of MLN genomic DNA. Different letters mean significant difference among groups (p < 0.05).

3.1.3.3. Expression of immune-related genes during *S. typhimurium* infection

In order to evaluate the porcine MLN response to *S. typhimurium*, qPCR expression profiling was performed on a panel of 42 immune-related genes encoding pattern recognition receptors, immune cells markers, innate/inflammatory and T cell response mediators. Statistically significant expression changes were observed in 26 genes along the time course analyzed (Table 2). Overall, the higher number of differentially expressed genes was observed at 2 and 6 dpi (20 and 14 genes, respectively) whereas only 6 genes had

their expression changed at 1 dpi. Interestingly, all the significant observed changes at 6 dpi consisted in down-regulation of gene transcripts (Fig. 3).

Table 2 - Changes in gene expression relative to uninfected controls (0 dpi) in porcine MLN at 1, 2 and 6 days after *S. typhimurium* infection. Fold change (FC) values with the same letters above are not significantly different (p < 0.05).

Gene	0 dpi		1 dpi		2 dpi		6 dpi	
	F. change	SD	F. change	SD	F. change	SD	F. change	SD
CASP1	1.00a	0.19	0.76ab	0.19	1.53c	0.17	0.54b	0.09
CCL2	1.00a	0.14	1.17ab	0.42	1.23a	0.27	0.62b	0.12
CCL3	1.00	0.29	1.06	0.20	1.64	0.22	1.05	0.24
CCL4	1.00	0.26	1.35	0.22	1.23	0.22	0.77	0.24
CCL5	1.00	0.24	0.95	0.18	0.89	0.12	1.26	0.34
CCL28	1.00a	0.25	0.74ab	0.24	0.35b	0.08	1.16a	0.14
CD11b	1.00a	0.17	0.69ab	0.23	0.43b	0.11	0.76a	0.16
CD14	1.00	0.24	1.32	0.36	1.79	0.56	0.92	0.33
CD40	1.00	0.14	0.95	0.24	1.26	0.20	0.82	0.14
CD40L	1.00a	0.18	0.71b	0.04	0.53c	0.03	0.90ab	0.16
CD209	1.00a	0.28	0.72a	0.36	0.13b	0.02	0.46a	0.22
CXCL2	1.00a	0.20	3.11b	1.22	2.85b	1.17	1.34ab	0.55
CXCL8	1.00a	0.20	1.18a	0.15	2.84b	0.41	0.49c	0.09
DEFB1	1.00	0.38	2.06	0.49	0.78	0.24	1.70	0.81
DEFB2	1.00a	0.14	0.98a	0.26	2.52b	0.59	1.05a	0.41
IFNγ	1.00a	0.31	1.91ab	0.66	3.50b	1.32	1.08a	0.41
IL1β	1.00a	0.20	6.85b	3.36	10.07b	4.43	1.03a	0.28
IL4	1.00a	0.27	0.50ab	0.12	0.23b	0.05	0.42b	0.11
IL5	1.00	0.20	0.66	0.23	0.61	0.14	0.84	0.22
IL6	1.00	0.35	0.97	0.42	0.93	0.32	0.62	0.10
IL10	1.00ab	0.16	0.76bc	0.18	1.14a	0.15	0.63c	0.09
IL12p40	1.00	0.24	0.63	0.22	0.37	0.17	0.47	0.17
IL-13	1.00a	0.28	0.55ab	0.27	0.24b	0.03	0.39ab	0.17
IL-18	1.00a	0.08	0.76b	0.11	0.51c	0.10	0.53c	0.08
IL-23p19	1.00	0.19	0.93	0.22	0.94	0.06	0.84	0.24
MyD88	1.00	0.15	0.85	0.17	0.80	0.14	0.67	0.07
NFkB1	1.00a	0.17	1.00a	0.24	0.62b	0.16	0.61b	0.13

Table 2 – *Continued*

Gene	0 dpi		1 dpi		2 dpi		6 dpi	
	F. change	SD	F. change	SD	F. change	SD	F. Change	SD
NOD1	1.00	0.26	0.89	0.30	1.19	0.21	0.60	0.20
NOD2	1.00ab	0.24	1.16bc	0.32	1.70c	0.26	0.68[a]	0.17
SELL	1.00a	0.23	0.76ab	0.18	0.56b	0.10	0.58b	0.12
SLC11A1	1.00a	0.43	1.80a	0.58	8.40b	1.22	0.90[a]	0.37
TLR1	1.00	0.10	0.69	0.15	0.75	0.15	0.75	0.10
TLR2	1.00a	0.09	1.01a	0.27	1.07a	0.21	0.59b	0.08
TLR3	1.00a	0.07	0.73ab	0.18	0.51b	0.13	0.61b	0.16
TLR4	1.00a	0.06	0.93a	0.22	0.82ab	0.22	0.58b	0.08
TLR5	1.00	0.29	0.45	0.19	0.64	0.15	0.57	0.23
TLR6	1.00a	0.12	0.58b	0.10	0.75ab	0.15	0.73b	0.11
TLR7	1.00a	0.04	0.55b	0.08	0.58b	0.06	0.56b	0.08
TLR8	1.00a	0.12	0.78a	0.12	1.30b	0.08	0.77[a]	0.15
TLR9	1.00	0.22	1.22	0.22	0.97	0.21	1.11	0.16
TLR10	1.00	0.14	0.73	0.17	0.71	0.15	0.78	0.14
TNFα	1.00a	0.23	1.41a	0.36	1.14a	0.23	0.65b	0.09

Changes in expression of genes coding for different innate/inflammatory response mediators were uncovered mainly at 2 dpi. Thus, significant mRNA up-regulation of IL1β, CXCL2, CXCL8, CASP1, SLC11A and DEFB2 was observed at this time point, whereas expression of CCL28 and SELL resulted down-regulated. Moreover, mRNA expression of IL1β and CXCL2 were also significantly upregulated at 1 dpi whereas CXCL8 and CASP1 showed down-regulation at 6 dpi. In spite of the absence of significant difference in mRNA expression at 1 or 2 dpi compared to control, genes coding for TNFα and CCL2 showed downregulation at 6 dpi. Many of the proinflammatory mediators up-regulated at 1 and 2 dpi have their mRNA expression under the control of the transcription factor NFκB. However, NFκB mRNA expression was significantly downregulated at 2 and 6 dpi.
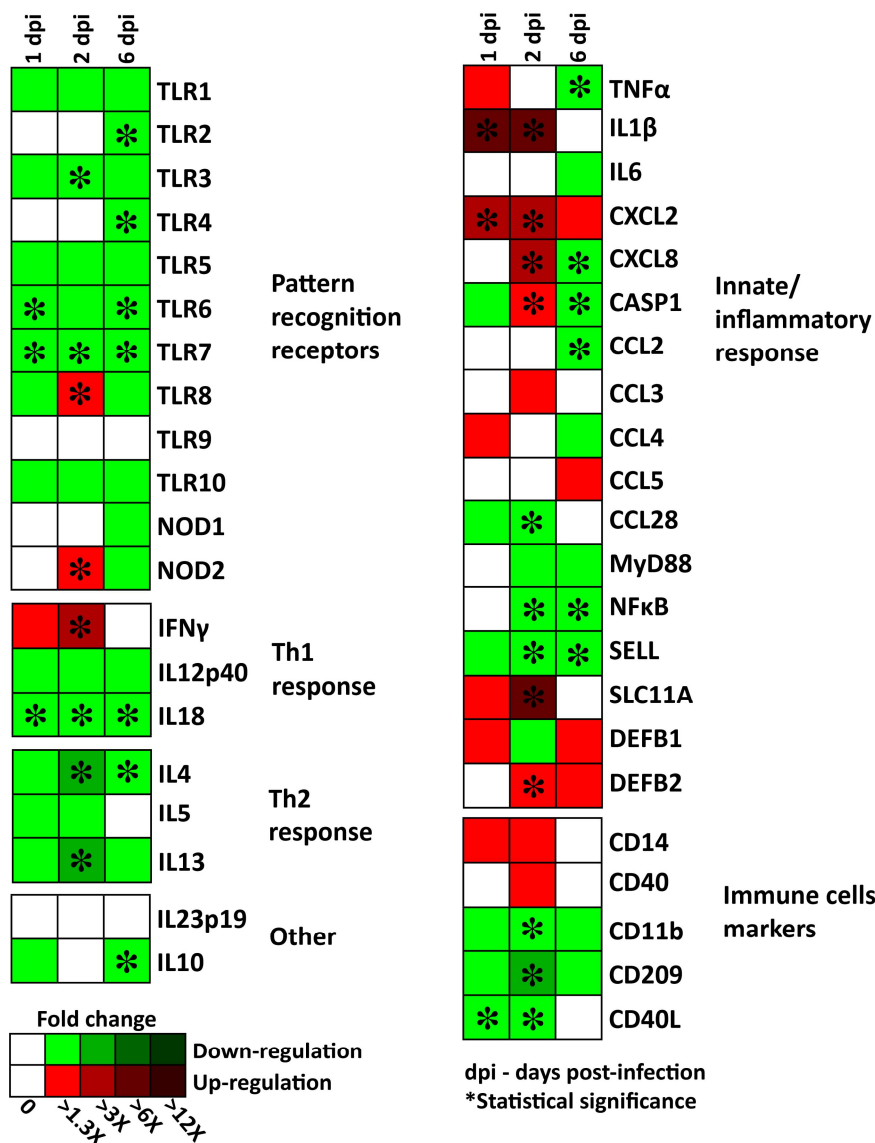
Figure 3. Expression of immune-related genes in MLN of pigs experimentally infected with *S. typhimurium* by qPCR. Data are shown as the fold change in gene expression in infected pigs compared to controls. Values lower than 1 were calculated as 1/fold change.

A down-regulation of genes coding for cytosolic and transmembrane pattern-recognition receptors (PRR) was asserted in our study, except for TLR8 and NOD2, which were up-regulated at 2 dpi.

Expression of genes coding for other cell surface proteins described as phenotype markers of swine immune cells was checked to estimate changes in MLN cellularity after infection. Changes in gene expression were not found out for CD14 or CD40. However, genes coding for CD11b and CD209 showed significant down-regulation at 2 dpi and CD40L at 1 and 2 dpi.

Finally, a diverse mRNA expression profile was observed among Th1 related genes. Although an up-regulation of IFNγ mRNA could be observed at 2 dpi, statistically significant changes in expression were not observed for IL12p40 and IL18 was down-regulated during the infection period studied. Concerning to Th2 response, down-regulation was verified for IL4 transcripts at 2 and 6 dpi and IL13 at 2 dpi. Furthermore, IL5 did not exhibited changes in expression after infection. Other genes encoding T cell costimulatory molecules were also studied. Thus, changes in IL23p19 mRNA expression were not detected and IL10 showed down-regulation at 6dpi.

3.1.3.4. Isolation and quantification of *S. typhimurium* in MLN of infected pigs

TaqMan real-time PCR technology was employed to quantify the presence of *S. typhimurium* in MLN at different times after infection. As shown in Fig. 2D, *S. typhimurium* burden changed significantly ($p = 0.005$) along the time course of infection. Pathogen load could be quantified at 1 dpi (85.4 ± 79.7 GE/800 ng DNA), peaked at 2 dpi (310.5 ± 171.1 GE/800 ng DNA), and decreased to unquantifiable levels at 6 dpi (0 GE/800 ng DNA), indicating the efficient clearance of most of bacteria from the tissue. Although *Salmonella* was not detected at 6 dpi or in one animal necropsied at 1 dpi, the screening by microbiological methods allowed us to determine the presence of live *S. typhimurium* in MLN of all animals belonging to groups 1, 2 and 6 dpi.

Nevertheless, the presence of bacteria was not detected in control animals, confirming their previously established *Salmonella* free status.

3.1.3.5. Conjunctive analysis of *S. typhimurium* burden, phagocyte count and immune-related genes expression

Spearman's rank correlation indicated a strong positive association between *Salmonella* burden and neutrophil count (Table 3 and Supplementary data file 1). Transcripts level of IFNγ, CXCL2, IL1β, CCL3 and SLC11a was also positively associated with the pathogen load in infected MLN, at a high level of significance ($p < 0.01$). Among genes which expression was negatively associated with *Salmonella* burden, TLR3, IL18, CD40L and CD11b could be highlighted. Expression of IFNγ, CXCL2 and IL1β was also positively associated with neutrophil count, whereas, mRNA levels of CD40L, IL4 and TLR3 were negatively associated. Differently from *Salmonella* load and neutrophil count, macrophages count showed a higher frequency of significant negative associations. Interleukin 13, CD209 and CD11b should be cited as genes which expression showed the most significant associations with macrophages count.

3.1.4. Discussion

MLN are important sites for the induction of immune response against invading pathogens in the gut [26]. In this work, we applied an *in vivo* approach to obtain insight into the response of porcine MLN to *S. typhimurium*. The effectiveness of the performed bacterial challenge was confirmed by the manifestation of typical clinical signs of pig salmonellosis by infected animals. Moreover, the presence of *S. typhimurium* in MLN at 1, 2 and 6 dpi was demonstrated employing microbiological and DNA based techniques.

Table 3 - Statistical association between mRNA gene expression and *S. typhimurium* load and neutrophil and macrophage count.

	S. Typhimurium	Neutrophils	Macrophages
S. Typhimurium	---	0.844**	0.517*
Neutrophils	0.844**	---	0.594*
Macrophages	0.517*	0.594*	---
CASP1	0.415	0.288	0.059
CCL2	0.452	0.226	-0.247
CCL3	0.645**	0.518*	0.252
CCL4	0.429	0.321	0.029
CCL5	-0.088	-0.129	0.112
CCL28	-0.311	-0.531	-0.392
CD11b	-0.712**	-0.571*	-0.710**
CD14	0.519*	0.550*	0.085
CD40	0.520*	0.338	0.091
CD40L	-0.731**	-0.759**	-0.616*
CD209	-0.473	-0.547*	-0.730**
CXCL2	0.630**	0.624**	0.181
CXCL8	0.605*	0.547*	0.203
DEFB1	0.006	-0.026	-0.110
DEFB2	0.541*	0.515*	0.423
IFNγ	0.668**	0.703**	0.202
IL1β	0.750**	0.650**	0.367
IL4	-0.622*	-0.720**	-0.706*
IL5	-0.595*	-0.432	-0.286
IL6	0.064	-0.100	-0.169
IL10	0.312	0.144	0.108
IL12p40	-0.515*	-0.297	-0.602*
IL13	-0.426	-0.397	-0.772**
IL18	-0.739**	-0.609*	-0.638**
IL23p19	0.035	-0.115	-0.286
MyD88	-0.155	-0.294	-0.392
NFκb	-0.225	-0.365	-0.511*
NOD1	0.290	0.053	0.066
NOD2	0.550*	0.391	0.230
SELL	-0.436	-0.591*	-0.549*
SLC11A1	0.727**	0.594*	0.424
TLR1	-0.201	-0.371	-0.418
TLR2	0.388	0.235	-0.236
TLR3	-0.771**	-0.624**	-0.521*
TLR4	0.033	0.029	-0.498*
TLR5	-0.163	-0.129	-0.395
TLR6	-0.304	-0.347	-0.355

Table 3 *Continued*

	S. Typhimurium	Neutrophils	Macrophages
TLR7	-0.415	-0.594*	-0.424
TLR8	0.429	0.365	0.186
TLR9	-0.040	-0.085	0.303
TLR10	-0.283	-0.521*	-0.408
TNFα	0.382	0.206	-0.222

Higher *S. typhimurium* loads were observed at 2 dpi, when a peak of corporal temperature was recorded and most of changes in gene expression were observed. In addition, histological analysis confirmed the existence of bacteria in the tissue and detected changes in MLN cellularity as a consequence of the infection.

Consistent with the latter, we observed that infection led to a strong infiltration of macrophages and neutrophils in MLN, which was highly correlated with *S. typhimurium* burden in the tissue. The recruitment of monocytes and neutrophils from blood to infected tissues is a requirement for controlling pathogens replication and ensuring host survival to infection [27]. L-Selectin (SELL), a glycoprotein constitutively expressed by porcine leucocytes [28], was down-regulated at 2 and 6 dpi. Negative correlations observed between the level of SELL transcripts and neutrophil/macrophage count in MLN confirms previous reports of SELL down-regulation by recruited monocytes [27] and neutrophils [29]. Chemokines are the main mediators involved in the recruitment and migration of leukocytes to and within tissues [30]. According with previously reported data [31,32], our experimental infection produced an up-regulation of chemokines in MLN. Moreover, significant correlations were observed between mRNA levels of CXCL8, CXCL2, and tissue neutrophil count. However, changes in expression of these chemokines were not significantly correlated to macrophages count. Interestingly, changes in expression of SLC11A1 showed positive

correlations with mRNA levels of most of pro-inflammatory genes, such as CXCL2, CXCL8, IFNγ, IL1β and CASP1 (Supplementary data file 1). SLC11A1 is an important innate host resistance factor to S. typhimurium, specially expressed in phagocytic cells, such as dendritic cells (DC) [33], macrophages and neutrophils [34]. In mice, the impact of SLC11A1 on the severity and outcome of *S. typhimurium* infection is determined by its influence on the speed and intensity of the host inflammatory response, facilitating the rapid activation of host defense [35]. In this work, we observed a strong up-regulation of SLC11A1 at 2 dpi and its expression was significantly correlated to the grade of tissue invasion by *Salmonella* and neutrophils infiltration. Consequently, this could indicate that regulation of SLC11A1 acts as a mechanism of orchestration of inflammatory response in MLN of *S. typhimurium* infected pigs, as has been previously reported in mice [33].

Herein, Salmonella infection resulted in downregulation of CD11b and its mRNA level was negatively correlated with pathogen burden as well as macrophages and neutrophils count in MLN. Differently from human, swine CD11b is only expressed by a subpopulation of granulocytes and lacks expression by monocytes and macrophages [36]. In addition, among the four DC subpopulations found throughout the porcine intestinal immune system, DC from Peyer's patches (PP) have been described as CD11b–, whereas DC in MLN are predominantly CD11b+ [37]. Previous reports highlight *S. typhimurium* transport from intestine to the draining MLN via PP DC as the most predominant penetration route in infection models [9,35,38]. Therefore, down-regulation of CD11b could be attributed to an increase in MLN of cells that do not express this cell marker such as macrophages, and probably DC from PP.

Activated caspase 1 (CASP1) contribute to the control of *Salmonella* infection by processing and maturating the pro-inflammatory cytokines IL1β and IL18 [39]. In this study, CASP1 exhibited up-regulation at 2 dpi, followed by down-

regulation at 6 dpi. However, its substrates showed a different expression pattern: IL1β was strongly upregulated at 1 and 2 dpi, whereas IL18 was down-regulated all along infection. In murine MLN and spleen, IL18 is the predominant CASP1 substrate that mediates resistance to oral *S. typhimurium* infection [40]. IL18 acts synergistically with IL12 in the induction of IFNγ production by antigen stimulated T cells in human and mice [41]. Nevertheless, we uncovered an increase of IFNγ expression, in spite of the absence of significant changes in IL12p40 regulation along infection. The lack of significant associations between mRNA levels of IL12p40/IL18 and IFNγ (Supplementary data file 1) could confirm the independence of IFNγ expression respect IL12p40 or IL18 regulation. Moreover, up-regulation of IFNγ could be explained by the fact that NK cells are important producers of this cytokine in pigs [41]. Together, these results might indicate that in porcine infections by *S. typhimurium*, IL18 and IL12 do not play the same role as in human and mice salmonellosis. It could also be inferred that repression of this cytokines is a mechanism whereby *Salmonella* may limit the protective cell-mediated immune response early in infection, as has been previously proposed [42].

Our results also evidenced a decrease in mRNA levels of genes coding for cytokines and receptors related to DC-T-cell interaction. CD40L expression is induced shortly after T-cell activation and represents an early activation marker of T lymphocytes [43]. Activated T cells enhance IL-12 production by interaction of their receptor ligand CD40L with CD40 on DCs or macrophages [44]. Since CD40L was down-regulated at 1 and 2 dpi, this could also be related to the expression profile uncovered for IL12p40. CD209 was also down-regulated at 2 dpi. This gene codes for a C-type lectin which mediates strong adhesion between DC to resting T cells and is essential in establishing the DC induced T cell proliferation [45]. Besides, it has been reported that CD209-driven interaction

between activated neutrophils and DC induce maturation of the latter and enable these cells to trigger an intense T cells proliferation and Th 1 polarization [46].

Since MLN underwent substantial changes in cellularity after infection, neutrophil extravasation primarily, downregulation CD40L and CD209 could be attributed to the infiltration of cells that do not express these molecules. However, the decrease in mRNA levels of IL12p40, which production is induced by activated T cells, as well as reports asserting the prevention of T cells activation as a strategy used by *Salmonella* to evade immune response [8] lead as to infer that this machinery could be employed by the bacteria in swine MLN infection.

TLRs and NODs function as sentinels of infection via recognition of pathogen-associated molecular patterns (PAMPs) and induction of appropriate innate and adaptive immune responses to invaders [47]. In this work, we found that except TLR-8 and NOD2, which were up-regulated at 2 dpi, most of the PRR were significantly down-regulated after *Salmonella* challenge. Rydstrom and Wick [30] relate that the absence of signaling through TLR4, TLR5 or both TLR4/5 simultaneously did not compromise phagocytes recruitment to PP and MLN. These authors inferred that such deficiency is probably compensated by recognition of bacterial ligands by other PRR. The occurrence of the TLR signaling at the very first moments of the bacterial challenge should not be excluded. According with both assumptions, we also observed an increase of phagocytes in MLN, in spite of repression of TLR2, TLR3, TLR4 TLR6 and TLR7.

Together, our results suggest a possible synergy between TLR8 and NOD2 in the recognition of *S. typhimurium* in pig infections. TLR8 and NOD2 are expressed by monocytes, macrophages and DC [48–50]. Yrlid et al. [51] state that the application of the agonistic TLR7/8 ligand R848 triggered a massive migration of intestinal DC into MLN. Intriguingly, our results revealed a highly significant correlation ($p < 0.01$) between mRNA levels of TLR8 and NOD2 (Supplementary

data file 1). Moreover, expression of none of these genes was correlated with macrophage or neutrophil count in MLN. Therefore, upregulation of NOD2 and TLR8 at 2 dpi could be attributed to the migration of *Salmonella* infected DC from intestine to MLN. The higher tissue pathogen load observed at 2dpi, in addition to previous reports asserting DC-carriage as the most important mechanism of *Salmonella* dissemination from gut to MLN [9,35,38], cooperate with this hypothesis.

Different methods were employed in this work to assure the presence of *Salmonella* in the tissue and elucidate its influence in immune response. Results revealed that the *Salmonella* burden in the tissue fluctuated during infection depending on host immune response. A coincident up-regulation of pro-inflammatory mediators and infiltration of phagocytes at 2 dpi reduced substantially the pathogen burden in MLN at 6 dpi. In spite of this, isolation of *S. typhimurium* from samples of pigs belonging to 6 dpi group revealed that the pathogen maintained itself in MLN. These findings are in agreement with published observations demonstrating that, after oral infection, *S. typhimurium* persists in myeloid cells in the MLN, despite host immune response [52].

In summary, our results sustain MLN as a vital barrier preventing systemic dissemination of *S. typhimurium* and controlling infection in pigs. According with our previously published proteomic data [53], the presence of *Salmonella* in these organs triggered the induction of innate immune response, marked by a substantial infiltration of phagocytes and up-regulation of pro-inflammatory genes. Such response resulted in a relevant decrease in pathogen burden, but host mechanisms were not able to eliminate *S. typhimurium* from tissue completely. Although porcine salmonellosis by *S. typhimurium* result in milder disease compared to mice, our results also lead us to infer that, in swine infections, *S. typhimurium* might interferes with the DC-T-cells interaction. This

strategy could be related to the maintenance of infected animals as bacterial carriers.

Acknowledgements

Appendix A. Supplementary data

Supplementary data associated with this article can be found, in the online version, at http://dx.doi.org/10.1016/j.cimid.2012.11.003.

References

[1] EFSA. The European union summary report on trends and sources of zoonoses, zoonotic agents and food-borne outbreaks in 2009. EFSA Journal 2011;9(3):2090.

[2] Wild PH, McEwan DG, Wagner S, Rogov VV, Brady NR, Richter B, et al. Phosphorylation of the autophagy receptor optineurin restricts *Salmonella* growth. Science 2011, http://dx.doi.org/10.1126/science.1205405.

[3] Boyen F, Haesebrouck F, Maes D, Van Immerseel F, Ducatelle R, Pasmans F. Non-typhoidal *Salmonella* infections in pigs: a closer look at epidemiology, pathogenesis and control. Veterinary Microbiology 2008;130:1–19.

[4] Callaway TR, Edrington TR, Anderson RC, Byrd JA, Nisbet DJ. Gastrointestinal microbial ecology and the safety of our food supply as related to *Salmonella*. Journal of Animal Science 2008;86:E163–72.

[5] Fosse J, Seegers H, Magras C. Prevalence and risk factors for bacterial food-borne zoonotic hazards in slaughter pigs: a review. Zoonoses and Public Health 2009;56:429–54.

[6] Wick MJ. Living in the danger zone: innate immunity to *Salmonella*. Current Opinion in Microbiology 2004;7:51–7.

[7] Eckmann L, Kagnoff MF. Cytokines in host defense against *Salmonella*. Microbes and Infection 2001;3:1191–200.

[8] Bueno SM, González PA, Schwebach JR, Kalergis AM. T cell immunity evasion by virulent *Salmonella enterica*. Immunology Letters 2007;111:14–20.

[9] Voedisch S, Koenecke C, David S, Herbrand H, Förster R, Rhen M, et al. Mesenteric lymph nodes confine dendritic cell-mediated dissemination of *Salmonella enterica* serovar Typhimurium and limit systemic disease in mice. Infection and Immunity 2009;77:3170–80.

[10] Veldhuizen EJA, Koomen I, Ultee T, van Dijk A, Haagsman HP. *Salmonella* serovar specific upregulation of porcine defensins 1 and 2 in a jejunal epithelial cell line. Veterinary Microbiology 2009;136:69–75.

[11] Ge S, Danino V, He Q, Hinton JCD, Granfors K. Microarray analysis of response of *Salmonella* during infection of HLA-B27- transfected human macrophage-like U937 cells. BMC Genomics 2010;11:456–68.

[12] Ciraci C, Tuggle CK, Wannemuehler MJ, Nettleton D, Lamont SJ. Unique genome-wide transcriptome profiles of chicken macrophages exposed to *Salmonella*-derived endotoxin. BMC Genomics 2010;11:545–55.

[13] Niewold TA, Veldhuizen EJA, van der Meulen J, Haagsman HP, de Wit AAC, Smits MA, et al. The early transcriptional response of pig small intestinal mucosa

to invasion by *Salmonella enterica* serovar typhimurium DT104. Molecular Immunology 2007;44:1316–22.

[14] Mastroeni P, Sheppard M. *Salmonella* infections in the mouse model: host resistance factors and *in vivo* dynamics of bacterial spread and distribution in the tissues. Microbes and Infection 2004;6(4):398–405.

[15] Liu X, Lu R, Xia Y, Sun J. Global analysis of the eukaryotic pathways and networks regulated by *Salmonella typhimurium* in mouse intestinal infection *in vivo*. BMC Genomics 2010;11:722–47.

[16] Bearson BL, Bearson SMD. Host specific differences alter the requirement for certain *Salmonella* genes during swine colonization. Veterinary Microbiology 2011, http://dx.doi.org/10.1016/j.vetmic.2010.12.026.

[17] Mittrücker HW, Kaufmann SHE. Immune response to infection with *Salmonella typhimurium* in mice. Journal of Leukocyte Biology 2000;67:457–63.

[18] Skjolaas KA, Burkey TE, Dritz S, Minton JE. Effects of *Salmonella enterica* serovar Typhimurium (ST) and Choleraesuis (SC) on chemokines and cytokine expression in swine ileum and jejuna epithelial cells. Veterinary Immunology and Immunopathology 2006;111: 199–209.

[19] Collado-Romero M, Arce C, Ramirez-Boo M, Carvajal A, Garrido JJ. Quantitative analysis of the immune response upon *Salmonella typhimurium* infection along the porcine intestinal gut. Veterinary Research 2010;41:23.

[20] Wang Y, Couture OP, Qu L, Uthe JJ, Bearson SMD, Kuhar D, et al. Analysis of porcine transcriptional response to *Salmonella enterica* serovar Choleraesuis suggests novel targets of NF_B are activated in the mesenteric lymph node. BMC Genomics 2008;9:437.

[21] Yubero N, Jimenez-Marín A, Barbancho M, Garrido JJ. Two cDNAs coding for the porcine CD51 (_V) integrin subunit: cloning, expression analysis, adhesion assays and chromosomal localization. Gene 2011, http://dx.doi.org/10.1016/j.gene.2011.04.006.

[22] Bullido R, Gomez del Moral M, Alonso F, Ezquerra A, Zapata A, Sánchez C, et al. Monoclonal antibodies specific for porcine monocytes/macrophages: macrophage heterogeneity in the pig evidenced by the expression of surface antigens. Tissue Antigens 1997;49:403–13.

[23] Park HJ, Kim HJ, Park SH, Shin EG, Kim JH, Kim HY. Direct and quantitative analysis of *Salmonella enterica* serovar Typhimurium using real-time PCR from artificially contaminated chicken meat. Journal of Microbiology and Biotechnology 2008;18:1453–8.

[24] Livak KJ, Schmittgen TD. Analysis of relative gene expression data using real-time quantitative PCR and the 2−__CT method. Methods 2001;25:402–8.

[25] Willems E, Leyns L, Vandesompele J. Standardization of real-time PCR gene expression data from independent biological replicates. Analytical Biochemistry 2008;379:127–9.

[26] Kwa SF, Beverley P, Smith AL. Peyer's patches are required for the induction of rapid Th1 responses in the gut and mesenteric lymph nodes during an enteric infection. Journal of Immunology 2006;176:7533–41.

[27] Rydström A, Wick MJ. Monocyte recruitment, activation, and function in the gut-associated lymphoid tissue during oral *Salmonella* infection. Journal of Immunology 2007;178:5789–801.

[28] Piriou-Guzylack L, Salmon H. Membrane markers of the immune cells in swine: an update. Veterinary Research 2008;39:54.

[29] Burdon PCE, Martin C, Rankin SM. The CXC chemokine MIP-2 stimulates neutrophil mobilization from the rat bone marrow in a CD49d-dependent manner. Blood 2005;105:2543–8.

[30] Rydström A, Wick MJ. Monocyte and neutrophil recruitment during oral *Salmonella* infection is driven by MyD88-derived chemokines. European Journal of Immunology 2009;39:3019–30.

[31] Wang Y, Qu L, Uthe JJ, Bearson SMD, Kuhar D, Lunney JK, et al. Global transcriptional response of porcine mesenteric lymph nodes to *Salmonella enterica* serovar Typhimurium. Genomics 2007;90:72–84.

[32] Uthe JJ, Royaee A, Lunney JK, Stabel TJ, Zhao SH, Tuggle CK, et al. Porcine differential gene expression in response to *Salmonella enterica* serovars Choleraesuis and Typhimurium. Molecular Immunology 2007;44:2900–14.

[33] Valdez Y, Diehl GE, Vallance BA, Grassl GA, Guttman JA, Brown NF, et al. Nramp1 expression by dendritic cells modulates inflammatory responses during *Salmonella typhimurium* infection. Cellular Microbiology 2008;10:1646–61.

[34] Wu H, Cheng D, Wang L. Association of polymorphisms of Nramp1 gene with immune function and production performance of large white pig. Journal of Genetics and Genomics 2008;35:91–5.

[35] Halle S, Bumann D, Herbrand H, Willer Y, Dahne S, Forster R, et al. Solitary intestinal lymphoid tissue provides a productive port of entry for *Salmonella enterica* serovar Typhimurium. Infection and Immunity 2007;75:1577–85.

[36] Domínguez J, Alvarez B, Alonso F, Thacker E, Haverson K, McCullough K, et al. Workshop studies on monoclonal antibodies in the myeloid panel with CD11 specificity. Veterinary Immunology and Immunopathology 2001;80:111–9.

[37] Bimczok D, Sowa EN, Faber-Zuschratter H, Pabst R, Rothkötter H-J. Site-specific expression of CD11b and SIRPa (CD172a) on dendritic cells: implications for their migration patterns in the gut immune system. European Journal of Immunology 2005;35:1418–27.

[38] Tam MA, Rydström A, Sundquist M, Wick MJ. Early cellular responses to *Salmonella* infection: dendritic cells, monocytes, and more. Immunological Reviews 2008;225:140–62.

[39] Fantuzzi G, Dinarello CA. Interleukin-18 and interleukin-1 beta: two cytokine substrates for ICE (caspase-1). Journal of Clinical Immunology 1999;19:1–11.

[40] Raupach B, Peuschel SK, Monack DM, Zychlinsky A. Caspase-1- mediated activation of interleukin-1_ (IL-1_) and IL-18 contributes to innate immune defenses against *Salmonella enterica* serovar Typhimurium infection. Infection and Immunity 2006;74:4922–6.

[41] Domeika K, Berg M, Eloranta ML, Alm GV. Porcine interleukin-12 fusion protein and interleukin-18 in combination induce interferon-γ production in porcine natural killer and T cells. Veterinary Immunology and Immunopathology 2002;86:11–21.

[42] Elhofy A, Marriott I, Bost KL. *Salmonella* infection does not increase expression and activity of the high affinity IL-12 receptor. Journal of Immunology 2000;165:3324–32.

[43] Daoussis D, Andonopoulos AP, Liossis SNC. Targeting CD40L: a promising therapeutic approach. Clinical and Diagnostic Laboratory Immunology 2004;11:635–41.

[44] Lyakh L, Trinchieri G, Provezza L, Carra G, Gerosa F. Regulation of interleukin-12/interleukin-23 production and the T-helper 17 response in humans. Immunological Reviews 2008;226:112–31.

[45] Geijtenbeek TBH, Torensma R, van Vliet SJ, van Duijnhoven GCF, Adema GJ, van Kooyk Y, et al. Identification of DC-SIGN, a novel cendritic cell–specific ICAM-3 receptor that supports primary immune responses. Cell 2000;100:575–85.

[46] Tsuda M, Inaba M, Sakaguchi Y, Fukui J, Ueda Y, Omae M, et al. Activation of granulocytes by direct interaction with dendritic cells. Clinical and Experimental Immunology 2007;150:322–31.

[47] Albiger B, Dahlberg S, Henriques-Normark B, Normark S. Role of the innate immune system in host defence against bacterial infections: focus on the Toll-like receptors. Journal of Internal Medicine 2007;261:511–28.

[48] Delbridge LM, O'Riordan MXD. Innate recognition of intracellular bacteria. Current Opinion in Immunology 2007;19:10–6.

[49] Gorden KB, Gorski KS, Gibson SJ, Kedl RM, Kieper WC, Qiu X, et al. agonists reveal functional differences between human TLR7 and TLR8. Journal of Immunology 2005;174:1259–68.

[50] Tohno M, Ueda W, Azuma Y, Shimazu T, Katoh S, Wang JM, et al. Molecular cloning and functional characterization of porcine nucleotide-binding oligomerization domain-2 (NOD2). Molecular Immunology 2008;45:194–203.

[51] Yrlid U, Milling SWF, Miller JL, Cartland S, Jenkins CD, MacPherson GG. Regulation of intestinal dendritic cell migration and activation by plasmacytoid dendritic cells, TNF-_ and type 1 IFNs after feeding a TLR7/8 ligand. Journal of Immunology 2006;176:5205–12.

[52] Monack DM, Bouley DM, Falkow S. *Salmonella typhimurium* persists within macrophages in the mesenteric lymph nodes of chronically infected Nramp1+/+ mice and can be reactivated by IFNγ neutralization. Journal of Experimental Medicine 2004;199:231–41.

[53] Martins RP, Collado-Romero M, Martínez-Gomáriz M, Carvajal A, Gil C, Lucena C, et al. Proteomic analysis of porcine mesenteric lymphnodes after *Salmonella typhimurium* infection. Journal of Proteomics 2012;75:4457–70.

3.2 Proteomic analysis of porcine mesenteric lymph-nodes after *Salmonella typhimurium* infection

Rodrigo Prado Martins[a], Melania Collado-Romero[a], Montserrat Martínez-Gomáriz [b], Ana Carvajal [c], Concepción Gil [b], Concepción Lucena [a], Ángela Moreno[a], Juan J. Garrido [a]

[a]Grupo de Genómica y Mejora Animal, Departamento de Genética, Universidad de Córdoba, Campus de Rabanales, 14071 Córdoba, Spain

[b]Unidad de Proteómica, Universidad Complutense de Madrid—Parque Científico de Madrid, 28040 Madrid, Spain

[c]Departamento de Sanidad Animal, Facultad de Veterinaria, Universidad de León, 24071, León, Spain

Abstract

In this study we employed for the first time an *in vivo* approach coupled to DIGE-based proteomics to explore the response of porcine mesenteric lymph nodes (MLN) to *Salmonella typhimurium* infection. MLN samples were collected from four control and twelve infected pigs (at 1, 2 and 6 days post infection) for histological analysis, protein and RNA purification. Afterwards, expressed proteins were screened by differential in gel analysis and data were analyzed by bioinformatic tools to generate interaction networks, and identify enriched signaling pathways and biological annotations. *S. typhimurium* labeling in tissue and phagocyte infiltration were analyzed by immunohistochemistry and RNA was employed to determine the relative expression of immune-related genes by quantitative RNA analysis. The proteome response of porcine MLN to infection was associated to the induction of processes such as phagocyte infiltration, cytoskeleton remodeling and pyroptosis. Moreover, our results suggest that *S. typhimurium* antigens are cross-presented via MHC-I in a proteasome-dependent manner in porcine MLN. Since pathogen burden in tissue was noticeably reduced at the end of the time course, we infer that host innate and adaptive immunity act in association in MLN to control *S. typhimurium* dissemination in swine infections.

Keywords: Pig, *Salmonella typhimurium,* Mesenteric lymph nodes, DIGE, Pyroptosis, Cross-presentation

3.2.1 Introduction

European pig herd is acknowledged as the second largest in the world, taking charge of the production of the most consumed meat in Europe [1]. Among the wide range of hazards transmitted to humans by the consumption of pork or pork products, *Salmonella* is considered a major health threat worldwide [2,3]. According to the European Food Safety Authority (EFSA), *Salmonella* is the most frequently reported cause of food-borne outbreaks in the European Union (EU) [4]. Besides, it is supposed that approximately 30% of the human salmonellosis cases are caused by *Salmonella enterica* serovar Typhimurium (herein, *S. typhimurium*) from pork or pork products [2]. In spite of extensive contributions exploring the murine salmonellosis, the pathogenesis of pig infections with broad host range serotypes of *Salmonella* was largely neglected until recently [5]. Pigs are typically asymptomatic carriers of *S. typhimurium* and this commensal-like state establishes a significant reservoir for *Salmonella* contamination of food during harvest and processing [6]. Although the persistence of *Salmonella* in gut-associated lymph nodes of infected pigs has been previously reported, the extraintestinal part of a *S. typhimurium* infection in swine is not well-documented [5]. A recent report demonstrated that the prevalence of *Salmonella* in the lymph nodes of slaughter pigs ranged from 0%to 39.6% in EU, being infected pigs the dominant route of transmission in countries with high *Salmonella* prevalence [4]. Therefore, a thorough knowledge of how *S. typhimurium* interacts with the porcine lymphoid organs and consequently maintains itself in infected hosts consists in an essential step for the development of efficient control measures aiming to protect our food supply in the farm-fork process. Infection induces changes in mRNA and protein expression profiles of host cells. Basing on this, comparative proteome analyses are often used to

generate more detailed understanding of molecular mechanisms behind diseases [7]. In fact, *in vivo* models combined with proteomic technological advances represent unprecedented means of characterizing host–pathogen interactions [8]. This approach enables a systematic identification and classification of host proteins involved in infection, providing new targets for disease prevention and treatment strategies [9]. For these reasons, in this study we employed a model of *in vivo* experimental infection followed by DIGE proteomics and bioinformatic data analysis to elucidate the molecular mechanisms undergone by swine porcine mesenteric lymph nodes (MLN) upon *S. typhimurium* infection.

3.2.2 Material and methods

3.2.2.1. *In vivo Salmonella* infection and tissue sampling

The experimental infection design was described elsewhere [10]. Briefly, sixteen weaned piglets of approximately four weeks of age and fecal-negative for *Salmonella* were randomly allocated to control (4 piglets) or infected groups (12 piglets). Control (0 day post-infection — dpi) pigs were necropsied 2 h before the experimental infection and those ones belonging to the infected groups were orally challenged with 108 cfu of *S. typhimurium* phagetype DT104. Afterwards, infected pigs were randomly sampled and necropsied at 1, 2 and 6 dpi (four animals at each time point). Finally, MLN from all experimental animals were collected after necropsies and immediately frozen in liquid nitrogen for protein isolation or fixed in 10% neutral buffered formalin for histological processing. All procedures involving animals were performed in accordance with the European regulations regarding the protection of animals used for experimental and other scientific purposes. Piglets were housed in experimental isolation facilities of the University of León (Spain). Animal care and procedures were in accordance with

the guidelines of the Good Experimental Practices (GEP), under the supervision of the Ethical and Animal Welfare Committee of the University of León (Spain).

3.2.2.2. Protein extraction and labeling

Samples were homogenized on ice in a proportion of 1.5 mL of buffer per 100 mg of tissue using a glass tissue-lyser. Lysis buffer was composed of 7 M urea, 2 M thiourea, 4% w/v CHAPS, 0.5 mM PMSF and protease inhibitor cocktail (Roche, Basel, Switzerland). After sonication (3×20 s pulses on ice, with cooling intervals of 2 min in between) and centrifugation (14,000 g for 10 min, at 4 °C), supernatants were precipitated with 2D-Clean-Up Kit (GE Healthcare, Buckinghamshire, UK) and resuspended in 100 μL of DIGE buffer (10mMTris, 7 Murea, 2 M thiourea, 2% w/v CHAPS). Subsequently, protein concentration was determined using Bradford Protein Assay (Bio-Rad, Hercules, CA, USA). CyDye labeling was performed following the manufacturer's instructions (GE Healthcare). Briefly, 50 μg of protein per sample was minimally labeled with 400 pmol of Cy3 or Cy5 fluorochromes (dissolved in 99.8% DMF) for 30min on ice in the dark. Then, reactions were quenched with lysine (10mM/50 μg of protein). An internal standard, which was included in all DIGE gels, was prepared by pooling equal amounts of protein from each biological sample and labelling with Cy2 dye in the same conditions of separate samples.

3.2.2.3. DIGE

Sixteen individual samples were randomly distributed across eight DIGE gels. To produce unbiased results and minimize system variation, half of samples from each time point were labeled with Cy5 and the remaining ones with Cy3 (for details, see Supplementary data file 1). For each gel, the same amount of internal standard, Cy3 and Cy5 labeled samples (50 μg each) was pooled and diluted with

an equivalent volume of rehydration buffer (7 M urea, 2 M thiourea, 4% w/v CHAPS, 100mMDTT and 2% pharmalytes, pH 3–11). Afterwards, pools were loaded into 24 cm 3–11 non-linear pH range IPG strips (GE Healthcare) by cup loading. Strips were previously hydrated for 8 h with 7 M urea, 2 M thiourea, 4% w/v CHAPS, 2% pharmalytes 3–11, DeStreak 100mM (GE Healthcare) and blue bromophenol traces. IEF was performed with an IPGphor II unit (GE Healthcare) at 20 °C. Before second dimension, stripswere equilibrated first for 12 min in reducing solution (6M urea, 100mM Tris–HCI pH 8.0, 30% v/v glycerol, 2% w/v SDS and 2% w/v DTT) and secondly for 5min in alkylating solution (6M urea, 100mM Tris–HCI pH 8.0, 30% v/v glycerol, 2% w/v SDS and 2.5% w/v iodoacetamide). IPG strips were subsequently loaded onto homogeneous 12% T, 2.6% C (piperazine diacrylamide) polyacrylamide gels and proteins were separated by electrophoresis at 20 °C, 15W/gel, using Ettan-DALTsix electrophoresis unit (GE Healthcare).

3.2.2.4. Image acquisition and DIGE analysis

Proteins were visualized using a Typhoon 9400 scanner (GE Healthcare) with CyDye filters. For the Cy3, Cy5 and Cy2 image acquisition, the 532 nm/580 nm, 633 nm/670 nm and 488 nm/520 nm excitation/emission wavelengths were used, respectively, and 100 µm as pixel size. Image cropping and filtering were carried out with Image Quant v.5.1 software (GE Healthcare). Analyses for detection of different abundance between spots from different replicates were performed with the DIA (differential in gel analysis) module of the DeCyder 6.5 package (GE Healthcare). Inter-gel variability was corrected by matching and normalization of the internal standard spot maps using the Biological Variance Analysis (BVA) module. The internal standard image gel with the greatest number of spots was used as a master gel. BVA module was also employed for

comparative cross-gel statistical analyses, basing on spot normalized volume ratio (Cy3:Cy2 and Cy5:Cy2). Variation in abundance among all experimental conditions was accessed by One-way ANOVA. For paired comparisons, independent Student's t-test was carried out. Spots present in at least 85% of gels and exhibiting changes in abundancewith a p-value less than 0.05 were considered as differentially abundant spots.

3.2.2.5. Mass spectrometry and protein identification

Differentially abundant spots were excised from gels for subsequent in-gel reduction, alkylation and digestion with trypsin [11]. Briefly, spots were washed twice with water, shrunk for 15min with 100% acetonitrile and dried in a Savant SpeedVac for 30min. Samples were then reduced with 10mM DTT in 25mM ammonium bicarbonate (56 °C, 30min) and alkylated with 55mM iodoacetamide in 25mM ammonium bicarbonate for 15 min in the dark. Finally, samples were digested overnight with 12.5 ng/μL sequencing-grade trypsin (Roche) in 25mMammoniumbicarbonate (pH8.5) at 37 °C. After digestion, the supernatant was collected, and 1 μL was spotted onto a MALDI target plate and allowed to air-dry at room temperature. Matrix (0.4 μL of a 3mg/mL) solution of α-cyano-4-hydroxy-cinnamic acid (CHCA; Sigma-Aldrich, St. Louis, USA) in 50%acetonitrilewas added to the dried peptide digest spots and allowed again to air-dry at room temperature. MALDI-TOF MS analysis was performed in a 4800 Proteomics Analyzer MALDITOF/TOF mass spectrometer (Applied Biosystems, Framingham, MA, USA) operated in positive reflector mode, with an accelerating voltage of 20,000 V. All mass spectra were calibrated internally using peptides from the autodigestion of trypsin. MALDI-TOF MS analysis produced peptide mass fingerprints and the peptides observed were collected and represented as a list of monoisotopic molecular weights with an S/N greater than 15. The suitable

precursors for MS/MS sequencing analyses were selected and fragmentation was carried out using the CID on (atmospheric gas was used) 1 KV ion reflector mode and precursor mass Windows±5 Da. The plate model and default calibration were optimized for the MS/MS spectra processing. For protein identification, the UniProtKB/Swiss-Prot Data Base was searched in batch mode using GPS Explorer v3.6 software (Applied Biosystems) with a licensed version 2.1 of MASCOT. Search parameters were: carbamidomethyl cystein as fixed modification, methionine oxidation as variable modification, peptide mass tolerance 50–100 ppm, peptide charge state +1, one missed trypsin cleavage site and MS/MS fragments tolerance 0.3 Da. The parameters for the combined search (peptide mass fingerprint and MS/MS spectra) were the same described above. In all protein identification, the probability scores were greater than the score fixed by MASCOT as significant with a p-value less than 0.05.

3.2.2.6. Systems biology analysis

Protein data sets were uploaded into ArrayUnlock (AU, Integromics, Granada, Spain) and Ingenuity Pathway Analysis (IPA, Ingenuity Systems, www.ingenuity.com) for bioinformatic analysis. The AU "Biological Enrichment" tool was used to find biological annotations associated to the list of differently abundant proteins. To this end, AU applies a statistical test based on the hypergeometric distribution to compute p-values and the false discovery ratio (FDR) of Benjamini and Hochberg to correct them. GO terms and KEGG pathways were chosen as annotations to be evaluated in the analysis (refer to AU manual for detailed information: http://www.integromics.com). Protein interaction networks were automatically generated, ranked by score and depicted on IPA as follows: each node in the network diagram represented a protein and its relationship with other molecules was represented by a line (solid and dotted

lines represent direct and indirect association respectively). Nodes with a colored background were input proteins detected in this study while non-colored nodes were proteins inserted by IPA based upon the Ingenuity Knowledge Base to produce a highly connected network. Fisher's exact test was used to calculate a p-value determining the probability that each biological function assigned to the data set was due to change alone. Score estimated the probability that a collection of proteins equal to or greater than the number in a network could be achieved by chance alone. Scores of 3 or higher were considered to have a 99.9% confidence of not being generated by random chance alone. IPA Knowledge Base was used as a reference set for statistical analysis of enriched functions/pathways.

3.2.2.7. Western blot analysis

Equivalent amounts of total protein (30 μg) from control and infected animals were electrophoretically fractionated in 12% (w/v) SDS-PAGE gels and transferred onto a PVDF membrane (Millipore, Bedford, MA, USA). After blockage with 5% skimmed milk in TBS-T (10mMTris pH 7.4, 150mMNaCl, 0.05%Tween-20) for 1 h at room temperature, membrane was incubated overnight at 4 °C with some of the following antibodies: antivimentin, clone V9 monoclonal antibody (Chemicon/Millipore, Billerica,MA, USA); rabbit polyclonal to FKBP52 (ab97306, Abcam, Cambridge, UK); anti-14-3-3 β (κ-19) rabbit polyclonal antibody (Santa Cruz Biotechnologies, Santa Cruz, CA, USA) and anti-L plastin polyclonal antibody (kindly gifted by Dr. Francisco Rivero from University of Hull, UK). Secondary peroxidase-linked antirabbit or anti-mouse antibodies were used to generate immunocomplexes that were visualized with an enhanced chemiluminescence reagent (Chemiluminescent HRP substrate, Millipore). Membranes were scanned in a FLA-5100 imager (Fujifilm, Tokyo, Japan) and signal intensity was determined

using Multigauge software (Fujifilm, Tokyo, Japan). Student's t test was conducted between control and infected groups using SPSS 15.0 for Windows (SPSS Inc, Chicago, IL, USA). A p-value below 0.05 was considered statistically significant. To confirm equal sample loading, allmembranes were reblotted with anti-GAPDH monoclonal antibody (GenScript, Picastaway, NJ, USA).

3.2.2.8. Histological analysis

Paraffin sections (5 µm) of formalin fixed sampleswere routinely processed and stained with hematoxylin and eosin (H&E). For immunohistochemistry, heat-mediated antigen retrieval in 0.01M citric acid and labeling were performed as described elsewhere [12], employing the anti-vimentin monoclonal antibody (Chemicon/Millipore), a monoclonal antibody specific for porcine macrophages (clone 4E9/11) [13] and a rabbit antiserum against the somatic antigen of *S. typhimurium*.

3.3.2.9. Real-time quantitative PCR

Real-time quantitative PCR (qPCR) technology was used to determine the relative expression of the genes coding for CASP1, IL1β, CXCL2, CXCL8 and IFNγ. RNA extractions, cDNA synthesis and qPCR assays were carried out according to Collado-Romero et al. [10]. Primer pairs used for amplifications can be found as supporting information (Supplementary data file 2). The relative gene expression was assessed by the $2^{-\Delta\Delta Cq}$ method [14] using cyclophilin-A and beta-actin as reference genes [15]. Afterwards, fold change values were standardized as proposed by Willems et al. [16]. Fold changes of 1 denoted no change in gene expression. Values lower than 1 and higher than 1 denoted down and up-regulation respectively. Standardized data were analyzed by Kruskal–Wallis and Mann–Whitney tests using the software SPSS 15.0 for Windows (SPSS Inc).

3.2.3 Results

3.2.3.1. Experimental infection and histological analysis

Clinical signs characterized as fever, lethargy, weight loss and diarrhea were observed in infected pigs. Although symptoms peaked at 2 dpi, a clinical improvement of disease was noticed along the time of infection, since animals showed normal feces and corporal temperature at 6 dpi. Lymphadenitis marked by a strong infiltration of neutrophils and macrophages was observed in infected animals (Fig. 1A, B). Besides, immunohistochemistry assays confirmed the presence of *S. typhimurium* in MLN after infection. In the same way of the clinical profile observed, *Salmonella* was more evident at 2 dpi and poorly detected at 6 dpi (Fig. 1C–F). Labeling of *S. typhimurium* antigens was observed in the cytoplasm of mononuclear cells and neutrophils located mainly in the diffuse lymphatic tissue around trabeculae.

3.2.3.2. DIGE analysis and identification of differently abundant proteins

DIGE approach was employed to detect changes in the proteome of porcine MLN after oral infection with *S. typhimurium*. Differential in gel analysis uncovered 54 spots exhibiting significant abundance changes as a consequence of the bacterial challenge (Fig. 2A). Paired analyses between infected and control groups detected 16, 43 and 16 differently changed spots at 1, 2 and 6 dpi, respectively. Furthermore, a predominance of spots that were significantly more abundant in relation to controls was observed in all infected groups (Fig. 2B). Among the screened spots, 48 could be identified and corresponded to 38 unique proteins (Table 1, see Additional information). In some cases multiple spots were identified as the same protein, thus indicating the occurrence of post-translational modifications or different isoforms.
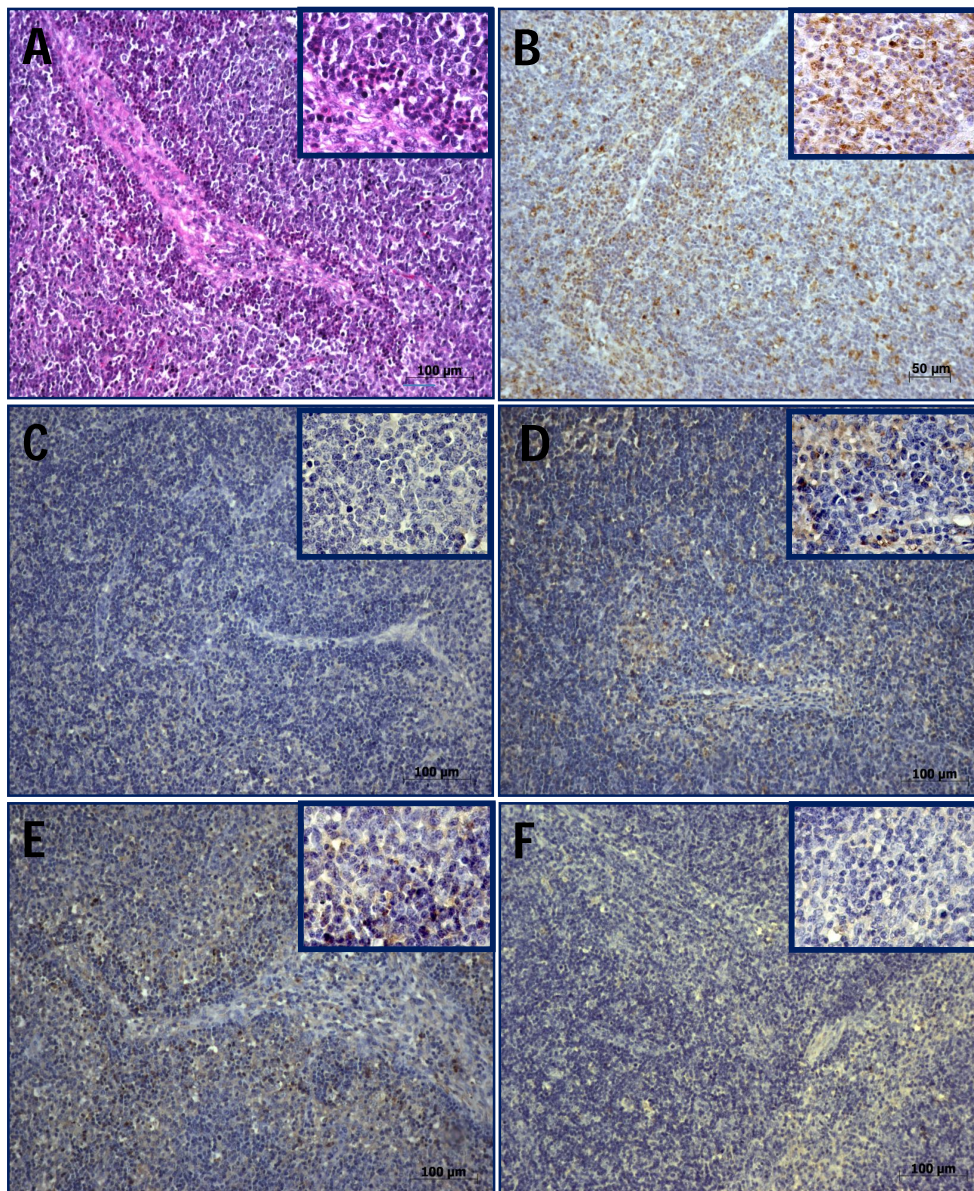
Figure 1 – Histological analysis of porcine mesenteric lymph nodes (MLN) upon *Salmonella typhimurium* infection. (A) H&E staining demonstrates an evident phagocyte infiltration around trabeculae at 2 days post infection (dpi). (B) Infiltration of macrophages after infection was also observed by immunohistochemistry. (C–F) *S. typhimurium* labeling at 0 (C), 1(D), 2 (E) and 6 (F) dpi. Labeling was more observed at 2 dpi and poorly detected at 6 dpi.

As shown in Fig. 2C, by comparing data from each of the infected groups, we detected only seven proteins exhibiting significant changes along the whole time course. These are actin (ACTB), growth factor receptor-bound protein 2 (GRB2), BTB/POZ domain-containing protein KCTD12 (KCTD12), protein-Lisoaspartate (D-aspartate) O-methyltransferase (PCMT1), PDZ and LIM domain protein 1 (PDLIM1), tubulin gamma 1 (TUBG1) and vimentin (VIM).
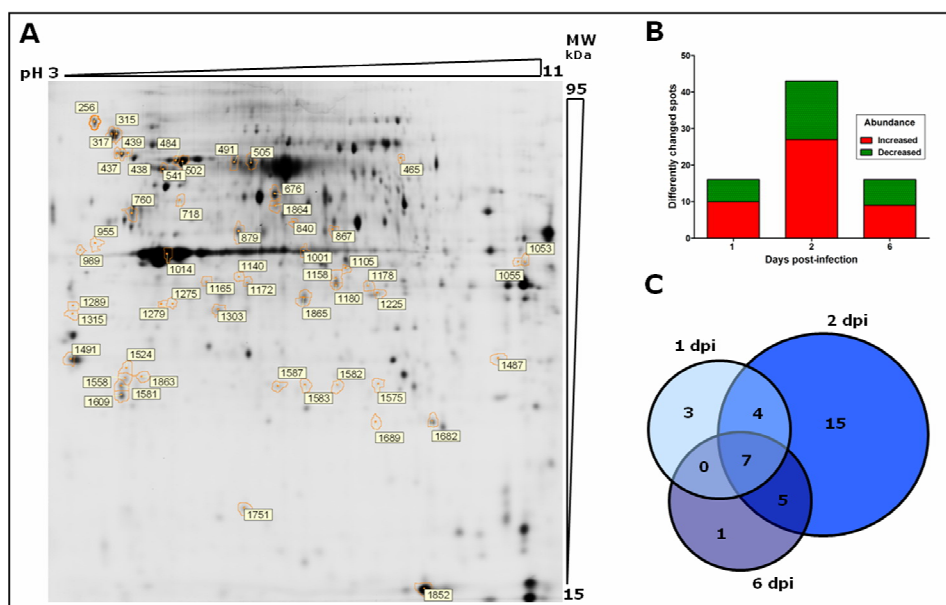
Figure. 2 – DIGE analysis of mesenteric lymph node proteins from controls and *Salmonella typhimurium* infected pigs. (A) Representative DIGE gel. Spots showing significant changes in abundance are indicated by numbers. (B) Bars demonstrate the number of spots exhibiting significant increase or decrease of abundance at 1, 2 and 6 days post-infection (dpi). (C) Venn diagram depicts the number of differently abundant proteins at each time point (1, 2 or 6 dpi) and commonly identified along the whole time course.

Table 1 - List of differently expressed protein in porcine MLN after oral infection with *S. typhimurium*.

Spot no.	Mass	pI	Score	Sequence coverage (%)	Protein ID	Name	Gene	1 vs 0		2 vs 0		6 vs 0		ANOVA
								p-value	Ratio	p-value	Ratio	p-value	Ratio	
1491	27899	4.73	447	53	P63104	14-3-3 protein zeta/delta	YWHAZ	0,16	-1,03	0,025	-1,18	0,01	-1,08	0,013
438	72402	5.07	278	11	P11021	78 kDa glucose-regulated protein	HSPA5	0,99	-1	0,046	1,3	0,91	1,01	0,049
439	72402	5.07	337	31	P11021	78 kDa glucose-regulated protein	HSPA5	0,77	1,02	0,058	1,22	0,56	-1,07	0,044
437	72402	5.07	367	14	P11021	78 kDa glucose-regulated protein	HSPA5	0,018	-1,25	0,32	-1,08	0,35	1,07	0,0033
1001	42052	5.29	410	26	Q6QAQ1	Actin, cytoplasmic 1	ACTB	0,32	-1,05	0,075	-1,08	0,023	-1,16	0,04
1014	42052	5.29	442	45	Q6QAQ1	Actin, cytoplasmic 1	ACTB	0,74	-1,01	0,0013	-1,13	0,1	-1,07	0,024
1165	42052	5.29	220	17	Q6QAQ1	Actin, cytoplasmic 1	ACTB	0,039	-1,3	0,046	-1,3	0,54	-1,08	0,021
879	47797	5.61	335	41	P61158	Actin-related protein 3	ACTR3	0,83	1,01	0,043	-1,08	0,81	-1,01	0,024
1864	57341	6.43	242	17	Q2XQV4	Aldehyde dehydrogenase, mitochondrial	ALDH2	0,24	1,09	0,0012	1,59	0,22	1,15	0,0016
1180	39020	6.43	224	23	P19619	Annexin A1	ANXA1	0,095	1,85	0,00016	2,86	0,59	1,15	0,0025
1158	39020	6.43	427	48	P19619	Annexin A1	ANXA1	0,058	2,08	5,40E-06	2,84	0,67	1,14	0,002
1581	30307	5.48	75	23	P18648	Apolipoprotein A-I	APOA1	0,74	1,04	0,012	-1,4	0,12	-1,21	0,0074
1689	22017	5.32	63	5	Q8HXK9	Apoptosis-associated speck-like protein containing a CARD	PYCARD	0,022	-1,35	0,71	-1,03	0,48	-1,06	0,034
1275	35964	5.51	101	23	Q96CX2	BTB/POZ domain-containing protein KCTD12	KCTD12	0,00092	-1,3	0,0016	-1,34	0,093	-1,28	0,031

Table 1 – *Continued*

Spot no.	Mass	pI	Score	Sequence coverage (%)	Protein ID	Name	Gene	1 vs 0		2 vs 0		6 vs 0		ANOVA
								p-value	Ratio	p-value	Ratio	p-value	Ratio	
1279	35964	5.51	51	4	Q96CX2	BTB/POZ domain-containing protein KCTD12	KCTD12	0,015	-1,24	0,014	-1,27	0,013	-1,4	0,0064
256	92698	4.75	98	10	Q29092	Endoplasmin	HSP90B1	1	1	0,0094	1,27	0,19	1,13	0,03
867	47096	6.30	303	46	A6M931	Eukaryotic initiation factor 4A-III	EIF4A3	0,96	-1	0,35	-1,03	0,065	-1,08	0,041
1487	25261	7.82	83	32	Q1JPH6	Eukaryotic translation initiation factor 4H	EIF4H	0,1	1,15	0,0063	1,39	0,14	1,13	0,0032
1053	39851	8.30	91	12	P04075	Fructose-bisphosphate aldolase A	ALDOA	0,13	-1,05	0,01	1,14	0,15	1,11	0,0072
1587	25304	5.89	390	39	P62993	Growth factor receptor-bound protein 2	GRB2	0,041	1,15	0,016	1,28	0,043	1,11	0,022
1575	24579	7.01	177	17	Q3T054	GTP-binding nuclear protein Ran	RAN	0,63	-1,08	0,023	1,65	0,39	1,26	0,039
1303	38151	5.60	298	25	P62871	Guanine nucleotide-binding protein G(I)/G(S)/G(T) subunit beta-1	GNB1	0,5	1,02	0,075	-1,09	0,82	-1,01	0,049
491	70340	5.60	175	11	Q6S4N2	Heat shock 70 kDa protein 1B	HSPA1B	0,96	1,01	0,012	1,61	0,4	-1,13	0,011
484	71082	5.37	548	45	P11142	Heat shock cognate 71 kDa protein	HSPA8	0,016	1,14	0,009	1,28	0,12	1,11	0,015
502	71082	5.37	471	40	P11142	Heat shock cognate 71 kDa protein	HSPA8	0,27	1,1	0,026	1,28	0,62	1,04	0,04
315	85121	4.93	230	20	O02705	Heat shock protein HSP 90-alpha	HSP90AA1	0,29	1,12	0,019	1,34	0,036	1,17	0,036

Table 1 – *Continued*

Spot no.	Mass	pI	Score	Sequence coverage (%)	Protein ID	Name	Gene	1 vs 0		2 vs 0		6 vs 0		ANOVA
								p-value	Ratio	p-value	Ratio	p-value	Ratio	
317	85121	4.93	375	31	O02705	Heat shock protein HSP 90-alpha	HSP90AA1	0,41	1,06	0,0078	1,41	0,33	1,12	0,015
1852	16212	7.10	405	66	P02067	Hemoglobin subunit beta	HBB	0,097	-1,46	0,0011	-2,02	0,033	-1,77	0,023
465	69788	8.68	379	21	O60506	Heterogeneous nuclear ribonucleoprotein Q	SYNCRIP	0,72	1,05	0,01	2,23	0,53	1,08	0,0038
1225	30097	6.61	97	12	Q14847	LIM and SH3 domain protein 1	LASP1	0,071	1,1	0,33	-1,06	0,022	1,2	0,0084
1865	36716	6.16	141	7	P11708	Malate dehydrogenase, cytoplasmic	MDH1	0,27	-1,05	0,021	-1,15	0,71	-1,02	0,013
1178	36314	6.76	112	14	Q5E9E1	PDZ and LIM domain protein 1	PDLIM1	0,022	1,34	0,00065	1,6	0,047	1,2	0,00089
1105	41137	6.77	57	2	Q08752	Peptidyl-prolyl cis-trans isomerase D	PPID	0,024	1,22	0,0034	1,41	0,058	1,12	0,0017
718	51839	5.31	147	17	Q9TRY0	Peptidyl-prolyl cis-trans isomerase FKBP4	FKBP4	0,21	1,15	0,03	1,32	0,068	1,23	0,019
541	70815	5.20	388	29	P13796	Plastin-2	LCP1	0,015	1,13	0,19	-1,08	0,34	1,08	0,043
1315	29092	4.57	185	30	P12004	Proliferating cell nuclear antigen	PCNA	0,16	1,1	0,0036	-1,29	0,61	-1,04	0,015
1682	11653	9.10	193	32	Q29576	Proteasome subunit beta type-8 (Fragment)	PSMB8	0,91	1,02	0,00073	1,71	0,023	1,49	0,0014

Table 1 – *Continued*

Spot no.	Mass	pI	Score	Sequence coverage (%)	Protein ID	Name	Gene	1 vs 0		2 vs 0		6 vs 0		ANOVA
								p-value	Ratio	p-value	Ratio	p-value	Ratio	
676	57146	5.98	134	12	P30101	Protein disulfide-isomerase A3	PDIA3	0,048	1,22	0,0067	1,61	0,072	1,65	0,04
1583	24745	6.71	76	15	P80895	Protein-L-isoaspartate(D-aspartate) O-methyltransferase	PCMT1	0,0091	1,13	0,00015	1,4	0,01	1,29	0,00017
1524	23464	5.12	227	28	P19803	Rho GDP-dissociation inhibitor 1	ARHGDIA	0,6	1,03	0,032	-1,14	0,56	-1,03	0,03
1558	23464	5.12	184	36	P19803	Rho GDP-dissociation inhibitor 1	ARHGDIA	0,79	1,01	0,0023	-1,19	0,095	-1,12	0,0071
1609	22836	5.09	191	23	Q9TU03	Rho GDP-dissociation inhibitor 2	ARHGDIB	0,7	1,04	0,035	-1,27	0,44	-1,07	0,037
1751	17292	5.76	158	54	Q6DUB7	Stathmin	STMN1	0,016	1,23	0,19	-1,1	0,3	1,14	0,013
1172	37833	7.03	89	9	Q2TBL6	Transaldolase	TALDO1	0,096	1,13	0,0066	1,33	0,048	1,21	0,0075
760	50804	4.94	507	58	Q2XVP4	Tubulin alpha-1B chain	TUBA1B	0,11	1,07	0,086	-1,1	0,93	-1	0,013
840	51458	5.75	154	20	Q0VCD2	Tubulin gamma-1 chain	TUBG1	0,00032	1,24	0,01	1,28	0,0017	1,28	0,004
955	53757	5.06	136	20	P31000	Vimentin	VIM	0,028	-2,1	0,007	-2,54	0,0062	-2,15	0,0017
989	51874	4.94	68	13	P48670	Vimentin (Fragment)	VIM	0,15	-1,39	0,048	-1,74	0,026	-1,67	0,025
505	N/A	N/A	N/A	N/A	N/A	N/A		0,25	-1,14	0,89	-1,02	0,036	-1,37	0,023
1055	N/A	N/A	N/A	N/A	N/A	N/A		0,81	-1,01	0,037	1,2	0,068	1,09	0,032
1140	N/A	N/A	N/A	N/A	N/A	N/A		0,041	1,23	0,023	1,34	0,065	1,3	0,033
1289	N/A	N/A	N/A	N/A	N/A	N/A		0,94	1	0,041	-1,25	0,097	-1,15	0,034
1582	N/A	N/A	N/A	N/A	N/A	N/A		0,59	1,06	0,01	1,56	0,32	1,16	0,012
1863	N/A	N/A	N/A	N/A	N/A	N/A		0,096	1,3	0,025	1,13	0,0038	1,41	0,031

3.2.3.3. Validation of selected proteins by Western blot and immunohistochemistry

To validate DIGE results, we performed Western blot analysis for four proteins: VIM, plastin-2 (LCP1), 14-3-3 (YWHAZ) and peptidyl–prolyl cis–trans isomerase FKBP4 (FKBP4). All of them showed the same abundance trends revealed by differential in gel analysis (Fig. 3B–I). Additionally, we also checked changes in abundance of VIM by immunohistochemistry assays (Fig. 3A). Consistent with DIGE, immunohistochemistry demonstrated that VIM was less abundant in infected animals when compared to controls. Besides difference in abundance, distribution of VIM in tissue was markedly different before and after infection. At 0 dpi, VIM was diffusely labeled in lymph nodes whereas at 2 dpi, staining was restricted to germinal centers and large irregularly-shaped mononuclear cells located near trabeculae.

3.2.3.4. Quantification of immune-related genes by qPCR

In order to confirm the regulation of host immune response mechanisms upon infection with *S. typhimurium*, qPCR expression profiling was performed for some genes encoding innate/ inflammatory and T cell response mediators. In general, screened genes showed a similar expression trend, which was marked by up-regulation at 2 dpi and decrease of mRNA levels or absence of significant changes at 6 dpi (Fig. 4).

3.2.3.5. Biological data interpretation

Bioinformatic tools were employed to biologically interpret protein list obtained from DIGE analysis, aiming to gain an insight into networks, biological processes, molecular functions and pathways associated with the proteome

response of porcine MLN to *S. typhimurium*. Three interaction networks were generated by IPA data analysis (Table 2) and the nature of relationships displayed
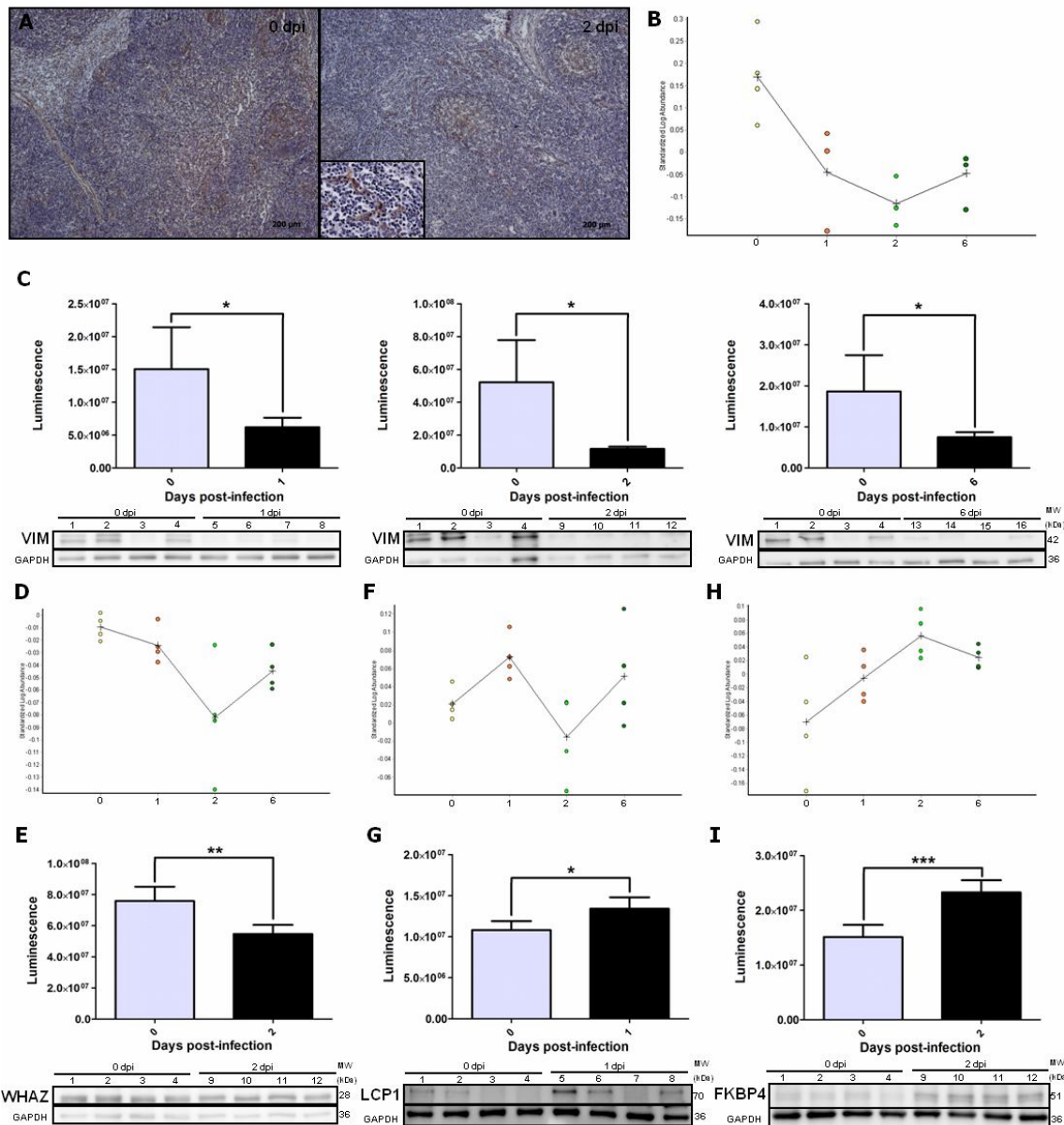

Figure 3 – Data validation by Western blot and immunohistochemistry. (A) Immunohistochemistry shows a decrease of VIM abundance in MLN and labeling of large irregularly-shaped mononuclear cells located near trabeculae after infection. (B–I) Standard abundance by DIGE and Western blot analysis of validated proteins at 1, 2 and 6 dpi. (B, C) VIM, (D, E) YWHAZ, (F, G) LCP1, (H, I) FKBP4.

by the molecules integrated in each network was accessed based on the scientific information contained in the Ingenuity Knowledge Criteria. The major network depicted the existence of 83 direct and 39 indirect relationships which integrated 20 of the proteins differently altered after *S. typhimurium* infection (Fig. 5).
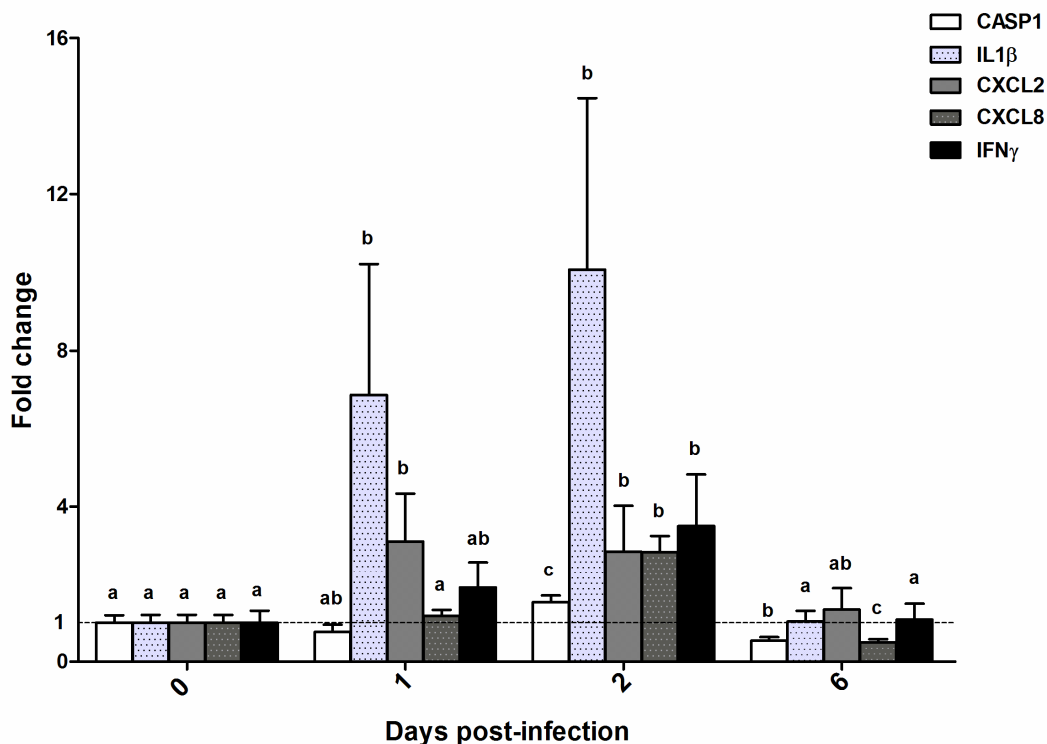
Figure 4 – Expression profiling of immune-related genes in mesenteric lymph nodes of pigs experimentally infected with *Salmonella typhimurium* by qPCR. Data are shown as the fold change in gene expression in infected pigs compared to controls Values lower than 1 and higher than 1 denote down and up-regulation respectively. The same letters above the bars indicate no significant differences ($p < 0.05$).

Furthermore, "Posttranslational modification", "Protein folding" and "Cellular assembly and organization" were identified as putative functions associated to the proteins included in this network. Network 1 also demonstrated the central role of the heat shock proteins in the proteome response of porcine MLN to *S.*

typhimurium as well as the regulatory interactions of these proteins with NFκB and caspase. As other relevant results of network analysis, the following could be highlighted: the activation relationship of GRB2 and ALDH2 (aldehyde dehydrogenase) with p38 MAP kinase depicted in network 2 and the direct activation/inhibition relationship between IFNγ and PSMB8 (proteasome subunit beta type-8) shown in network 3 (Supplementary data file 1).

Table 2 - Protein interaction networks associated to the response of porcine MLN to *S. typhimurium* infection.

ID	Score[1]	Focus molecule[2]	Molecules in the network[3]	Top Functions
1	54	20	14-3-3, **ACTB**, Actin, **ACTR3**, Alpha tubulin, **ANXA1**, **ARHGDIA**, **ARHGDIB**, Arp2/3, Caspase, Ck2, **EIF4A3**, F Actin, **FKBP4**, **HBB**, Hsp70, Hsp90, HSP, **HSP90AA1**, **HSP90B1**, **HSPA5**, **HSPA8**, **HSPA1B**, **LASP1**, **LCP1**, MHC Class I (complex), NFkB (complex), **PDIA3**, **PYCARD**, RNA polymerase II, **STMN1**, **TUBA1B**, **TUBG1**, Tubulin, **YWHAZ**	Post-Translational Modification, Protein Folding, Cellular Assembly and Organization
2	20	10	Akt, **ALDH2**, **ALDOA**, Ap1, **APOA1**, CaMKII, ERK1/2, FAM59A, FSH, **GNB1**, **GRB2**, Histone h3, Histone h4, IG9, Insulin, Jnk, LDL, Lh, LOC81691, MAP2K1/2, Mapk, MIR155HG, Nfat (family), P38 MAPK, **PCMT1**, **PCNA**, PDGF BB, **PDLIM1**, PI3K (complex), Pkc(s), PLC gamma, Rac, **SYNCRIP**, Trypsin, **VIM**	Cellular Movement, Cell Cycle, Lipid Metabolism
3	14	7	BPNT1, CDC37L1, CEACAM3, CHI3L2, CLEC5A, DEFB104A/DEFB104B, DNAJB7, **EIF4H**, FKBP6, Gbp4, GBP6, H60a, HSP90AB1, IFNG, IKBKE, **KCTD12**, KMO, **MDH1**, MLEC, Myhs, NDRG4, PGRMC2, **PPID**, **PSMB8**, Raet1b, **RAN**, SLC28A1, SLC5A2, **TALDO1**, Taok2 (mouse), TGFB1, TNF, TRAF6, TREM3, TTC28	Cell Death, Cell-To-Cell Signaling and Interaction, Inflammatory Response

[1] Calculated with Right-tailed Fisher's Test; [2] Number of imput molecules in the network; [3] Input molecules are highlighted in bold.

Gene ontology (GO) annotations associated to differently abundant proteins were found out by the AU "Biological Enrichment" tool. "Cell motility" and "Antiapoptosis" were the top enriched biological processes identified (Supplementary data file 4). In addition, "Protein folding" and "Rho GDP-dissociation inhibitor activity" were uncovered as the molecular functions more related to the differently abundant proteins (Supplementary data file 5). Pathway analysis was based on the Ingenuity Canonical Pathways Libraries and KEGG
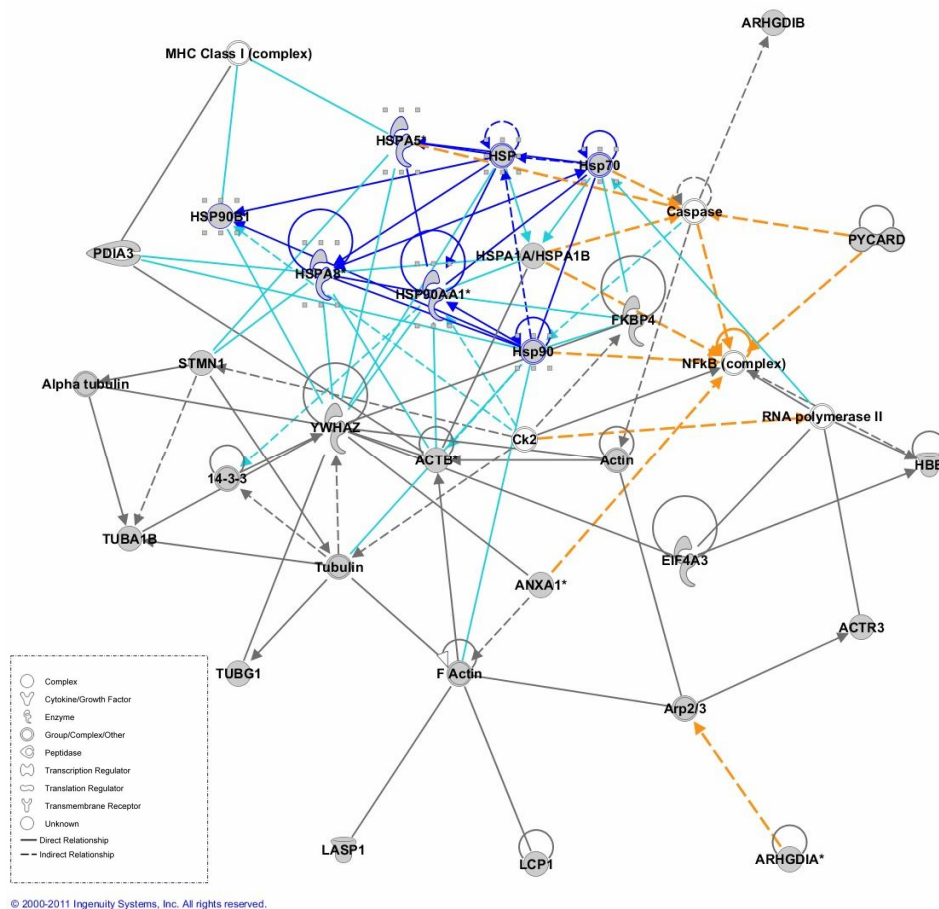
Figure 5 – Gene network analysis of porcine MLN after *S. typhimurium* infection. "Post-translational modification, Protein folding, Cellular assembly and organization" gene networks. Activation relationships are highlighted in yellow. Blue lines represent interactions entailing heat shock proteins. Light blue lines represent interactions between heat shock proteins and other molecules.

database. The top canonical and KEGG pathways significantly altered after the bacterial challenge are described in Table 3. Corroborating data from network analysis, heat shock proteins were observed to take part in different molecular routes. We also detected a similar tendency in DIGE analysis for differently abundant proteins associated to the "Antigen processing and presentation pathway" (Fig. 6A). Interestingly, all of them exhibited an increase of abundance at 2 dpi (Fig. 6B).

Table 3 - Top four enriched canonical and Kegg pathways in porcine MLN after S. typhimurium infection.

Pathways	p-value[1]	Ratio[2]	Input molecules
Kegg Pathways			
Antigen processing and presentation	1.4E-06	5.7E-02	PDIA3, HSP90AA1, HSPA8, HSPA5, HSPA1B
Pathogenic *Escherichia coli* infection	2.7E-04	6.1E-02	TUBA1B, ACTB, YWHAZ
MAPK signaling pathway	3.3E-04	1.8E-02	HSPA1B, HSPA5, HSPA8, GRB2, STMN1
Shigellosis	4E-04	6.1E-02	TUBA1B, ACTB, YWHAZ
Ingenuity Canonical Pathways			
Glucocorticoid Receptor Signaling	5.9E-08	2.7E-02	HSPA8, HSP90B1, HSPA1B, GRB2, ANXA1, FKBP4, HSP90AA1, HSPA5
14-3-3-mediated Signaling	1.4E-07	5E-02	GRB2, PDIA3, TUBG1, YWHAZ, VIM, TUBA1B
Aldosterone Signaling in Epithelial Cells	9.8E-07	3.5E-02	HSPA8, HSP90B1, HSPA1B, PDIA3, HSP90AA1, HSPA5
Protein Ubiquitination Pathway	1.5E-05	2.2E-02	HSPA8, HSP90B1, HSPA1B, HSP90AA1, PSMB8, HSPA5

1 Fisher's exact test; 2 Ratio (number of input molecules in a given pathway, divided by total number of molecules that make up that pathway)

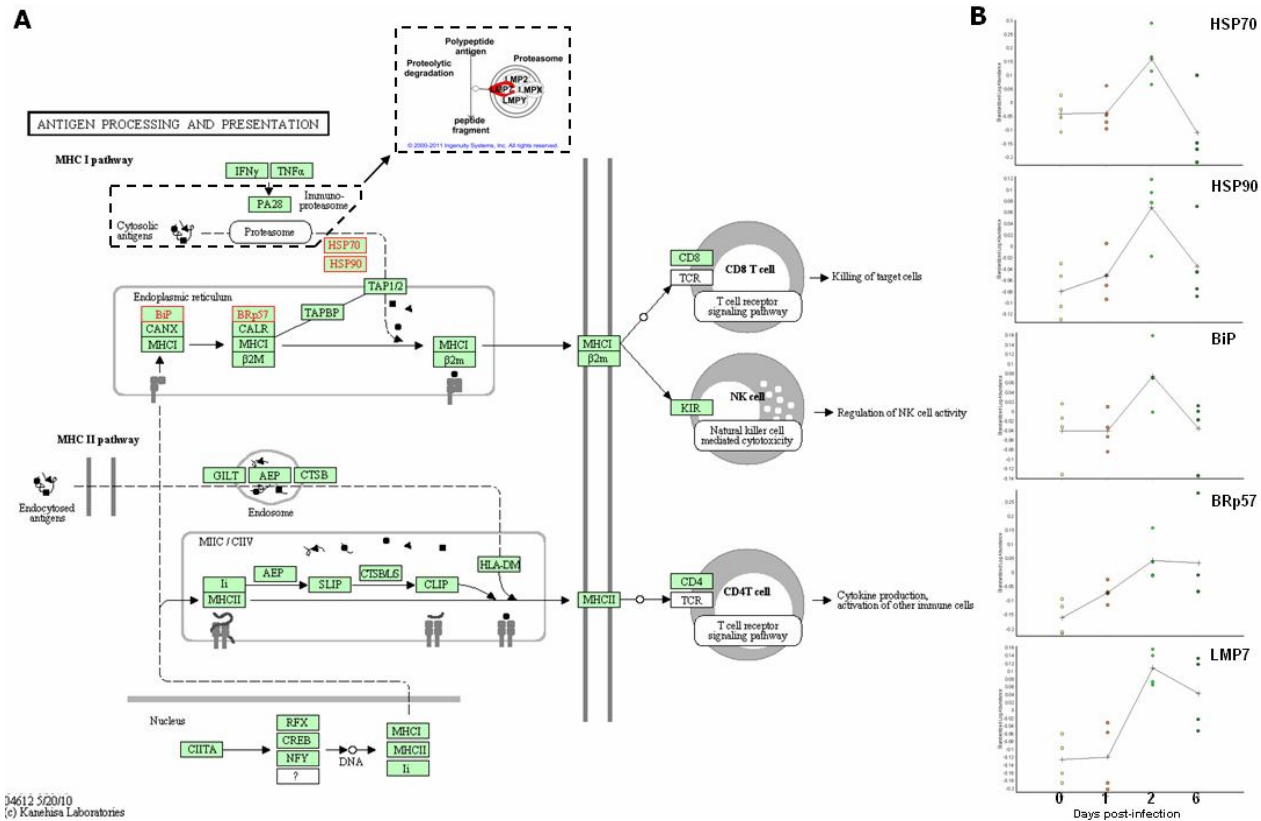**Figure 6** – Antigen processing and presentation pathway. Differently abundant proteins associated to this pathway are highlighted in red (A) and their standard abundance after infection by DIGE is depicted in (B). Dotted line indicates a pathway detail from Ingenuity Pathway Analysis. The image was generated by Kegg pathways from the Kanehisa laboratories and is subject to their copyright conditions.

3.2.4. Discussion

Proteome approaches are being increasingly used in many different systems to investigate host–microbe interactions. In this context, in vivo models are crucial to reflect the multiple events undergone by host upon pathogen infection. Although the systemic pathology induced by *S. typhimurium* has been extensively studied using the mouse model [6], the complex molecular mechanisms underlying the intestinal infection caused by bacteria in food-producing animals are still not fully understood [17]. To address this issue, in this work we employed for the first time an in vivo approach coupled to DIGE based proteomic analysis to detect changes in the porcine MLN proteome in response to *S. typhimurium* infection.

After bacteria challenge, the effectiveness of the experimental infection was confirmed by the observation of clinical signs of enteric disease in all infected animals. Distinct to mice, *S. typhimurium* generally causes little or no systemic involvement in pigs [17]. Nevertheless, in our in vivo model we observed in MLN the presence of the pathogen associated to the cytoplasm of infiltrated phagocytes, in concordance with previously reported evidences that, in mice, *S. typhimurium* is shuttled to MLN by infected phagocytes [18,19]. Since major protein changes were detected at 2 dpi, coinciding with a higher presence of *S. typhimurium* in infiltrated phagocytes, it could be inferred that proteome response of porcine MLN to the infection is strongly related to changes in tissue cellularity and pathogen burden. Consistent with this, we found that "Cell motility" was the most significantly enriched biological process after *S. typhimurium* infection (see Supplementary data file 4).

In general, our results indicated a modulation of diverse normal host functions upon *S. typhimurium* infection. This can be related with the complex

interplay between *Salmonella* and its host that involves the coordinated stimulation and downregulation of cell functions by type III secretion systems 1 and 2 (T3SS1 and T3SS2) effectors for benefits of bacteria [20]. Firstly, bacterial internalization involves manipulation of the Rho family GTPases resulting in actin cytoskeleton rearrangements [21,22]. In our study, we observed that regulators of Rho protein signaling such as GDP dissociation inhibitors (GDI)ARHGDIA (Rho GDI-1) and ARHGDIB (Rho GDI-2) were less abundant after *Salmonella* infection. Because GDI hinder the dissociation of guanosine diphosphate from Rho proteins,maintaining GTPases in an inactive form [23], our proteomic data suggest an increasing of GTPases activity in porcine infected MLN as a result of the repression of Rho GDI activity. Although T3SS effectors modulate host Rho GTPases activity for the benefit of the bacteria, mechanisms of host immune response, such as phagocytosis and chemotaxis, are driven by extensive local reorganization of the actin cytoskeleton dependent on Rho GTPase activity. Therefore, cytoskeletal changes undergone by MLN in response to infection reflect amix of outcomes induced by both *Salmonella* and host. Following actin polymerization by activation of the Rho GTPases, recovery of normal cellular architecture was observed once *S. enterica* has completely invaded target cells [24]. However, after bacterial uptake, *Salmonella* can initiate a second round of actin polymerization, resulting in formation of an F-actin coat around replicating intracellular bacteria [20]. In line with this, we observed changes in proteins involved in processes such as actin filament binding and bundle formation. Thus, PDLIM1, a kinase known for their critical role in regulating actin polymerization downstream of the Rho GTPase cascade [25], was more abundant at 1, 2 and 6 dpi. On the other hand, ACTB exhibited a decrease of abundance along the whole time course. According to Galan and Zhou [22] the *Salmonella* effector SipA binds to actin promoting a significant reduction in the concentration of its monomeric conformation. In addition, SipA increases the stability of actin bundles by

modulating plastin actin-bundling activity [26]. Interestingly, we observed that L-plastin was more abundant in the beginning of infection and this result could consist in another evidence of SipA activity in MLN. In the same way of ACTB, VIM, one of the constituents of cytoskeletal intermediate filaments (IF) network, exhibited a decrease of abundance after infection. Moreover, immunohistochemistry assays revealed that this protein was evidently accumulated in cells which morphology and localization in tissue were equivalent to *Salmonella* infected phagocytes. Protective IF cages similar to those composed by F-actin also coalesce around *Salmonella*-containing vacuoles [27]. Assembly of both proteins during *Salmonella* intracellular replication is reported to be interdependent and disruption of either leads to release of bacteria in the cytoplasm [28]. Moreover, annexin A1 (ANXA1), which was initially related to anti-inflammatory functions [29], appears to be involved in controlling association of F-actin with phagosomes thereby affecting phagosome formation. ANXA1 binds to, bundles and colocalizes with F-actin during phagocytic cup formation and on mature phagosomes [30]. Intriguingly, this protein exhibited the most prominent increase of abundance in the porcine MLN after infection. Thus, the uncovered reduction of monomeric forms of actin and vimentin as well as the augment of PDLIM1 and ANXA1 in MLN probably causes rearrangements in the cytoskeleton of infected cells that are necessary for phagosome formation and *Salmonella* replication. Triggering of GTPase activity in MLN was also disclosed by the abundance increase of GTP-binding nuclear protein Ran (RAN), found in this study. RAN is a major regulator of nucleocytoplasmic transport, controlling its rate and directionality by cycling between inactive (GDP-bound) and active (GTP-bound) conformations [31]. Recent studies assert that RAN is noticeably upregulated in fish after viral or bacterial infection [32] and its activity is associated to the enhancement of phagocytosis [31]. Evidences inmammals demonstrate that RAN is also involved in LPS endotoxin response [33] and

nuclear import of STAT3 [34]. The increase of RAN abundance observed in this study could consist in a GTPase response carried out by the host against *S. typhimurium*. However, the role of this protein in *Salmonella* infections has not been elucidated so far.

In addition to cytoskeleton rearrangements, *S. typhimurium* infection induced cell death mechanisms, which in combination to the inflammatory cell infiltration observed in our study, could point toward the occurrence of pyroptosis in porcine MLN. Pyroptosis is a CASP1 dependent inflammatory form of cell death induced by *Salmonella* and other intracellular microorganisms that is characterized by the release of potent mediators of inflammation such as IL1b and IL18 [35]. Although our proteomic study did not allow for an observation of the changes in CASP1, we do see it at mRNA level at 2 dpi accompanied by a high increase of IL1b gene expression (Fig. 4). In agreement with that finding, functional analysis of the proteomic results disclosed an enrichment of the mitogenactivated protein kinase (MAPK) signaling pathway upon infection (Table 3), additionally verified bymRNA quantification of the downstream pro-inflammatory chemokines CXCL2 and CXCL8, which were both up-regulated at 2 dpi. These results represent a further indication of pyroptosis induction, since the production of pro-inflammatory cytokines is carried out via activation of MAPK and consequent regulation of the transcription factors NF-κB and AP1 [22,36].

Although pyroptosis represents an important innate immune effector mechanism against intracellular bacteria, *Salmonella* has developed strategies to overcome it [37,38]. Apparently, this pathogen voids pyroptosis effectiveness by delaying its onset and infecting new macrophages after escaping from lysed cells [35]. However, released bacteria should be able to survive to neutrophil uptake and killing by reactive oxygen species, in order to re-infect cells and maintain their replicative cycle in tissue [38]. Intriguingly, our results indicate that *Salmonella* burden in MLN was reduced along infection. This is probably related

to the strong infiltration of phagocytic cells observed at 2 dpi that could be causing the substantial decrease of *S. typhimurium* labeling in tissue at 6 dpi. In addition, we observed an enrichment of the anti-apoptosis process after infection. Although the role of each protein associated to this mechanism is unknown for us, we speculate that apoptosis is avoided by swine, hampering cell-to-cell spread of bacteria through subsequent rounds of macrophage infection. Therefore, our results could demonstrate that in spite of manipulating host machinery, *S. typhimurium* is not able to effectively evade the porcine MLN response. Nevertheless, the presence of live *S. typhimurium* in tissue at 6 dpi (datanot shown) reinforces the hypothesis that this pathogen develops some mechanism to maintain itself in MLN at low levels. Further research will be necessary to bring significant insight into how and how long *S. typhimurium* persists in porcine MLN after infection.

Changes in proteins related to the modulation of host second line of defense were also identified after infection. Thus, we uncovered an increase in abundance of proteins involved in different steps of the antigen processing and presenting pathway (Table 3). Strikingly, these proteins exhibited similar quantitative changes, being all of them more abundant at 2 dpi, when *S. typhimurium* and proteome changes were more evident. Additionally, activation of T-cells was also deduced by the increase in mRNA levels of IFNγ (see Fig. 4), a cytokine that promotes Th1 differentiation leading to cellular immunity. Therefore, our data suggest that the process of antigen presentation properly functions in porcine MLN after *S. typhimurium* infection.

It is known that antigenic peptides presented by MHC-I are produced through cytosolic degradation of intracellular proteins by proteasome [39]. Otherwise, presentation of exogenous antigens has been classically attributed to MHC class II [40]. Additionally, the term cross-presentation was introduced as an alternative mechanism to define a process in which antigens acquired from the

extracellular environment are present by antigen-presenting cells (APCs) to CD8+ T cells via their own MHC-I molecules [41]. Interestingly, this mechanism could explain the clear indications of adaptive immunity induction via MHC-I which is derived from the proteomic results obtained in our work. Since *Salmonella* is confined in host cell inside phagosomes, its antigens theoretically would be protected from cytosolic degradation by proteasome, unless the phagosome is a competent organelle for antigen cross-presentation as has been previously stated by Houde et al. [42]. In this alternative scenario, phagocytosed proteins reach cytosol by chaperone retrotranslocation mechanisms, subsequently degradated by proteasomes located in the cytoplasmic side of phagosomes and then, the generated peptides gain access to the phagosome lumen via TAP, bind MHC-I molecules and activate CD8+ T-cells [40,42]. Transcriptomic analysis carried out by us (Martins et al., unpublished data) highlighted the upregulation of TAP and MHC-I mRNA in MLN of *S. typhimurium* infected pigs. In the proteomic study present here, HSP90 and other three chaperones associated with degradation and retrotranslocation of proteins to cytosol (HSP70, BiP/HSPA5 and BRp57/PDIA) [43] were detected at higher levels in infected samples. Also, the proteasome subunit beta type-8 (PSMB8 or LMP7) was also found to be more abundant in MLN after infection. The hydrolyzing activities of proteasomes are conferred upon stimulation of cells with IFNγ [39]. This process results in the replacement of its 20S core subunits by LMP2 (iβ1), MECL1 (iβ2) and LMP7 (iβ5), constituting the so-called immunoproteasome [42]. In line with the direct activation/inhibition relationship between IFNγ and PSMB8 depicted in network 3 (see Supplementary data file 3) and the previously referred reports [39,41], we found out that the highest levels of PSMB8 in tissue is coinciding with the increase of IFNγ mRNA at 2 dpi. Since proteasomal activity is dependent on the ubiquitination of its targets [41], the significant enrichment of the "Protein ubiquitination pathway" uncovered by IPA analysis gives an additional evidence

of the enhancement of protein degradation by immunoproteasome as a result of infection.

In conclusion, our results suggest that, in spite of modulating normal host functions and replicating intracellularly, *S. typhimurium* fails to effectively damper immune response elements during infections in pigs. The proteome response of porcine MLN to infection was associated to the induction of innate immunity processes such as phagocyte infiltration and pyroptosis. Moreover, we could infer that *S. typhimurium* antigens are cross-presented via MHC-I in a proteasome-dependent manner and this mechanism probably triggers an early cytotoxic response against bacteria. Although both innate and adaptive immune responses might control pathogen dissemination, further research will be necessary to elucidate the strategies exploited by *S. typhimurium* to establish the asymptomatic-carrier state in swine infections.

Supplementary material related to this article can be found online at doi:10.1016/j.jprot.2012.03.045.

Acknowledgments

References

[1] Fosse J, Seegers H, Magras C. Prevalence and risk factors for bacterial food-borne zoonotic hazards in slaughter pigs: a review. Zoonosis Public Health 2009;56:429–54.

[2] Methner U, Rammler N, Fehlhaber K, Rösler U. *Salmonella* status of pigs at slaughter — bacteriological and serological analysis. Int J Food Microbiol 2011;151:15–20.

[3] Foley SL, Lynne AM, Nayak R. *Salmonella* challenges: prevalence in swine and poultry and potential pathogenicity of such isolates. J Anim Sci 2008;86:E149–62.

[4] Anon. The European Union summary report on trends and sources of zoonoses, zoonotic agents and food-borne outbreaks in 2009. EFSA J 2011;9:1–378.

[5] Boyen F, Haesebrouck F, Maes D, Van Immerseel F, Ducatelle R, Pasmans F. Non-typhoidal *Salmonella* infections in pigs: a closer look at epidemiology, pathogenesis and control. Vet Microbiol 2008;130:1–19.

[6] Bearson BL, Bearson SMD. Host specific differences alter the requirement for certain *Salmonella* genes during swine colonization. Vet Microbiol 2011;150:215–9.

[7] Bendixen E, Danielsen M, Larsen K, Bendixen C. Advances in porcine genomics and proteomics — a toolbox for developing the pig as a model organism for molecular biomedical research. Brief Funct Genomics 2010;9:208–19.

[8] Zhang CG, Chromy BA, McCutchen-Maloney SL. Host–pathogen interactions: a proteomic view. Expert Rev Proteomics 2005;2:187–202.

[9] Hartlova A, Krocova Z, Cerveny L, Stulik J. A proteomic view of the host–pathogen interaction: the host perspective. Proteomics 2011;11:3212–20.

[10] Collado-Romero M, Arce C, Ramírez-Boo M, Carvajal A, Garrido JJ. Quantitative analysis of the immune response upon *Salmonella* typhimurium infection along the porcine intestinal gut. Vet Res 2010;41:23.

[11] Sechi S, Chait BT. Modification of cysteine residues by alkylation. A tool in peptide mapping and protein identification. Anal Chem 1998;70:5150–8.

[12] Yubero N, Jiménez-Marín A, Barbancho M, Garrido JJ. Two cDNAs coding for the porcine CD51 (αV integrin subunit: cloning, expression analysis, adhesion assays and chromosomal localization. Gene 2011;481:29–40.

[13] Bullido R, Gomez del Moral M, Alonso F, Ezquerra A, Zapata A, Sánchez C, et al. Monoclonal antibodies specific for porcine monocytes/macrophages: macrophage heterogeneity in the pig evidenced by the expression of surface antigens. Tissue Antigens 1997;49:403–13.

[14] Livak KJ, Schmittgen TD. Analysis of relative gene expression data using real-time quantitative PCR and the 2−ΔΔCT method. Methods 2001;25:402–8.

[15] Vandesompele J, De Preter K, Pattyn F, Poppe B, Van Roy N, De Paepe A, et al. Accurate normalization of real-time quantitative RT-PCR data by geometric averaging of multiple internal control genes. Genome Biol 2002;3:1–12.

[16] Willems E, Leyns L, Vandesompele J. Standardization of real-time PCR gene expression data from independent biological replicates. Anal Biochem 2008;379:127–9.

[17] Paulin SM, Jagannathan A, Campbell J, Wallis TS, Stevens MP. Net replication of *Salmonella* enterica serovars Typhimurium and Choleraesuis in porcine intestinal mucosa and nodes is associated with their differential virulence. Infect Immun 2007;75:3950–60.

[18] Bueno SM, Wozniak A, Leiva ED, Riquelme SA, Carreño LJ, Hardt W-D, et al. *Salmonella* pathogenicity island 1 differentially modulates bacterial entry to dendritic and non-phagocytic cells. Immunology 2010;130:273–87.

[19] Haimovich B, Venkatesan MM. Shigella and *Salmonella*: death as a means of survival. Microbes Infect 2006;8:568–77.

[20] Pizarro-Cerda J, Cossart P. Bacterial adhesion and entry into host cells. Cell 2006;124:715–27.

[21] Malik-Kale P, Jolly CE, Lathrop S, Winfree S, Luterbach C, Steele-Mortimer O. *Salmonella* — at home in the host cell. Front Microbiol 2011;2:125.

[22] Galán JE, Zhou D. Striking a balance: modulation of the actin cytoskeleton by *Salmonella*. Proc Natl Acad Sci USA 2000;97: 8754–61.

[23] DerMardirossian C, Bokoch GM. GDIs: central regulatory molecules in Rho GTPase activation. Trends Cell Biol 2005;15:356–63.

[24] Holden DW. Trafficking of the *Salmonella* vacuole in macrophages. Traffic 2002;3:161–9.

[25] te Velthuis AJW, Isogai T, Gerrits L, Bagowski CP. Insights into the molecular evolution of the PDZ/LIM family and identification of a novel conserved protein motif. PLoS One 2007;2:e189.

[26] Silva CV, Cruz L, Araújo NS, Angeloni MB, Fonseca BB, Gomes AO, et al. A glance at Listeria and *Salmonella* cell invasion: different strategies to promote host actin polymerization. Int J Med Microbiol 2012;302:19–32.

[27] Guignot J, Servin AL. Maintenance of the *Salmonella*-containing vacuole in the juxtanuclear area: a role for intermediate filaments. Microb Pathog 2008;45:415–22.

[28] Haglund CM, Welch MD. Pathogens and polymers: microbe–host interactions illuminate the cytoskeleton. J Cell Biol 2011;195:7–17.

[29] Parente L, Solito E. Annexin 1: more than an anti-phospholipase protein. Inflamm Res 2004;53:125–32.

[30] Patel DM, Ahmad SF, Weiss DG, Gerke V, Kuznetsov SA. Annexin A1 is a new functional linker between actin filaments and phagosomes during phagocytosis. J Cell Sci 2011;124:578–88.

[31] Zhao Z, Jiang C, Zhang X. Effects of immunostimulants targeting Ran GTPase on phagocytosis against virus infection in shrimp. Fish Shellfish Immunol 2011;31:1013–8.

[32] Han F, Wang XQ, Yao CL, Wang ZY. Molecular characterization of Ran gene up-regulated in large yellow croaker (Pseudosciaena crocea) immunity. Fish Shellfish Immunol 2010;29:327–33.

[33] Kang AD, Wong PM, Chen H, Castagna R, Chung SW, Sultzer BM. Restoration of lipopolysaccharide-mediated B-cell response after expression of a cDNA encoding a GTP-binding protein. Infect Immun 1996;64:4612–7.

[34] Cimica V, Chen HC, Iyer JK, Reich NC. Dynamics of the STAT3 transcription factor: nuclear import dependent on Ran and importin-β1. PLoS One 2011;6:e20188.

[35] Miao EA, Rajan JV. *Salmonella* and caspase-1: a complex interplay of detection and evasion. Front Microbiol 2011;2:85.

[36] Broz P, Monack DM. Molecular mechanisms of inflammasome activation during microbial infections. Immunol Rev 2011;243:174–90.

[37] Guiney DG, Fierer J. The role of the spv genes in *Salmonella* pathogenesis. Front Microbiol 2011;2:129.

[38] Miao EA, Leaf IA, Treuting PM, Mao DP, Dors M, Sarkar A, et al. Caspase-1-induced pyroptosis is an innate immune effector mechanism against intracellular bacteria. Nat Immunol 2010;11:1136–42.

[39] Kloetzel PM, Ossendorp F. Proteasome and peptidase function in MHC-class-I-mediated antigen presentation. Curr Opin Immunol 2004;16:76–81.

[40] Cresswell P, Ackerman AL, Giodini A, Peaper DR, Wearsch PA. Mechanisms of MHC class I-restricted antigen processing and cross-presentation. Immunol Rev 2005;207:145–57.

[41] Lattanzi L, Rozera C, Marescotti D, D'Agostino G, Santodonato L, Cellini S, et al. IFNγ boosts epitope cross-presentation by dendritic cells via modulation of proteasome activity. Immunobiology 2011;216:537–47.

[42] Houde M, Bertholet S, Gagnon E, Brunet S, Goyette G, Laplante A, et al. Phagosomes are competent organelles for antigen cross-presentation. Nature 2003;425:402–6.

[43] Imai T, Kato Y, Kajiwara C, Mizukami S, Ishige I, Ichiyanagi T, et al. Heat shock protein 90 (HSP90) contributes to cytosolic translocation of extracellular antigen for cross-presentation by dendritic cells. Proc Natl Acad Sci USA 2011;108:16363–8.

3.3 Pig infections by *Salmonella enterica* serovar Typhimurium: an insight into the molecular mechanisms carried out in mesenteric lymph-nodes

Rodrigo Prado Martins [1], Carmen Aguilar [1], James E. Graham [2], Ana Carvajal [3], Rocío Bautista [4], M. Gonzalo Claros [4], Juan J. Garrido [1]

1 Grupo de Genómica y Mejora Animal, Departamento de Genética, Facultad de Veterinaria, Universidad de Córdoba, Campus de Rabanales, Edificio Gregor Mendel C5, 14071 Córdoba, Spain.

2 Department of Microbiology and Immunology, University of Louisville School of Medicine, 40202 Louisville, Kentucky, USA.

3 Departamento de Sanidad Animal, Facultad de Veterinaria, Universidad de León, 24071 León, Spain.

4 Plataforma Andaluza de Bioinformática, Universidad de Málaga, Parque Tecnológico de Andalucía, 29590 Málaga, Spain

Abstract

In this study, we sought to elucidate the early mechanisms triggered in porcine mesenteric lymph-nodes (MLN) upon in vivo *Salmonella* Typhimurium infection. For this, a robust approach was employed to analyse host response and verify the expression of virulence genes by pathogen found in tissue. *Salmonella* Typhimurium strain used in this bacterial challenge was able to express the screened virulence effectors in MLN, suggesting that the development of a mild disease in infected swine is not attributed to an absence of virulence strategies triggering by pathogen. In fact, results indicate that despite its capacity of hampering immune response, a combination of host triggered innate immunity mechanisms and early T-cell cytotoxic response might overcome virulence strategies employed by pathogen. Clathrin-mediated endocytosis appears to take part in the pathogenesis of infection, but the role of this pathway in host and pathogen-mediated processes remains to be clarified. Furthermore, we infer that due to an inability of *Salmonella* Typhimurium to suppress flagellin and prgJ expression in porcine MLN, host is able to induce infected cell death by pyroptosis, protecting itself of pathogen spread beyond gut-associated lymph-nodes.

3.3.1 Introduction

Infections by *Salmonella* are a major health problem in the developing and developed world. In the European Union, despite the current decreasing trend of human cases, *Salmonella* persists as the main cause of food-borne outbreaks [1]. Pork is considered to be a significant source of *Salmonella* to humans next to eggs and poultry meat [2]. In fact, according to the European food safety authority (EFSA), *Salmonella enterica* serovar Typhimurium (herein *Salmonella* Typhimurium) is the second serovar most frequently reported in human salmonellosis and infection by this pathogen is mostly associated with the consumption of contaminated pork [1].

Since food industry and direct contact with infected animals represent the main sources of non-typhoid *Salmonella* [3], prevention of human disease depends significantly on controlling infection in livestock hosts [4]. *Salmonella* Typhimurium infected pigs generally carry this serotype asymptomatically in the tonsils, intestines and gut-associated lymphoid tissue, posing an important threat to animal and human health [5]. Epidemiological studies assert that *Salmonella* prevalence in slaughter swine lymph nodes varies widely at country level, ranging from 0 to 29% [2]. Although salmonellosis in pigs has been subject of research [5], a thorough knowledge of the pathogenesis of porcine infections with broadhost range *Salmonella* serotypes is still necessary and a better understanding of the biological processes that control host-pathogen interaction and *Salmonella* persistence in porcine lymphatic tissue could provide new targets for treatment and control of salmonellosis in this species.

Combination of system-wide approaches and *in vivo* infection models is expected to generate precise and novel data to the study of porcine salmonellosis [6]. In fact, whole-genome expression analysis has been used to

identify genes and molecular pathways involved in the pig response to *Salmonella* infections [7, 8]. More recently, proteomic techniques were employed by us as a step towards a detailed understanding of the disease mechanisms [9, 10]. Thus, the objective of the current study was to expand the available knowledge by investigating the early processes carried out in the mesenteric lymph-nodes (MLN) of pigs experimentally infected with *Salmonella* Typhimurium. To achieve that, host response was monitored by several approaches including microarray gene expression, bioinformatic data enrichment, western blot, quantitative real-time PCR, immunohistochemistry and confocal microscopy analysis. In addition, selective capture of transcribed sequences (SCOTS) technique [11] was performed to analyze the *in vivo* expression of some *Salmonella* Typhimurium genes in order to investigate important pathogenesis determinants on the pathogen side.

3.3.2 Materials and methods

3.3.2.1 Experimental infection and tissue sampling

Sixteen crossbred weaned piglets of approximately four weeks of age, serologically and fecal-negative for *Salmonella* were used in an experimental infection described elsewhere [12]. Briefly, twelve piglets were orally infected with 10^8 cfu of a *Salmonella* Typhimurium phagetype DT104 strain isolated from a naturally infected pig [12], whereas control group (4 animals) received sterile medium. Non-infected control pigs were necropsied prior to the experimental infection (0 day post-infection – dpi) and four randomly chosen infected piglets were necropsied at 1, 2 or 6 dpi. Samples of MLN were collected from all experimental animals and immediately frozen in liquid nitrogen for RNA and protein isolation or fixed in 10% neutral buffered formalin for histological

processing. All procedures involving animals were performed in accordance with the European regulations regarding the protection of animals used for experimental and other scientific purposes. Piglets were housed in experimental isolation facilities of the University of León (Spain). Animal care and procedures were in accordance with the guidelines of the Good Experimental Practices (GEP), under the supervision of the Ethical and Animal Welfare Committee of the University of León (Spain).

3.3.2.2 RNA purification

After treatment with RNAlater-ICE (Ambion, Inc, Austin, TX, USA), MLN samples were soaked in RLT buffer (Qiagen, Valencia, CA, USA) and disrupted in a rotor-stator homogenizer. RNA was isolated by using the AllPrep DNA/RNA/Protein Mini Kit (Qiagen), digested with the RNase-Free DNase Set (Qiagen) according to manufacturer instructions and routinely precipitated with ethanol. RNA integrity was evaluated using the Experion RNA chips (Bio-Rad, Hercules, CA, USA) before being quantified using a ND-1000 spectrophotometer (Nanodrop Technologies, Wilminton, USA).

3.3.2.3 Microarray analysis

Gene expression analysis was carried out using the GeneChip Porcine Genome Array by Affymetrix platform (Affymetrix Inc., Santa Clara, CA, USA) at the Genomics Unit of CABIMER (Andalusian Center for Molecular Biology and Regenerative Medicine, Seville, Spain). This chip contains 23,937 probe sets to interrogate 23,256 transcripts in pig, which represents 20,201 genes. The One-Cycle Eukaryotic Target Labeling Assay was used to obtain biotinylated cRNA to be used in the subsequent chip hybridization according to manufacturer instructions (Expression Analysis Technical Manual, Affymetrix). The biotinylated

cRNA targets were then cleaned up, fragmented, and hybridized with the GeneChip Porcine Genome Array following Affymetrix recommended protocols. Chips were washed, stained with a GeneChip Fluidics Station 450 (Affymetrix) using the standard fluidics protocol and scanned with an Affymetrix GeneChip Scanner 3000 (Affymetrix). Probe signal intensities were captured and processed with the GeneChip Operating Software 1.4.0.036 (Affymetrix) and the resulting CEL files were reprocessed using robust multi-array average normalization (RMA) [13]. Because the aim of analysis was to detect changes in gene expression along the time-course, differentially expressed (DE) genes were accessed by the BATS (Bayesian Analysis of Time Series) software package [14], using default settings. Bayes Factor (BF) value of 0.05 was used as cutoff to rank significantly regulated transcripts. Since the Affymetrix Porcine GeneChip is not fully annotated in all the features, it was re-annotated with Blast2GO [15] with a minimum E-value of 10^{-10} and a minimum similarity of 50%.

3.3.2.4 Systems biology analysis

The list of genes that showed significant changes in expression was uploaded into Ingenuity Pathway Analysis (IPA, Ingenuity Systems, www.ingenuity.com) for bioinformatic analysis. Additionally, DAVID Bioinformatic Database [16] was used applying the default settings to refine some data from IPA analysis. Gene interaction networks were automatically generated, ranked by score and depicted on IPA as follows: each node in the network diagram represented a gene and its relationship with other molecules was represented by a line (solid and dotted lines represent direct and indirect association respectively). Nodes with a red background were input genes detected in this study while grey nodes were molecules inserted by IPA based upon the Ingenuity Knowledge Base to produce a highly connected network. Score estimated the

probability that a collection of genes equal to or greater than the number in a network could be achieved by chance alone. Scores of 3 or higher were considered to have a 99.9% confidence of not being generated by random chance alone. For statistical analysis of enriched functions/pathways, IPA Knowledge Base was used as a reference set and Fisher's exact test was employed to estimate the significance of association. P-values bellow 0.05 were considered statistically significant. For canonical pathways graphical representation, ratio indicated the percentage of genes taking part in a pathway that could be found in uploaded data set and –log(p-value) meant the level of confidence of association. Threshold line represented a p-value of 0.05.

3.3.2.5 Relative gene expression analysis by qPCR

Real-time quantitative PCR (qPCR) assays were performed as previously described [12]. Fold change values were calculated by the $2^{-\Delta\Delta Cq}$ method [17] using beta-actin as reference gene. Afterwards, data were standardized as proposed by Willems et al. [18] and analyzed by Kruskal–Wallis and Mann–Whitney tests using the software SPSS 15.0 for Windows (SPSS Inc, Chicago, IL, USA). Fold changes of 1 denoted no change in gene expression. Values lower and higher than 1 denoted down and up-regulation respectively. To be represented in Table 1, fold change of down-regulated genes was calculated as $-1/2^{-\Delta\Delta Cq}$. Primer pairs used for amplifications can be found as supporting information [see Additional File 1].

3.3.2.6 Western blot analysis

For protein extractions, MLN samples from all experimental animals were separately homogenized on ice with lysis buffer (7 M urea, 2 M thiourea, 4% w/v CHAPS, 0.5 mM PMSF) using a glass tissue-lyser and protein lysate concentration

was determined using Bradford Protein Assay (Bio-Rad). Subsequently, protein from individual replicates belonging to the same group was pooled (30 ug total), electrophoretically fractionated in 12% (w/v) SDS-PAGE gels and transferred onto a PVDF membrane (Millipore, Bedford, MA, USA). Western blot assays were carried out as described by Martins et al. [10] employing the following primary antibodies: 4B7/8 (anti-SLAI) [19], 1F12 (anti-SLAII) [19], anti-CTLA4 (Epitomics,Burlingame, CA, USA) and anti-Clathrin light chain (ab24579, Abcam, Cambridge, UK). To confirm equal sample loading, membranes were reblotted with anti-GAPDH monoclonal antibody (GenScript, Picastaway, NJ, USA) and no statistical differences for GAPDH abundance were observed between groups in all assays. Membranes were scanned in a FLA-5100 imager (Fujifilm, Tokyo, Japan) and signal intensity was determined using Multigauge software (Fujifilm, Tokyo,Japan) as previously described [10].

3.3.2.7 Histopathology, immunohistochemistry and confocal microscopy analysis

Paraffin sections (5 μm) of formalin fixed samples were routinely processed and stained with hematoxylin and eosin (H&E) to evaluate tissue morphology. For immunohistochemistry assays, a standard avidin-biotin peroxidase method was performed as described elsewhere [20] employing 1F12 monoclonal antibody for swine histocompatibility class II antigen detection and a biotinylated anti-mouse Ig (Dako, Barcelona, Spain) as secondary antibody. Immunofluorescence using confocal microscopy was performed employing the mouse anti-SLAII 1F12 antibody, rabbit anti-*Salmonella* somatic antigen [10] and rabbit anti-*Salmonella* Typhimurium flagellin [21]. Fluorescein isothiocyanate (FITC)-conjugated goat anti-rabbit IgG (Sigma-Aldrich, St. Louis, MO, USA) and Alexa Fluor 594 anti-mouse IgG (Life Technologies, Carlsbad, CA, USA) were used

as secondary antibodies. Immunostaining was performed as described by Robertson et al. [22]. Briefly, deparaffinized sections of formalin fixed MLN were blocked for 30 min with 1% bovine serum albumin and 2% foetal calf serum in PBS. Then, sections were overnight incubated at 4°C with primary antibodies, three times washed with PBS for 5 min and incubated for 1 h at 37°C with fluorescent secondary antibodies. For negative controls, primary antibody was omitted. Finally, sections were three times washed for 5 min in PBS containing 1.43 μM 4',6-diamidino-2-phenylindole (DAPI, Life Technologies). Samples were subsequently evaluated and imaged using a LSM 5 Exciter confocal microscope (Carl Zeiss, Jena, Germany).

3.3.2.8 Cell death analysis

Formalin fixed MLN samples were evaluated for cell death by Terminal deoxynucleotidyl transferase dUTP nick end labeling (TUNEL), employing the TUNEL Apoptosis Detection Kit for Paraffin-embedded Tissue Sections (GenScript, Picastaway, NJ, USA) according to manufacturer instructions. Briefly, proteinase K treated samples were permeabilized with 0.1% Triton X-100 and 0.1% sodium citrate for 10 minutes and incubated with Blocking Solution II (GenScript) for 30 minutes. Subsequently, tissues were covered with 50 µl of TUNEL Reaction Mixture (GenScript), incubated at 37 °C for 1 h in a dark humidified chamber and washed in PBS. Sections were examined in a LSM 5 Exciter confocal microscope (Carl Zeiss MicroImaging GmbH, Jena, Germany) using excitation wave 450-500 nm and emission wave 515-565 nm (green). Fluorescence intensity was quantified with the ImageJ software 1.46r [23] and data were analyzed by ANOVA (p-value cutoff of 0.05) using SPSS 15.0 for Windows (SPSS Inc).

3.3.2.9 Selective capture of transcribed sequences (SCOTS)

Selective capture of *Salmonella* transcripts from MLN of pigs at 2 dpi was performed by the SCOTS method [11], following the procedure described by Sheikh et al. [24]. Briefly,5 µg of total RNA from infected MLN samples was converted into first strand cDNA by using random priming and Superscript III reverse transcription (Life Technologies). Subsequently second strand cDNA was produced employing DNA polymerase I (Klenow fragment, Life Technologies). To create a corresponding *in vitro Salmonella* Typhimurium cDNA sample for comparison, the same bacterial isolate employed in the experimental infection was grown to early-log growth phase (OD_{600}=0.3) and late-log growth phase (OD_{600}=0.8) in Luria Bertani (LB) broth. Afterwards, *Salmonella* Typhimurium transcripts were selectively captured from *in vivo* and *in vitro* double stranded cDNA by hybridization to sonicated biotinylated genomic *Salmonella* DNA, which was previously blocked with *Salmonella* ribosomal DNA fragments. Microbial cDNA-genomic DNA hybrids were then captured by binding to streptavidin-coated beads (Dynabeads M-280 streptavidin, Invitrogen) and bacterial transcripts were eluted by alkaline denaturation. Eluted bacterial cDNA was then PCR-amplified with conserved primers and finally purified using Qiagen PCR column purification kit (Qiagen). After that, one round captured and purified cDNA from both *in vitro* and *in vivo* conditions were quantified by spectrophotometry and used as template (10 ng) for qPCR assays as described above. Primer pairs used for amplifications can be found as supporting information [see Additional file 2]. Gene expression levels were estimated employing *gyrA* as reference gene. Since tissue from uninfected pigs was negative for *Salmonella*, those samples could not be used as reference for fold change calculations of pathogen gene expresion. Besides, most of screened genes showed Cq values inferior to those observed for *gyrA* in infected MLN. For these

reasons, gene expression levels were alternatively estimated as follows: *gyrA* Cq – target gene Cq. Higher values meant higher expression levels and vice-versa.

3.3.3. Results

3.3.3.1 Overview of gene expression in porcine MLN upon *Salmonella* Typhimurium infection

Microarray technology coupled to a Bayesian analysis was employed to explore the transcriptional response of porcine MLN to *Salmonella* Typhimurium at 1, 2 and 6 dpi. BATS method was specifically designed for the analysis of time series microarray data [10]. For this reason, this strategy was established aiming to provide a general panorama of changes undergone by tissue at the mRNA level during the early response to infection. Taking into account the entire studied time course, a total of 290 transcripts, representing 285 unique genes, showed levels of expression that changed significantly (BF<0.05) over time as a result of the bacterial challenge [see Additional file 3].

3.3.3.2 Validation of microarray data by qPCR

To validate microarray data, qPCR assays were performed on a panel of fourteen genes identified by BATS analysis. As expected, all of them were confirmed to be significantly regulated (p<0.05) after infection (Table 1). Furthermore, an identical expression trend along time was observed for most of the screened genes by qPCR and microarray analysis.

3.3.3.3 Biological interpretation of microarray data

To translate microarray data into functional biological information, bioinformatics tools were employed to gain an insight into networks, functions

and pathways associated to the transcriptomic response of porcine MLN to *Salmonella* Typhimurium [see Additional file 4].
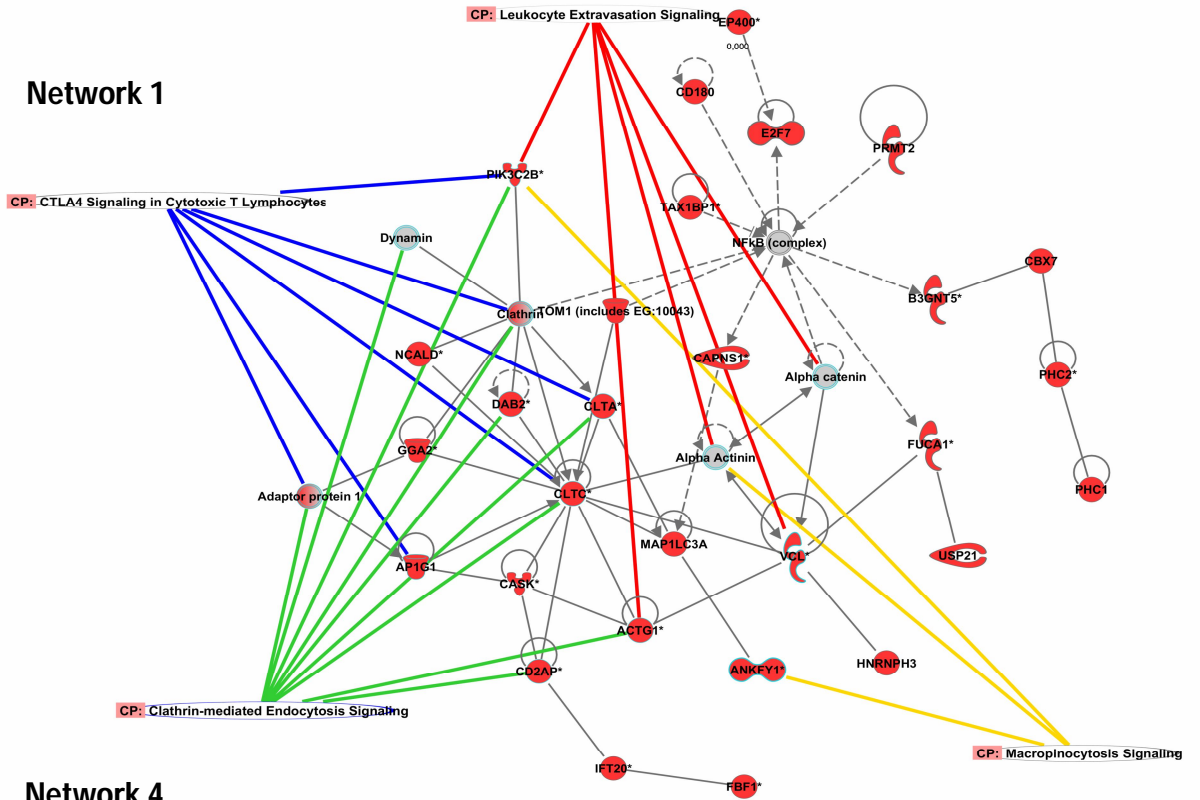
Table 1   Microarray data validation by qPCR -

Gene	MICROARRAY				qPCR			
	Fold change			BF	Fold change			p-value
	1 dpi	2 dpi	6 dpi		1 dpi	2 dpi	6 dpi	
CD180	1.7	2.6	1.5	0.0000429	1.1	1.8	1.2	0.010
CD1A	1.1	-1.4	1.2	0.00047793	-1.4	-2.5	1.2	0.013
DAB2	-1.2	-2.6	-1.2	6.62E-13	-3.1	-6.5	-2.6	0.001
EIF4H	-1.1	-1.1	-1.1	0.0000101	-1.5	-1.4	-1.8	0.021
ENPP6	1.3	2.0	-1.2	0.0000448	1.2	1.8	-1.7	0.000
F13A1	1.4	2.2	-1.1	0.00000227	1	1.7	-2.2	0.012
HLA-B[b]	1.0	-1.1	-1.2	0.00023747	-1.4	-1.4	-1.9	0.047
HLA-DRB5[b]	1.0	-1.1	1.0	0.0000311	-1.4	-1.6	-2	0.036
HSPA1B[a]	3.3	1.4	-1.1	0.0001166	2.5	1.4	-1.3	0.025
HSPH1	2.3	1.7	-1.0	0.00000424	1.5	1.1	-2	0.003
IL16	-1.0	-1.2	-1.1	8.12E-07	1	-1.1	-1.5	0.035
LPCAT2	1.2	2.3	1.0	0.0000146	1.4	2	-1.3	0.010
PSMC2	-1.0	-1.0	-1.1	0.00105861	-1.1	-1.4	-1.8	0.036
TRAC	-1.0	-1.1	-1.1	0.00000951	-1.5	-1.8	-1.8	0.010

aData from microarray analysis are mean values from two different probes. bAmplified with SLA-B and SLA-DRB5 primers.

IPA analysis generated 17 gene interaction networks integrated by molecules associated to mechanisms that play a relevant role in infectious processes, such as cell-mediated immune response, cell-to-cell signalling and interaction, tissue morphology, cell movement and cell death. Significantly, networks 1 and 4 (Figure 1) revealed direct relationships between molecules taking part in five of the ten top enriched canonical pathways after infection (Figure 2). Moreover, network 4 demonstrated the central role of heat shock proteins and MHC encoding genes in the establishment of different mechanisms carried out in MLN in response to *Salmonella* Typhimurium.

Network 1

CP: Leukocyte Extravasation Signaling

CP: CTLA4 Signaling in Cytotoxic T Lymphocytes

CP: Clathrin-mediated Endocytosis Signaling

CP: Macropinocytosis Signaling

Network 4

CP: Dendritic Cell Maturation

CP: Antigen Presentation Pathway

CP: Cytotoxic T Lymphocyte-mediated Apoptosis of Target Cells

CP: Communication between Innate and Adaptive Immune Cells
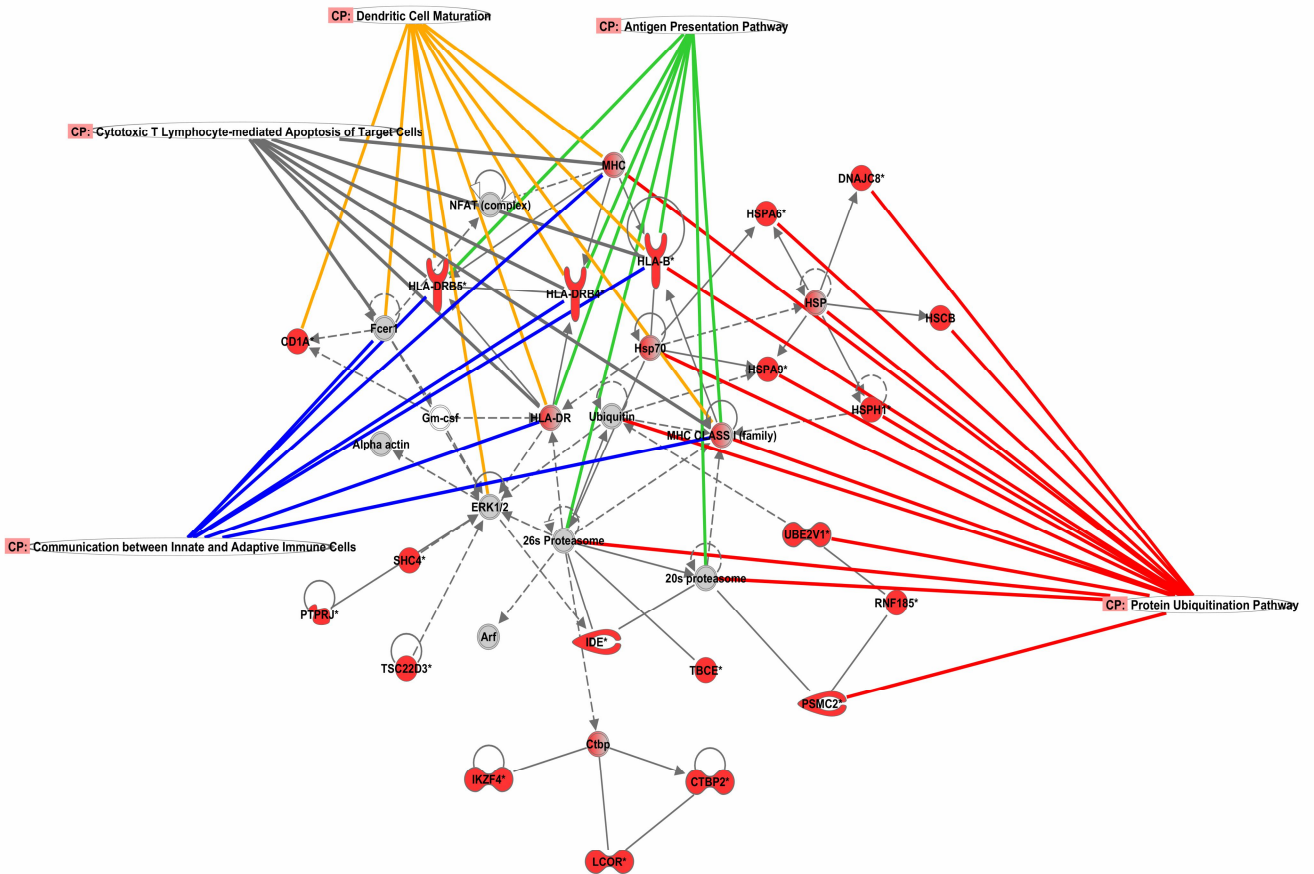
CP: Protein Ubiquitination Pathway

Figure 1 (*previous page*) - **Gene network analysis by Ingenuity Pathway Analysis (IPA)** Visual representation of networks 1 and 4. Red and grey nodes are input and IPA-inserted molecules respectively. Colored lines highlight genes that take part in an enriched Canonical Pathway.
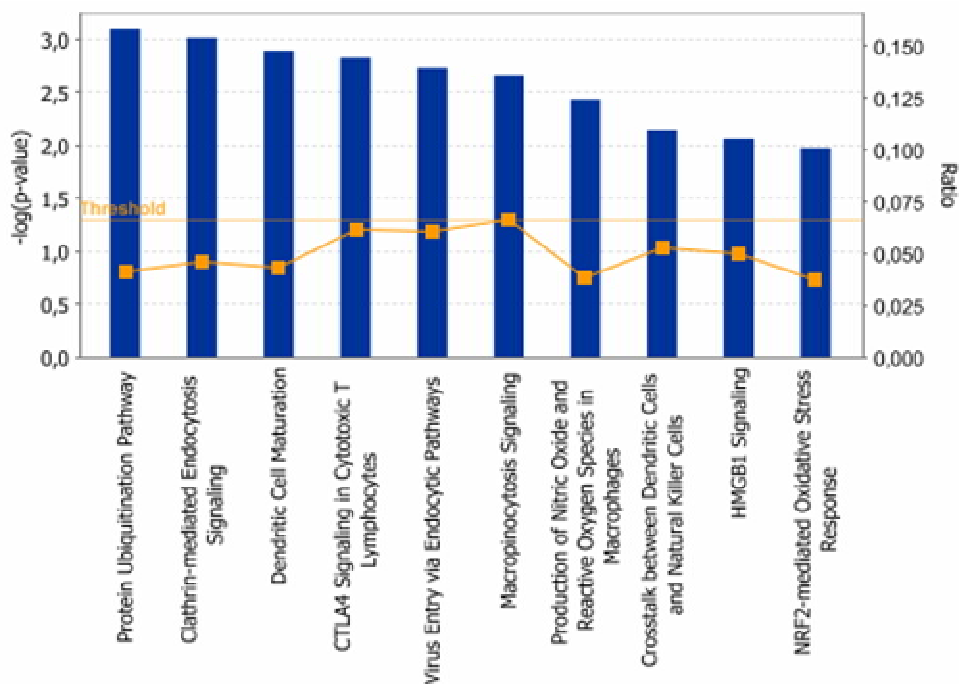

Figure 2 - Top 10 enriched canonical pathways. Blue bars and yellow squares denote –log(p-value) and ratio respectively. Threshold line represents a p-value of 0.05.

IPA also ascertained the enrichment of biological functions other than those identified by network analysis (Table 2). Thus, "Inflammatory disease" was the Ingenuity biofunction more significantly related to the differently expressed genes, followed by "Protein synthesis" and "Antigen presentation". Thus, "Inflammatory disease" was the Ingenuity biofunction more significantly related to the differently expressed genes, followed by "Protein synthesis" and "Antigen presentation".

Table 2 - Top five biological functions enriched in MLN of pigs infected with *Salmonella* Typhimurium*.*

Annotations	p-Value[a]	Input genes (n)
Inflammatory Disease	4,64E-05 -2,65E-02	13
Protein Síntesis	6,52E-05 -1,86E-02	32
Antigen Presentation	1,8E-04 -1,68E-02	5
Cell Death	1,8E-04 -2,67E-02	78
Cell-To-Cell Signaling and Interaction	1,8E-04 -2,67E-02	27

3.3.3.4 Modulation of immune response mechanisms

Wide transcriptomic data analysis by bioinformatics tools revealed an enrichment of distinct mechanisms involved in the triggering of immune response in porcine MLN upon *Salmonella* Typhimurium infection. Furthermore, network analysis demonstrated a possible connection between them and regulation of common genes (Figure 1). To explain in depth the significance of these results, a series of assays including western blot, qPCR, immunohistochemistry and confocal analysis was performed.

As illustrated in Figure 3A, the association between pathways "CTLA-4 signaling in cytotoxic T lymphocytes" and "Clathrin-mediated endocytosis signaling" was confirmed by the regulation of shared genes. Thus, we checked by western blot the abundance along time of cytotoxic T-lymphocyte-associated protein 4 (CTLA-4) and clathrin light chain A (CLTA), the key molecules in each pathway. An opposite trend was observed for these proteins, since CLTA was more abundant in infected animals whereas CTLA4 showed reduced levels after infection (Figure 3B). Since changes in *CTLA4* expression could not be detected by microarray analysis, we verified *CTLA4* mRNA levels by qPCR (Figure 3C). In accordance with western blot assays, *CTLA4* was observed to be significantly
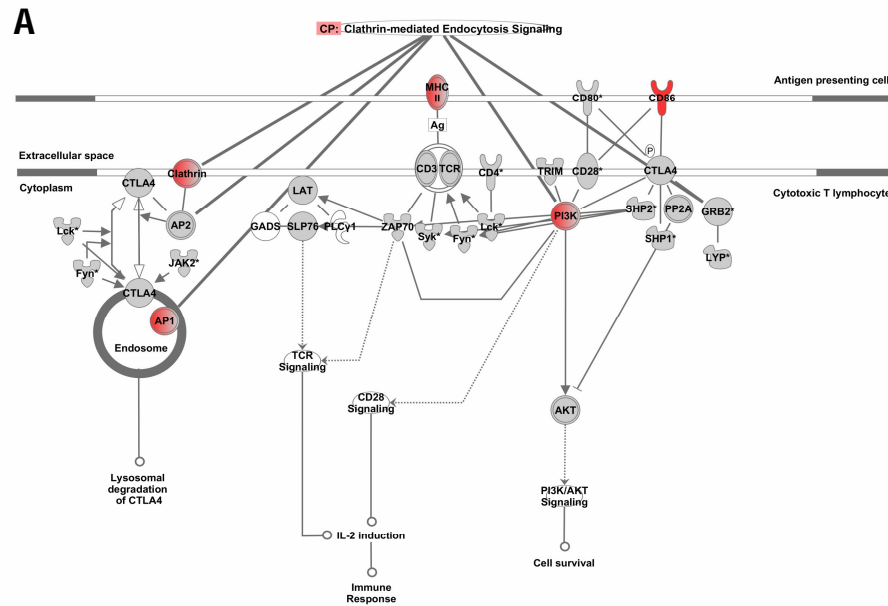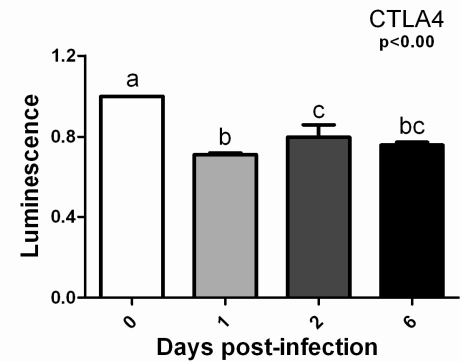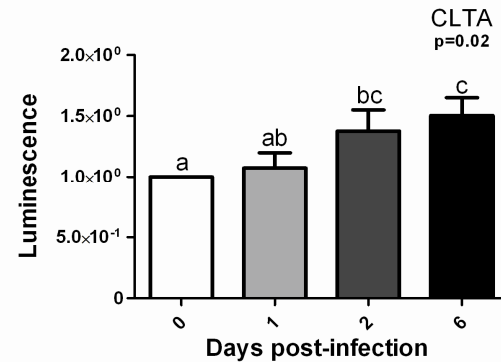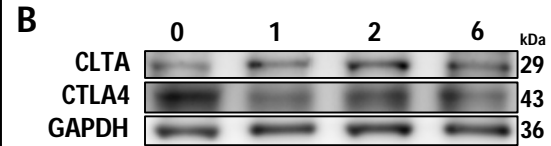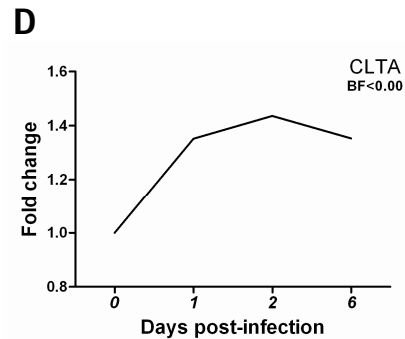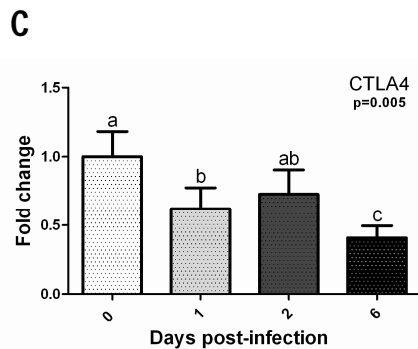
Figure 3 Interaction between CTLA-4 signaling in cytotoxic T lymphocytes and Clathrin-mediated endocytosis signaling pathways. A: visual representation of CTLA-4 signaling in cytotoxic T lymphocytes pathway stressing the regulation of molecules taking part in Clathrin-mediated endocytosis signaling. Red and grey nodes are input and IPA-inserted molecules respectively. B: western blot analysis of CTLA4 and CLTA in MLN at 1, 2 and 6 dpi. C: mRNA quantification of *CTLA4* by qPCR. D: expression pattern of *CLTA* mRNA by microarray analysis.

down-regulated in infected animals at 1 and 6 dpi. Concerning *CLTA*, a similar trend towards up-regulation was observed at mRNA (Figure 3D) and protein levels.

System biology analysis accomplished in this study also revealed the involvement of MHC encoding genes in many mechanisms triggered in MLN in response to *Salmonella* Typhimurium. For this reason, changes undergone by these molecules were evaluated employing different approaches. As shown in Figure 4A, western blot analysis demonstrated that major histocompatibility antigens class I (MHCI) and class II (MHCII) were more abundant in tissue at 1 dpi. Similarly, immunohistochemistry revealed a higher expression of MHCII at initial stages of infection, being labeling mainly detected in large irregularly-shaped mononuclear cells (Figure 4B-E). Interestingly, *Salmonella* location in MLN was previously observed by us in the cytoplasm of mononuclear phagocytes and neutrophils [10, 21]. So, confocal microscopic analysis was subsequently carried out to address the hypothesis that the increase of MHCII positive cells and the presence of *Salmonella* Typhimurium in tissue could be closely related events. As depicted in Figure 4H-K, *Salmonella* Typhimurium was detected in the cytoplasm of MHCII positive cells, morphologically identical to those identified by immunohistochemistry. Curiously, *MHCI* and *MHCII* (annotated in data sets as HLA-B and HLA-DRB, respectively) mRNA expression were found to be down-regulated by microarray analysis. Furthermore, as exposed in Table 1 and Figure 4F-G, similar results were uncovered by qPCR, confirming a divergence between transcriptomic and proteomic data obtained in MLN for these receptors.

3.3.3.5 Tissue morphology and cell death

"Cell death" was one of the most significantly altered biological functions after infection and integrated the highest number of differently expressed genes
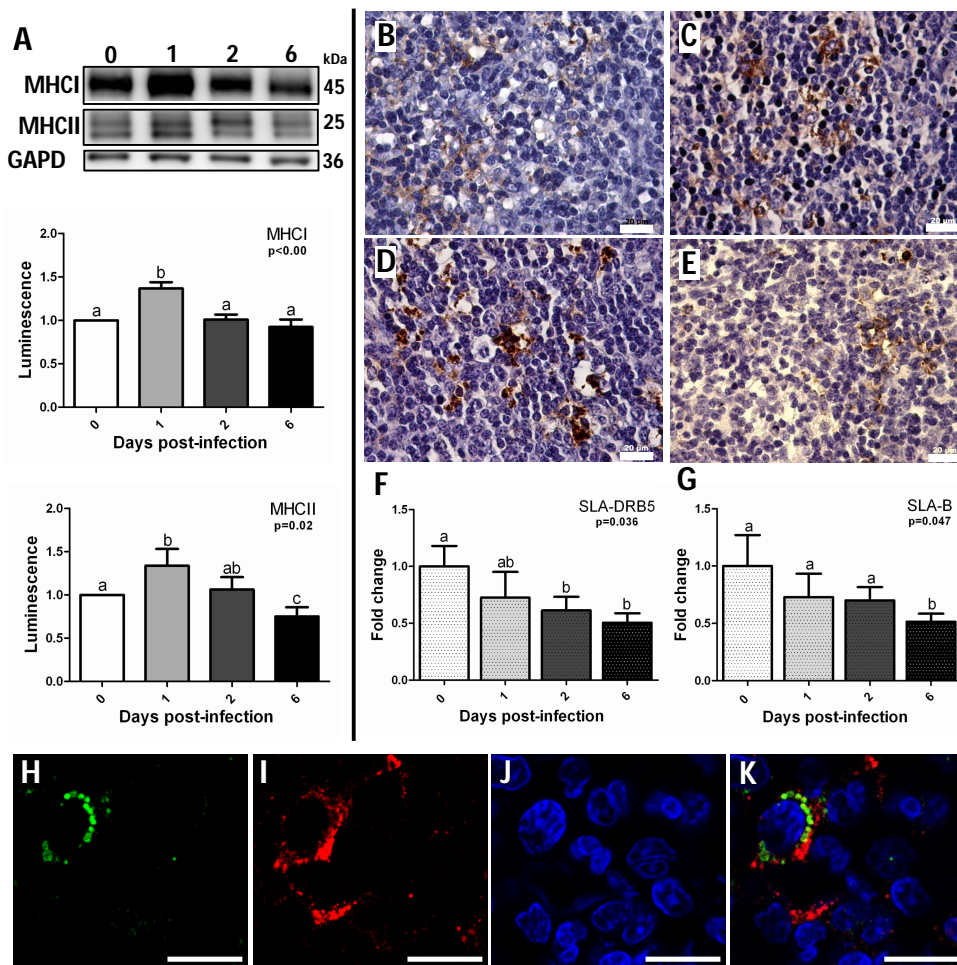
Figure 4 Analysis of MHC molecules in porcine MLN after *Salmonella* Typhimurium infection. A: western blot analysis of MHC class I and II at 1, 2 and 6 dpi. B-E: MHCII labeling in tissue at 0 (B), 1(C), 2 (D) and 6 (E) dpi by immunohistochemistry. Scale bar = 20 μm. F-G: mRNA quantification of SLA-DRB5 (MHCII) (F) and SLA-B (MHCI) (G) by qPCR. H-K: confocal analysis of *Salmonella* Typhimurium infected MLN demonstrate the presence of the pathogen in MHCII positive cells. *Salmonella* Typhimurium-FITC (H), MHCII-Alexa Fluor® 594 (I), DAPI (J) and merge (K).

(n=78). In order to find GO subcategories associated to genes implicated in this function, data set arranged into "Cell death" by IPA was loaded in DAVID Bioinformatic Database. As expected, enriched terms were related to cell proliferation, differentiation and death [see Additional file 5]. Among them, "Negative regulation of apoptosis" and "Antiapoptosis" could be highlighted

because most of genes taking part in these processes were overexpressed all along the time course, suggesting an inhibition of apoptosis. To deepen and sharpen these results, TUNEL analysis followed by confocal microscopy was performed aiming to elucidate the mechanisms of cell death in MLN after *Salmonella* Typhimurium infection. As shown in Figure 5A-D and 5I, DNA damage detected by TUNEL staining peaked at 1 dpi and decreased at 2 and 6 dpi compared to controls. Afterwards, expression level of the main pyroptosis and apoptosis inducers (*CASP1* and *CASP3*, respectively) was quantified by qPCR. *CASP1* mRNA was significantly up-regulated at 2 dpi and down-regulated at 6 dpi (Figure 5J), whereas no significant changes were observed for *CASP3* (Figure 5K). Finally, lymph-node sections were additionally H&E-stained to analyse the structural changes undergone by tissue as a consequence of infection (Figure 5E-H). Besides the loss of the typical lymph-node micro-architecture, phagocytes infiltration was the main tissue alteration revealed after infection, being observed mainly at 1 and 2 dpi.

3.3.3.6 *Salmonella* Typhimurium localization and gene expression *in vivo*

Confocal microscopy analysis was performed to localize *Salmonella* Typhimurium in tissue. Although bacteria were detected in MLN along the whole time course, higher *Salmonella* labelling was observed at 2 dpi (data not shown), agreeing with our previous observations [10, 21]. Pathogen was labelled as spherical structures located in the perinuclear zone of mononuclear cells (Figure 6A) as observed for bacteria confirmed to be localized in MHCII positive cells (Figure 4H-K). Conversely, in some cases, staining of regular bacilli shaped structures was uncovered (Figure 6B) and z-stack images suggested that *Salmonella* showing this labelling pattern could be positioned extracellularly [see Additional file 6]. Nevertheless, further experiments are necessary to confirm this
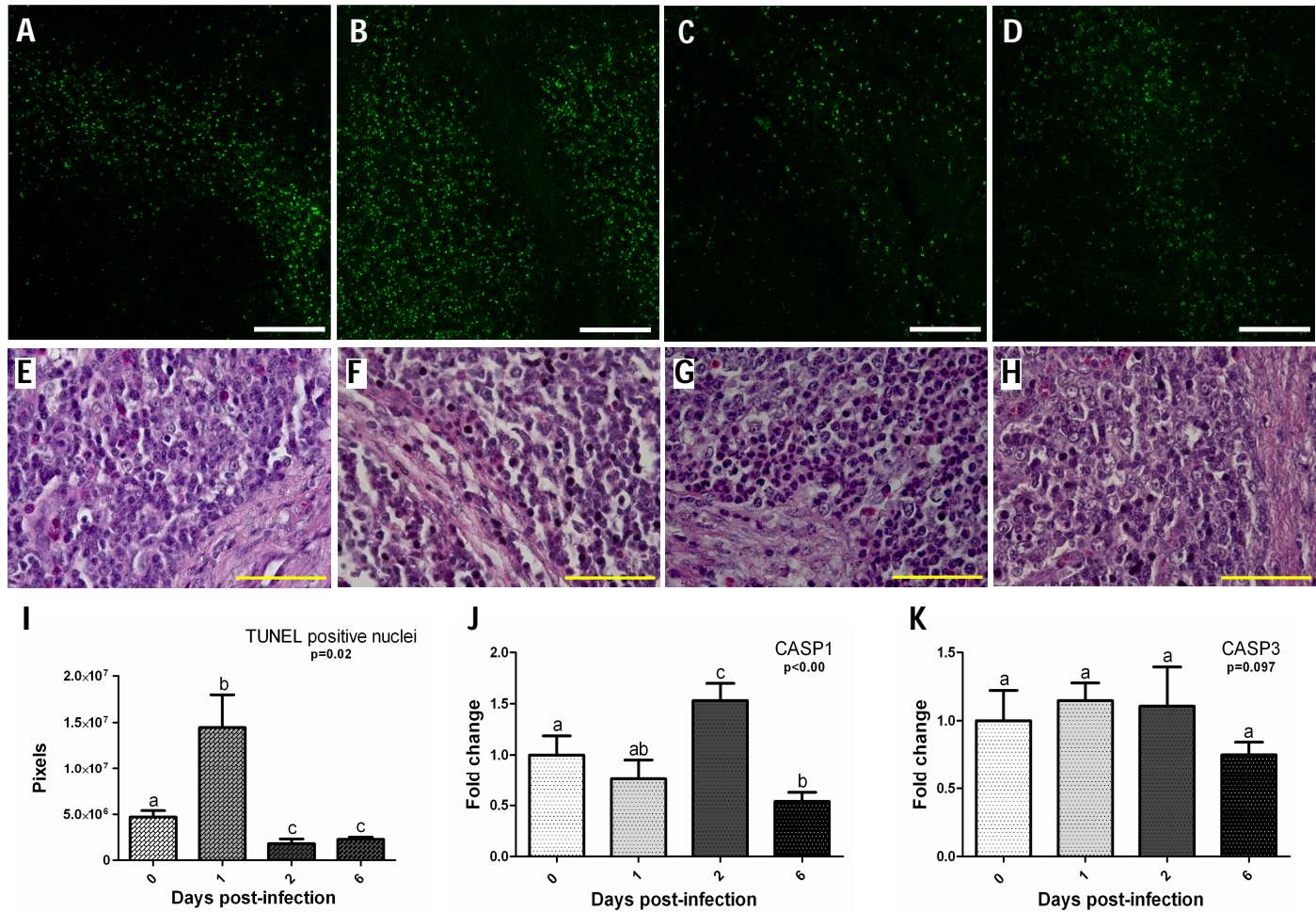
Figure 5 Cell death and histopathologic analysis of MLN from *Salmonella* Typhimurium infected pigs. A-D: Terminal deoxynucleotidyl transferase dUTP nick end labeling (TUNEL) analysis at 0 (A), 1(B), 2 (C) and 6 (D) dpi. Scale bar = 100 μm. E-H: H&E staining of at 0 (E), 1(F), 2 (G) and 6 (H) dpi. Scale bar = 50 μm. I: Quantification of TUNEL fluorescent labeling shows an increase of positive nuclei at 1 dpi and decrease to levels inferior to controls at 2 and 6 dpi. J-K: mRNA quantification of *CASP1* (J) and *CASP3* (K) by qPCR.
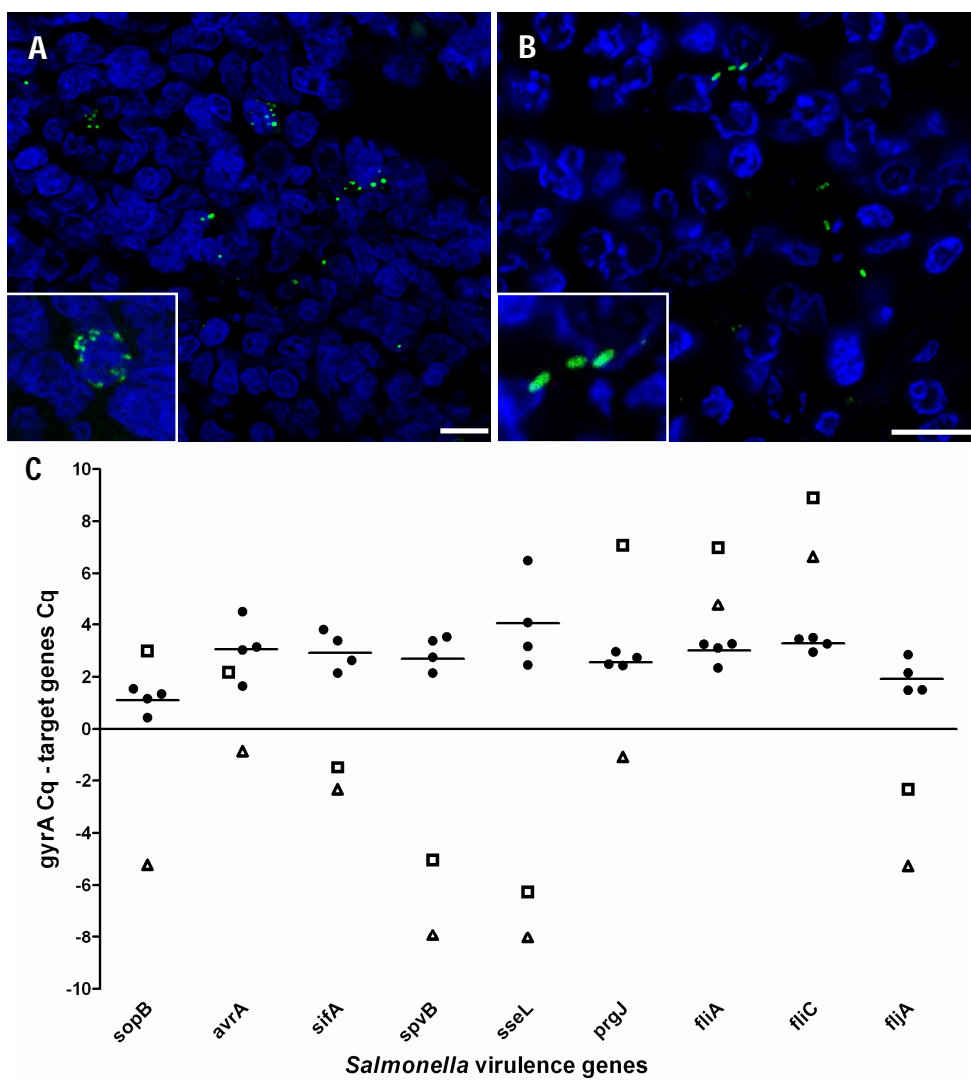
Figure 6 *Salmonella* Typhimurium labeling and gene expression in porcine MLN. A-B: Different labeling profiles found for *Salmonella* Typhimurium in porcine MLN. Scale bar = 10 µm. (A) Pathogen detection as spherical structures in the perinuclear zone of mononuclear cells. (B) Staining of bacilli shaped structures. E: Analysis of *Salmonella* Typhimurium gene expression by SCOTS *in vivo* and *in vitro*. Black dots and bars respectively represent individual and mean expression values from analysis of cDNA from pig infected MLN. Triangles (early logarithmic phase) and squares (late logarithmic phase) denote gene expression data from *Salmonella* Typhimurium cultures. Higher values mean higher expression levels and vice-versa.

hypothesis. Ultimately, expression of some *Salmonella* genes *in vivo* was also studied by SCOTS approach and compared to *in vitro* condition. Type III secretion systems (TTSS) encoded genes (*sopB, avrA, sifA, sseL* and *prgJ*) and *spvB* were found to be expressed by *Salmonella* Typhimurium in porcine MLN. Notably, comparing to *in vivo* condition, lower expression of these genes was detected in early log growth phase cultures. Similarly, higher levels of *sifA, spvB* and *sseL* mRNA expression were found in MLN when compared to late log growth phase culture. Results regarding genes coding for flagella components and regulators showed higher expression levels *in vitro* for *fliA, fliC* whereas *fljA* mRNA was observed more expressed *in vivo* (Figure 6C).

3.3.4. Discussion

Gut-associated lymphoid tissues have been proved to be an important niche for *Salmonella* Typhimurium during pig infections [5]. For this reason, in this work we aimed to dissect host response mechanisms occurring in the porcine MLN upon interaction with *Salmonella* Typhimurium. Besides, attempting to integrate information from both parties involved in disease, expression in tissue of some *Salmonella* genes was also studied after pig oral inoculation. It is known that *Salmonella* pathogenicity island 1 and 2 (SPI-1 and SPI-2) TTSS genes are required for intestinal and systemic infection respectively [25, 26]. Here, we found that both SPI-1 (*sopB* and *avrA*) and SPI-2 (*sifA* and *sseL*) encoded virulence factors were expressed in infected tissue, suggesting that invasion and intracellular survival inducers were employed by *Salmonella* to adapt itself to MLN milieu and cause infection.

Furthermore, system biology analysis reported in this study uncovered the enrichment of different endocytosis pathways, according to accumulating observations that *Salmonella* interacts extensively with host endocytic pathways

[27]. Thus, "Macropinocytosis pathway" was found by us to be implicated in the response of MLN to infection, in agreement with available knowledge that *Salmonella* TTSS effectors promote massive actin polymerization and lead to bacterial internalization by macropinocytic membrane extensions [28]. In addition, "Clathrin-mediated endocytosis signalling" was identified as the second most significantly affected canonical pathway upon infection. Although studies have demonstrated that clathrin-mediated endocytosis is used in bacterial-induced internalization, *Salmonella* is not able to employ this machinery to invade [29]. Therefore, we speculated that the enrichment of this process, added to the disclosed mediation of the "Protein ubiquitination pathway" after infection, is related to preceding evidences that *Salmonella* employ its SPI encoded effector SifA to remove mature MHCII complexes from cell surface, by enhancing their ubiquitination, in a clathrin and AP2-dependent way [30, 31, 32].

We observed that the *Salmonella* Typhimurium strain used in this work was able to express *sifA* in porcine MLN, suggesting that this evasion strategy could be triggered by pathogen to circumvent host response. *Salmonella* is expected to induce a strong immune response through specific antigen presentation to CD4 restricted T cells in the context of MHCII antigens [33]. Nevertheless, by reducing MHCII levels in antigen presenting cells, this pathogen may limit the induction of host T helper 1 (Th1) response. In line with this, it was previously observed by us [21] and others [34] that pig infections with *Salmonella* Typhimurium do not produce an up-regulation of Th1 response inducers in MLN.

The disclosed involvement of MHC molecules in several enriched mechanisms highlighted the central role of these receptors in the pig response to *Salmonella.* Curiously, both MHCI and MHCII encoding genes were observed to be down-regulated in porcine MLN after infection, although results from western blot and microscopy analysis revealed a significant increase in the abundance of these receptors at initial stages of infection. We envisage that these finds could

be attributed to infected antigen presenting cells that, upon contact with bacteria in intestine, express high levels of MHC and migrate to MLN. As depicted here and previously [10, 21], infection results in substantial changes in tissue cellularity, marked mainly by infiltration of phagocytes. Additionally, we were able to detect *Salmonella* Typhimurium in the cytoplasm of cells showing high levels of MHCII and the enrichment of "Dendritic Cell maturation" pathway as a consequence of the bacterial challenge. Our inference could be further supported by previous studies that report shuttle of *Salmonella* Typhimurium from intestine to mesenteric lymph-nodes by infected antigen presenting cells [5, 35].

In spite of the sophisticated strategies evolved by *Salmonella* Typhimurium to modulate host defence, our data indicated that the induction of some components of porcine adaptive immunity appears not to be repressed in infected MLN. Network analysis also associated "Clathrin-mediated endocytosis signaling" to "CTLA4 signaling in cytotoxic T lymphocytes pathway", bringing to light the role of the former process in adaptive immunity triggering. CTLA-4, an important negative regulator of the T cell immune response [36], is endocytosed via a clathrin and dynamin-dependent route in activated T-cells [37]. According to Johanns et al. [38], up-regulation of *CTLA-4* in regulatory T cells restrains effector T cell activation at early infection time points and allows the increase of bacterial burden during murine salmonellosis. Similarly, Inoue et al. [36] state that CTLA-4 mediated Treg immunosuppression is critical in preventing host from eliminating certain invasive pathogens. Given that, CTLA-4 down-regulation observed in this study, concurrent with clathrin up-regulation after the bacterial challenge could indicate the repression of a mechanism of T cell inhibition in porcine MLN upon *Salmonella* Typhimurium infection. However, since clathrin appears to be involved in the establishment of both host immunity mechanisms and virulence strategies evolved by pathogen, a deeper investigation of processes mediated by

this molecule during infection could provide novel knowledge on the pathogenesis of porcine salmonellosis.

High MHCI levels observed by western blot reinforce our previous evidences that *Salmonella* antigens are cross-presented in swine MLN [10], bringing out the induction of other adaptive immunity process upon infection. Cross-presentation results in CD8+ T cells priming by antigen presenting cells via their own MHCI molecules [33]. Interestingly, it has been reported that *Salmonella* is not able to reduce MHCI surface expression of infected cells and consequently avoid host early cytotoxic response [30, 31, 32]. Therefore, cross-presentation might contribute to *Salmonella* Typhimurium clearance in porcine MLN, in agreement with the stimulation of *Salmonella*-specific CD8 T cells readily observed in mice and human infections [40]. In addition, an evidence of humoral response induction was also uncovered by us. *CD180*, an inducer of B cells proliferation, activation and differentiation [41], was up-regulated all along infection. So, besides cellular immunity, humoral response seems to be promptly carried out in porcine MLN after *Salmonella* Typhimurium infection.

Among several layers of immune defence developed by mammals, cell death is a key component of host response aginst infection. Elimination of an infected cell can be beneficial or detrimental to both host and pathogen. Thus, each party utilizes a number of strategies to regulate the outcome of this process in its favour [42]. In a previous study, we suggested that apoptosis is avoided and infected cell undergoes pyroptosis in MLN of *Salmonella* Typhimurium infected swine [10]. Cells dying by pyroptosis have biochemical and morphological features of both apoptotic and necrotic cells [43]. As in apoptosis, pyroptotic cells show DNA fragmentation, nuclear condensation and positive TUNEL staining [42]. However, pyroptosis inherently results in inflammation due to caspase-1-mediated maturation of pro-IL-1β and pro-IL-18 and release of the cytoplasmic content, whereas apoptotic cell is considered to be immunologically silent [44].

Evidences of pyroptosis induction and apoptosis dampening in infected MLN were disclosed in the current study, supporting our previous reports [10, 21]. Besides the increase of TUNEL positive labelling at 1 dpi and infiltration of inflammatory cells observed in tissue, microarray data mining detected an enrichment of processes such as "Negative regulation of apoptosis" and "Antiapoptosis" after the bacterial challenge, in addition to up-regulation of genes encoding for inhibitor of apoptosis proteins (IAP) like XIAP and PDCL3. Induction of apoptosis has been asserted as a strategy that facilitates *Salmonella* cell-to-cell spread during systemic infection [45]. Nevertheless, it has also been reported that AvrA, a *Salmonella* effector protein, prevents the apoptotic elimination of host cell niche as a pathogen evasion mechanism [46]. Intriguingly, we observed *in vivo* expression of SpvB and SseL, both major *Salmonella* Typhimurium apoptosis inducers, and the apoptosis inhibitor AvrA, indicating that *Salmonella* appeared to execute virulence mechanisms to modulate apoptosis in porcine MLN in its favour. However, the balance of pathogen and host processes apparently avoided apoptosis induction and resulted in infected cell death by pyroptosis, producing pathogen discharge to the extracellular milieu and clearance of bacteria by innate mechanisms. In consequence of this response, swine MLN might be able to act as a barrier to dissemination of infection, as suggested by the notable reduction of pathogen burden in tissue previously reported by us [21].

Concordant with this, an elegant study by Miao et al. [47] stated that *Salmonella* Typhimurium is able to damper pyroptosis for its own advantage by avoiding flagellin expression during infection of mice. Interestingly, we found out expression of *Salmonella* Typhimurium flagella component (FliC) and regulators (FliA and FljA) in infected MLN. Additionally, flagella expression by infecting bacteria found in tissue was also corroborated by labelling using a specific polyclonal antibody. *S. enterica* alternately expresses two different flagellar

filament proteins, FljB and FliC, in a process known as flagellar phase variation. In spite of the high homology level found between these proteins, their middle surface exposed sequence of amino acids are divergent, resulting in distinct antigenicities [48]. Of note, our results demonstrated higher expression levels for *fliC* and its regulator *fliA in vitro* than *in vivo*. On the other hand, *fljA*, which is cotranscribed with *fljB*, was more expressed in *Salmonella* Typhimurium found *in vivo*. Moreover, this gene was notably less expressed than *fliA* and *fliC* in both early and late logarithmic phase cultures. Basing on this, we deduced a skewing toward FliC flagellin expression by bacteria *in vitro*. Besides, we drew the inference that a more heterogeneous flagellin expression is found in *Salmonella* Typhimurium replicating *in vivo* and that induction of flagellar phase variation could be a strategy adopted by this pathogen to hinder pig immune response. Expression of prg*J* was also uncovered in swine MLN. Curiously, repression of this efector has been reported as a mechanism of pyroptosis inhibition *in vivo* [49]. Thus, it could be inferred that absence of flagellin and *prgJ* repression by *Salmonella* Typhimurium found in tissue might enable pig to use pyroptosis to clear bacteria in gut associated lymph-nodes, protecting itself from pathogen dissemination.

Nevertheless, an issue that should be addressed by our assumption is why pathogen burden in tissue peaks after pyroptosis triggering. Miao and Rajan [49] state that in a single cell, pyroptosis only takes place at late times of infection, following bacteria replication. So, we speculated that increase of pathogen load at 2 dpi is resultant of release of replicated *Salmonella* from cells dead by pyroptosis. This could justify the detection of bacteria by confocal microscopy that, differently from structures labelled inside MHCII positive cells, showed a regular rod shape and appeared to be out of host cells. Extracellular localization of pathogen could be further supported by a previous report [50],

which asserts that *Salmonella* Typhimurium predominantly survives in an extracellular niche in the tonsils of infected pigs.

Notably, the presence of TUNEL positive cells in tissue was significantly reduced at 2 and 6 dpi, suggesting a decrease of cell death by apoptosis or pyroptosis. As with any physiological process, excessive pyroptosis is detrimental to host [42]. So, modulation of this pathway by host aiming to restore tissue integrity should be expected. Actually, we observed up-regulation of *MAP3K7* and *TRAF7*, both involved in NF-kB and survival pathways activation, at 2 and 6 dpi. However, evidences indicate that inhibition of caspase-dependent apoptosis primes cells towards programmed necrosis [51]. Since mechanisms that dictate the cellular decision to survive by activating NF-kB or to die through apoptosis or necroptosis are still unclear [52], further research is necessary to clarify these results.

In conclusion, provided results led us to infer that although the *Salmonella* Typhimurium strain employed in this study was able to express some of its major virulence effectors in porcine MLN, a combination of host triggered innate immunity mechanisms and an early T-cell cytotoxic response might overcome virulence strategies employed by pathogen. Besides preventing apoptosis, swine appears to take advantage of flagellin and prgJ expression by pathogen to induce pyroptosis in MLN. In this context, pyroptosis might consist in a host protective mechanism that prevents pathogen spread beyond gut-associated lymph-nodes. Furthermore, clathrin-mediated endocytosis appears to take part in the pathogenesis of infection. Nevertheless, role of this process in host and pathogen mediated processes remains to be clarified.

Competing interests

The authors declare that they have no competing interests.

Authors' contributions

RPM was responsible for the whole study, including lab work, data analysis and interpretation, as well as the writing of the manuscript. CA participated in the confocal analysis. JEG collaborated with SCOTS analysis. AC performed the experimental infection and collected the tissue samples. RB and MGC performed microarray data processing. JJG conceived and designed the project and participated in the interpretation and discussion of results, as well as in the writing of the manuscript. All authors read and approved the final manuscript.

Acknowledgements

References

1. EFSA. The European Union Summary Report on Trends and Sources of Zoonoses, Zoonotic Agents and Food-borne Outbreaks in 2009: *EFSA J* 2011, 9:2090.

2. Baptista FM, Halasa T, Alban L, Nielsen LR: Modelling food safety and economic consequences of surveillance and control strategies for *Salmonella* in pigs and pork. *Epidemiol Infect* 2011, 139:754-764.

3. Sánchez-Vargas FM, Abu-El-Haija MA, Gómez-Duarte OG: *Salmonella* infections: An update on epidemiology, management, and prevention. *Travel Med Infect Dis* 2011, 9:263-277.

4. Gopinath S, Carden S, Monack D: Shedding light on *Salmonella* carriers. *Trends Microbiol* 2012, 20:320-327.

5. Boyen F, Haesebrouck F, Maes D, Van Immerseel F, Ducatelle R, Pasmans F: Non-typhoidal *Salmonella* infections in pigs: a closer look at epidemiology, pathogenesis and control. *Vet Microbiol* 2008, 130:1-19.

6. Tuggle CK, Bearson SM, Uthe JJ, Huang TH, Couture OP, Wang YF, Kuhar D, Lunney JK, Honavar V: Methods for transcriptomic analyses of the porcine host immune response: application to Salmonella infection using microarrays. *Vet Immunol Immunopathol* 2010, 138: 280-291.

7. Wang YF, Couture OP, Qu L, Uthe JJ, Bearson SMD, Kuhar D, Lunney J, Nettleton D, Dekkers JCM, Tuggle CK. Analysis of porcine transcriptional response to *Salmonella enterica* serovar Choleraesuis suggests novel targets of NFkappaB are activated in the mesenteric lymph node. BMC Genomics 2008, 9:437.

8. Huang TH, Uthe JJ, Bearson SM, Demirkale CY, Nettleton D, Knetter S, Christian C, Ramer-Tait AE, Wannemuehler MJ, Tuggle CK. Distinct peripheral blood RNA responses to *Salmonella* in pigs differing in *Salmonella* shedding levels: intersection of IFNG, TLR and miRNA pathways. *PLos One* 2011, 6:e28768.

9. Collado-Romero M, Martins RP, Arce C, Moreno Á, Lucena C, Carvajal A, Garrido JJ. An in vivo proteomic study of the interaction between *Salmonella* Typhimurium and porcine ileum mucosa. *J Proteomics* 2012, 75: 2015-2026.

10. Martins RP, Collado-Romero M, Martínez-Gomáriz M, Carvajal A, Gil C, Lucena C, Moreno A, Garrido JJ: Proteomic analysis of porcine mesenteric lymph-nodes alter *Salmonella typhimurium* infection. *J Proteomics* 2012, 75: 4457-4470.

11. Graham JE, Clark-Curtiss JE: Identification of Mycobacterium tuberculosis RNAs synthesized in response to phagocytosis by human macrophages by selective capture of transcribed sequences (SCOTS). *Proc Natl Acad Sci USA* 1999, 96:11554–11559.

12. Collado-Romero M, Arce C, Ramirez-Boo M, Carvajal A, Garrido JJ: Quantitative analysis of the immune response upon *Salmonella typhimurium* infection along the porcine intestinal gut. *Vet Res* 2010, 41:23.

13. Irizarry RA, Hobbs B, Collin F, Beazer-Barclay YD, Antonellis KJ, Scherf U, Speed TP: Exploration, normalization, and summaries of high density oligonucleotide array probe level data. *Biostatistics* 2003, 4:249-264.

14. Angelini C, Cutillo L, De Canditiis D, Mutarelli M, Marianna Pensky: BATS: a Bayesian user-friendly software for Analyzing Time Series microarray experiments. *BMC Bioinformatics* 2008, 9:415

15. Conesa A, Götz S, García-Gómez JM, Terol J, Talón M, Robles M: Blast2GO: a universal tool for annotation, visualization and analysis in functional genomics research. *Bioinformatics* 2005, 21:3674-3676.

16. Huang da W, Sherman BT, Lempicki RA: Systematic and integrative analysis of large gene lists using DAVID bioinformatics resources. *Nat Protoc* 2009, 4:44-57.

17. Livak KJ, Schmittgen TD: Analysis of relative gene expression data using real-time quantitative PCR and the $2^{-\Delta\Delta CT}$ method. *Methods* 2001, 25:402-408.

18. Willems E, Leyns L, Vandesompele J: Standardization of real-time PCR gene expression data from independent biological replicates. *Anal Biochem* 2008, 379:127-129.

19. Bullido R, Gomez del Moral M, Alonso F, Ezquerra A, Zapata A, Sánchez C, Ortuño E, Alvarez B, Domínguez J: Monoclonal antibodies specific for porcine

monocytes/macrophages: macrophage heterogeneity in the pig evidenced by the expression of surface antigens. *Tissue Antigens* 1997, 49:403-413.

20. Yubero N, Jiménez-Marín A, Barbancho M, Garrido JJ: Two cDNAs coding for the porcine CD51 (α_V integrin subunit: cloning, expression analysis, adhesion assays and chromosomal localization. *Gene* 2011, 481:29-40.

21. Martins RP, Collado-Romero M, Arce C, Lucena C, Carvajal A, Garrido JJ: Exploring the immune response of porcine mesenteric lymph nodes to *Salmonella enterica* serovar Typhimurium: an analysis of transcriptional changes, morphological alterations and pathogen burden. *Comp Immunol Microbiol Infect Dis 2013,*36: 149-160.

22. Robertson D, Savage K, Reis-Filho JS, Isacke CM: Multiple immunofluorescence labelling of formalin-fixed paraffin-embedded (FFPE) tissue. *BMC Cell Biol* 2008, 9:13-22.

23. Schneider CA, Rasband WS, Eliceiri KW: NIH Image to ImageJ: 25 years of image analysis. *Nat Methods* 2012, 9:671-675.

24. Sheikh A, Charles RC, Sharmeen N, Rollins SM, Harris JB, Bhuiyan MS, Arifuzzaman M, Khanam F, Bukka A, Kalsy A, Porwollik S, Leung DT, Brooks WA, LaRocque RC, Hohmann EL, Cravioto A, Logvinenko T, Calderwood SB, McClelland M, Graham JE, Qadri F, Ryan ET: *In vivo* expression of *Salmonella enterica* serotype Typhi genes in the blood of patients with typhoid fever in Bangladesh. *PLoS Negl Trop Dis* 2011, 5:e1419.

25. Boyen F, Pasmans F, Van Immerseel F, Morgan E, Adriaensen C, Hernalsteens JP, Decostere A, Ducatelle R, Haesebrouck F. *Salmonella* Typhimurium SPI-1 genes promote intestinal but not tonsillar colonization in pigs. *Microbes Infect* 2006, 8: 2889-2907.

26. Yoon H, McDermott JE, Porwollik S, McClelland M, Heffron F: Coordinated regulation of virulence during systemic infection of *Salmonella enterica* serovar Typhimurium. *PLoS Pathog* 2009, 5:e1000306.

27. Srikanth CV, Mercado-Lubo R, Hallstrom K, McCormick BA: *Salmonella* effector proteins and host-cell responses. *Cell Mol Life Sci* 2011, 68:3687-3697.

28. Veiga E, Cossart P: The role of clathrin-dependent endocytosis in bacterial internalization. *Trends Cell Biol* 2006, 16:499-504.

29. Cossart P, Veiga E: Non-classical use of clathrin during bacterial infections. *J Microsc* 2008, 231:524-528.

30. Lapaque N, Hutchinson JL, Jones DC, Méresse S, Holden DW, Trowsdale J, Kelly AP: *Salmonella* regulates polyubiquitination and surface expression of MHC class II antigens. *Proc Natl Acad Sci USA* 2009, 106:14052-14057.

31. Van Parys A, Boyen F, Verbrugghe E, Leyman B, Bram F, Haesebrouck F, Pasmans F: *Salmonella* Typhimurium induces SPI-1 and SPI-2 regulated and strain dependent downregulation of MHC II expression on porcine alveolar macrophages. *Vet Res* 2012, 43:52.

32. Mitchell EK, Mastroeni P, Kelly AP, Trowsdale J: Inhibition of cell surface MHC class II expression by *Salmonella. Eur J Immunol* 2004, 34:2559-2567.

33. Eckmann L., Kagnoff MF: Cytokines in host defense against *Salmonella. Microbes Infect* 2001, 3:1191-1200.

34. Uthe JJ, Royaee A, Lunney JK, Stabel TJ, Zhao SH, Tuggle CK, Bearson SM: Porcine differential gene expression in response to Salmonella enterica serovars Choleraesuis and Typhimurium. *Mol Immunol* 2007, 44: 2900-2914.

35. Tam MA, Rydström A, Sundquist M, Wick MJ: Early cellular responses to Salmonella infection: dendritic cells, monocytes, and more. *Immunol Rev* 2008, 225:140-162.

36. Inoue S, Bo L, Bian J, Unsinger J, Chang K, Hotchkiss RS: Dose-dependent effect of anti-CTLA-4 on survival in sepsis. *Shock* 2011, 36:38-44.

37. Qureshi OS, Kaur S, Hou TZ, Jeffery LE, Poulter NS, Briggs Z, Kenefeck R, Willox AK, Royle SJ, Rappoport JZ, Sansom DM: Constitutive clathrin-mediated

endocytosis of CTLA-4 persists during T cell activation. *J Biol Chem* 2012, 287:9429-9440.

38. Johanns TM, Ertelt JM, Rowe JH, Way SS: Regulatory T cell suppressive potency dictates the balance between bacterial proliferation and clearance during persistent *Salmonella* infection. *PLoS Pathog* 2010, 6:e1001043.

39. Houde M, Bertholet S, Gagnon E, Brunet S, Goyette G, Laplante A, Princiotta MF, Thibault P, Sacks D, Desjardins M: Phagosomes are competent organelles for antigen cross-presentation. *Nature* 2003, 425:402-406.

40. Lee SJ, Dunmire S, McSorley SJ: MHC class-I-restricted CD8 T cells play a protective role during primary *Salmonella* infection. *Immunol Lett* 2012, 148:138-143.

41. Chaplin JW, Kasahara S, Clark EA, Ledbetter JA: Anti-CD180 (RP105) activates B cells to rapidly produce polyclonal Ig via a T cell and MyD88-independent pathway. *J Immunol* 2011, 187:4199-4209.

42. Labbé K, Saleh M: Pyroptosis: A Caspase-1-dependent programmed cell death and a barrier to infection. In *Progress in Inflammation Research: The Inflammasomes.* Edited by Couillin I, Pétrilli V, Martinon F. Basel: Springer Basel AG; 2011:17-36.

43. Duprez L, Wirawan E, Vanden Berghe T, Vandenabeele P: Major cell death pathways at a glance. *Microbes Infect* 2009, 11:1050-1062.

44. Fink SL, Cookson BT: Apoptosis, pyroptosis, and necrosis: mechanistic description of dead and dying eukaryotic cells. *Infect Immun* 2005, 73:1907-1916.

45. Haimovich B, Venkatesan MM: *Shigella* and *Salmonella*: death as a means of survival. *Microbes Infect* 2006, 8:568-577.

46. Wu H, Jones RM, Neish AS. The *Salmonella* effector AvrA mediates bacterial intracellular survival during infection *in vivo. Cell Microbiol* 2012, 14:28-39.

47. Miao EA, Leaf IA, Treuting PM, Mao DP, Dors M, Sarkar A, Warren SE, Wewers MD, Aderem A: Caspase-1-induced pyroptosis is an innate immune effector mechanism against intracellular bacteria. *Nat Immunol* 2010, 11:1136-1142.

48. Bonifield HR, Hughes KT: Flagellar phase variation in *Salmonella* enterica is mediated by a posttranscriptional control mechanism. *J Bacteriol* 2003, 185:3567-3574.

49. Miao EA, Rajan JV: *Salmonella* and caspase-1: a complex interplay of detection and evasion. *Front Microbiol* 2011, 2:85.

50. Van Parys A, Boyen F, Volf J, Verbrugghe E, Leyman B, Rychlik I, Haesebrouck F, Pasmans F. *Salmonella* Typhimurium resides largely as an extracellular pathogen in porcine tonsils, independently of biofilm-associated genes csgA, csgD and adrA. *Vet Microbiol* 2010, 144:93-99.

51. Moquin D, Chan FK: The molecular regulation of programmed necrotic cell injury. *Trends Biochem Sci* 2010, 35:434-441.

52. Christofferson DE, Yuan J: Necroptosis as an alternative form of programmed cell death. *Curr Opin Cell Biol* 2010, 22:263-268.

3.4 Innate and adaptive immune mechanisms are effectively induced in ileal Peyer's patches of *Salmonella typhimurium* infected pigs

Rodrigo Prado Martins[a], Valentina Lorenzi[a], Cristina Arce[a], Concepción Lucena[a], Ana Carvajal[b], Juan José Garrido[a]

[a]Grupo de Genómica y Mejora Animal, Departamento de Genética, Facultad de Veterinaria, Universidad de Córdoba, Campus de Rabanales, Edificio Gregor Mendel C5, 14071
Córdoba, Spain
[b]Departamento de Sanidad Animal, Facultad de Veterinaria, Universidad de León, 24071 León, Spain

Abstract

In this report we employed laser-capture microdissection (LCM) coupled to qPCR technology and bioinformatic analysis to characterize, for the first time, the response of Peyer's patches (PP) from orally infected animals to *Salmonella typhimurium*, in a model of non-typhoidal salmonellosis. Pathogen was highly found in the cytoplasm of phagocytes in PP and differential gene expression analysis indicated an up-regulation of proinflammatory molecules, establishment of a Th1 driven response and triggering of DC and T-cell activity. Furthermore, predictions by bioinformatic analysis pointed to an activation of processes regarding stimulation and maturation of DC, influx of leukocytes in tissue and T lymphocytes priming and differentiation. In short, the approach used in this study proved to be a promising strategy to explore infectious processes. Indeed, it revealed an effective induction of innate and adaptive immune mechanisms in swine PP which appear to be distinct from those observed in mesenteric lymph nodes and closely related to response of gut mucosa.

Keywords - Peyer's patches, *Salmonella typhimurium*, Laser-capture microdissection, Immune response.

3.4.1 Introduction

Despite the current improvement in sanitation and hygiene, *Salmonella* persists as a significant cause of disease worldwide. Data from the Centers for Disease Control (CDC) assert that *Salmonella* alone causes approximately 1 million foodborne infections annually in the United States (CDC, 2011). Similarly, *Salmonella* is reported as the main cause of food-borne outbreaks in the European Union, being *Salmonella enterica* serovar Typhimurium (herein *Salmonella typhimurium*) the second most frequently isolated serovar from human infections (EFSA, 2012).

Advances in mammalian models of *Salmonella* infection are expected to result in new understanding of salmonellosis pathogenesis, contributing to the control and cure of human cases (Gopinath et al., 2012). In this context, pigs can be stressed as an ideal model for investigating human non-typhoidal salmonellosis, since upon infection with *S. typhimurium* swine undergo a self-limiting enterocolitis similar to the clinical manifestation observed in man.

Studies on the murine model of typhoid fever state that to cause infection, ingested *S. typhimurium* primarily invade M cells in the small intestine and then accesses Peyer's patches (PP), resulting in a massive inflammatory response in these organs (Broz et al.,2012). Therefore, besides their role in the immune surveillance of the intestinal lumen, PP are relevant mediators of infections by *S. typhimurium*. Although previous studies have employed gut loops models to extrapolate the response of PP to *S. typhimurium* (Meurens et al., 2009; Nunes et al., 2010), the function of these organs in the context of oral non-typhoidal infections has never been explored to date. To address this issue, we employed for the first time laser-capture microdissection (LCM) coupled to qPCR

technology and bioinformatic analysis to provide an accurate view of the immune mechanisms modulated in PP of pigs orally infected with *S. typhimurium*.

3.4.2. Material and methods

3.4.2.1. Experimental infection

Eight crossbred piglets of approximately four weeks of age, confirmed to be fecal-negative for Salmonella, were randomly allocated to control or infected groups (four animals each), being control (0 day post-infection — dpi) pigs necropsied 2 h before the experimental infection. Pigs belonging to the infected group were orally challenged with 108 cfu of *S. typhimurium* phagetype DT104 and euthanized at 2 dpi. Ileum samples were collected from all piglets and immediately frozen in liquid nitrogen for RNA isolation or fixed in 10% neutral buffered formalin for immunohistochemistry

3.4.2.2. Laser-capture microdissection and RNA preparations

Frozen gut samples from all experimental animals were embedded in optimal cutting temperature compound (Sakura Finetek USA, Torrance, CA, USA) and cut into serial 20 lm sections. Before microdissection, eight cryostat sections from each pig were mounted on glass slides and treated with RNAlater-ICE (Ambion) according to manufacturer instructions. Subsequently, PP follicles were laser-microdissected and captured from terminal ileum sections avoiding contamination by adjacent cells with a PALM Micro-Beam device (Carl Zeiss MicroImaging GmbH, Jena, Germany), by Auto-Laser Pressure Catapulting (LPC) mode (Fig. 1A–C). Catapulted tissue was soaked in 15 ll of RLT buffer (Qiagen, Valencia, CA, USA) poured in 200 ll microtubes caps and RNA purifications were carried out employing the RNeasy Mini Kit (Qiagen). Eluted RNA was digested

with RNase-Free DNase Set (Qiagen) and RNA quality was checked by Experion RNA analysis (Bio-Rad, Hercules, CA, USA). Finally, RNA was amplified using the SuperScript™ RNA Amplification System (Invitrogen, Carlsbad, CA, USA), as indicated by manufacturer.

3.4.2.3. Real-time quantitative PCR (qPCR)

Amplified RNA from infected and control animals was reverse transcribed to cDNA using the qScript cDNA Synthesis kit (Quanta BioSciences, Gaithersburg, MD, USA) and qPCR assays were performed according to Martins et al. (2013) to determine the relative expression of 30 genes coding for molecules taking part in distinct immune response processes such as inflammation, DC-T cell interaction and T helper cell response. Primers used for amplifications can be found as supporting information (see Supplementary File 1). Afterwards, relative gene expression was assessed by the $2^{-\Delta\Delta Cq}$ method (Livak and Schmittgen, 2001). In this analysis, qPCR data were presented as the fold change in gene expression normalized to an endogenous reference gene and relative to the uninfected controls. Fold change values higher than 1 meant upregulation. Values inferior to 1 were calculated as -1/fold change and denoted down-regulation. Data were analyzed by Student's t-test using the software SPSS 15.0 for Windows® (SPSS, Inc). A p-value bellow 0.05 was considered statistically significant.

3.4.2.4. Bioinformatic data analysis

Ingenuity Pathway Analysis (IPA, Ingenuity Systems, www.ingenuity.com) Downstream Effects tool was used to identify functions that are expected to be activated in tissue, given the observed gene expression patterns. Predictions were made by z-score algorithm and values higher and lower than 2 meant that activation state was statistically increased and decreased respectively. IPA Path

Designer was also employed to illustrate some mechanisms modulated by genes evaluated in this study.

3.4.2.5. Immunohistochemistry

To verify the presence of *S. typhimurium* in PP, paraffin sections (5 μm) of formalin fixed samples were routinely processed and immunostained as described elsewhere (Martins et al., 2013), employing a specific anti-*Salmonella* rabbit antiserum.

3.4.3 Results and discussion

Ileal loops models have provided valuable information regarding the response of gut mucosa to *Salmonella*. Nevertheless, accumulating evidences indicate that ingested *Salmonella* undergo phenotypical changes during its passage along host gastrointestinal tract that influence the infectious process (Alvarez-Ordóñez et al., 2011). Thus, it could be speculated that infection conditions employed by this approach is substantially different from those found in natural infections. Basing on this, in this report we describe for the first time the regulation of immune response mechanisms in the PP of orally infected animals, in the context of nontyphoidal salmonellosis. Besides, LCM was used to isolate and analyze cell exclusively from PP follicles. Microdissection has been successfully employed in cancer research to provide precise knowledge on tumor biology (Cheng et al., 2013). Here, LCM coupled to qPCR technology enabled us to characterize changes in infected PP with reduced interference from non-target cells, generating more accurate data than previously reported.

Immunohistochemistry assays demonstrated that *S. typhimurium* was notably found in PP (Fig. 1D and E), agreeing with preceding reports that highlight these organs as the main portal of pathogen entry to host mucosa (Broz et al.,
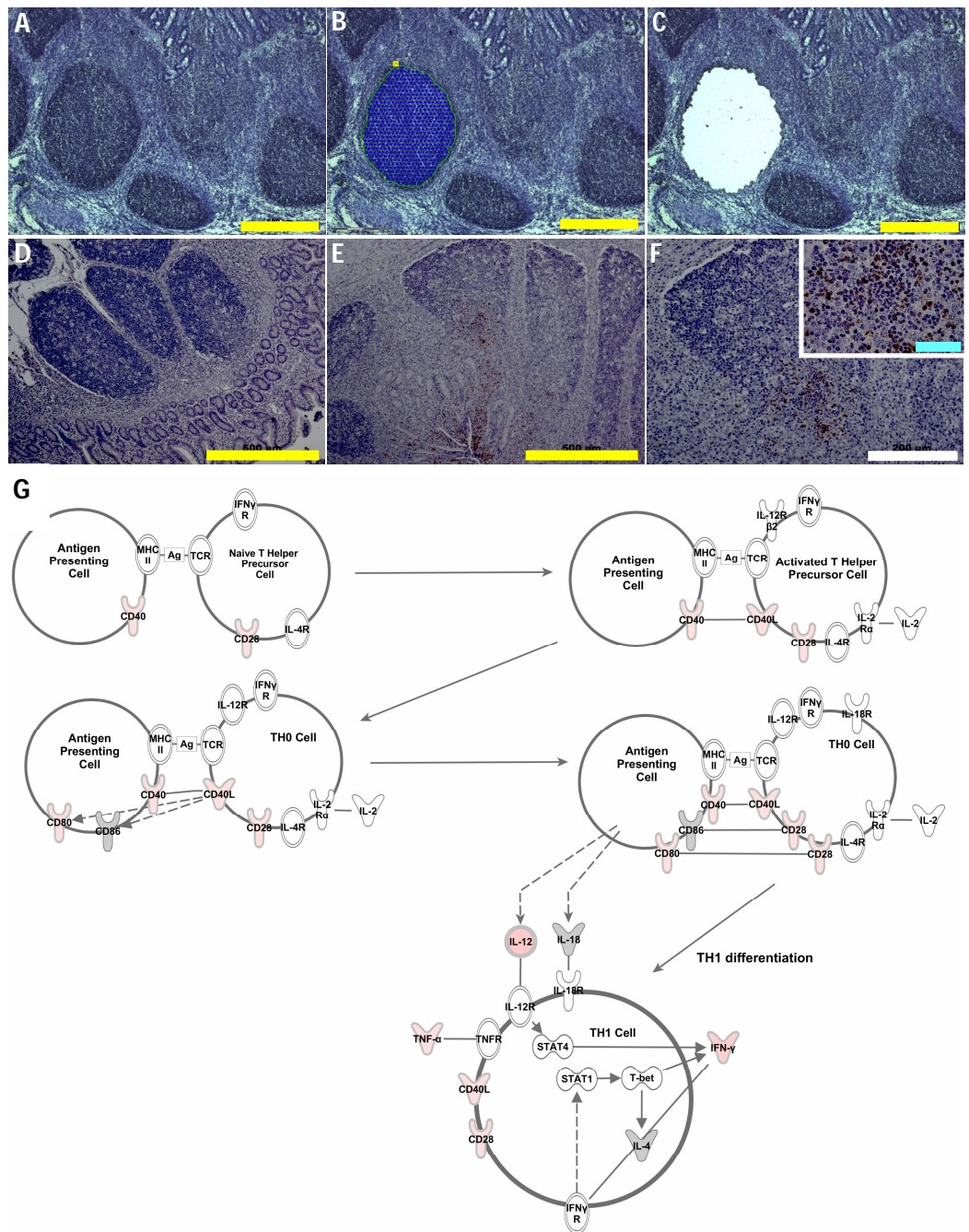
Figure 1. - Laser-capture microdissection, pathogen detection and gene expression analysis in Peyer's patches of *S. typhimurium* infected pigs. (A–C) LCM: After their identification in tissue (A), PP follicles were selected (B) and collected by Auto-Laser Pressure Catapulting mode (C). (D–F) Immunohistochemistry: *S. typhimurium* was immunolabeled in control (D) and infected tissue (E–F). Yellow, white and blue bars correspond to 500, 200 and 50 lm respectively. (G) Visual representation of T-helper cell

2012; Schauser et al., 2004). Moreover, differential expression analysis revealed significant regulation of 21 out 30 genes encoding pattern-recognition receptors (PRR), chemokines, DC and T-cell activation markers, Th response mediators and other immune-related molecules (Table 1). Proinflammatory genes such as IL1b, CXCL2 and TNFa were found to be upregulated as a consequence of infection. This response could be associated to recognition of invading Salmonella via PRR by macrophages and dendritic cells in PP, resulting in pathogen phagocytosis, secretion of chemokines and recruitment of additional inflammatory cells into the site of invasion (Broz et al., 2012). In line with this, a strong up-regulation was uncovered for all screened PRR (TLR2, 4, 5, 8 and NOD2) and pathogen labeling was mainly observed in the cytoplasm of large irregular-shaped mononuclear cells and some polymorphonuclear cells (Fig. 1F). Inflammation induced by IL1 has been considered a key mechanism in *Salmonella* pathogenesis at mucosa level (Raupach et al., 2006). However, a previous report employing porcine gut loops did not detect up-regulation of IL1β and chemokines encoding genes in PP upon *S. typhimurium* infection (Meurens et al., 2009). Although we believe that this discrepancy could be attributed to differences between approaches, PP areas not analyzed by us, such as dome and interfollicular zones, might affect the response of these organs to infection. Thus, this fact could also justify the observed differences between current study and others on the whole PP.

In general, results indicated that similarly to the murine typhoid model (Tam et al., 2008), mechanisms of innate immune response are effectively induced in PP during swine oral infections by *S. typhimurium*. Apart from contributing to bacterial clearance in tissue, as suggested by our previous observations (Martins et al.,2013), this response could be related to triggering of host second line of defense. Genes coding for molecules involved in DC activation (CD80, CD83, CD40, IL12p40, IL23p19 and CCR7) were found to be up-regulated in infected PP (Supplementary File 2).

Table 1 - Relative gene expression in Peyer's Patches of pigs experimentally infected with *S.typhimurium*, at 2 dpi.

Gene	0 dpi		2 dpi		p-value[b]
	FC[a]	SD	FC	SD	
CASP1	1	1.26	2.66	3.51	0.266
CCL19	1	0.12	3.47	0.81	0.000
CCL21	1	0.72	2.98	3.09	0.292
CCR7	1	0.57	5.98	2.16	0.002
CD11b	1	0.32	6.53	1.51	0.000
CD28	1	1.01	6.96	3.38	0.028
CD40	1	0.29	3.66	0.89	0.001
CD40L	1	0.27	2.02	0.56	0.020
CD80	1	0.62	9.69	6.34	0.006
CD83	1	0.20	2.07	0.41	0.012
CD86	1	0.34	1.19	0.50	0.710
CTLA4	1	0.69	3.96	2.91	0.142
CXCL2	1	0.33	5.78	2.85	0.002
IL1β	1	1.29	79.22	43.06	0.004
IL4	1	1.02	1.38	1.05	0.868
IL12p40	1	0.97	20.22	19.15	0.007
IL13	n.a.	n.a.	n.a.	n.a.	n.a.
IL16	1	0.73	1.43	1.41	0.902
IL17A	n.a.	n.a.	n.a.	n.a.	n.a.
IL18	1	0.42	1.07	0.52	0.940
IL21	1	0.32	3.93	2.97	0.032
IL23	1	0.16	2.58	0.25	0.000
IFNγ	1	0.96	17.66	9.94	0.005
NOD2	1	0.72	16.48	20.82	0.042
SELL	1	0.13	-2.5	0.026	0.000
TLR2	1	0.82	17.14	8.37	0.013
TLR4	1	0.11	2.23	0.92	0.015
TLR5	1	0.38	14.05	7.45	0.001
TLR8	1	0.56	4.67	2.17	0.005
TNFα	1	0.24	2.41	0.51	0.002

a Fold change mean values (n = 4 per group). Values higher than 1 meant upregulation. Those inferior to 1 were calculated as _1/fold change and denoted down-regulation. b p-values bellow 0.05 were considered statistically significant. n.a.: not amplified.

The same was observed for molecules required for T-cell mediated processes (IFNγ, CD40L, CD28, CCL19 and IL21). Of note, high mRNA levels were observed for IFNγ and IL12p40, despite the absence of IL18 up-regulation. Although this interleukin act synergistically with IL12 in the induction of IFNγ production and cell-mediated immunity, a previous study demonstrated that IL-18 is relevant for resistance to the systemic infection but not during the intestinal phase of salmonellosis (Raupach et al., 2006). Concurrently, down-regulation or absence of expression was uncovered for Th2 (IL4 and IL13) and Th17 (IL17A) inducers, suggesting a trend to Th1 orientation in *S. typhimurium* infected PP (Fig. 1G). In accordance with these observations, Collado-Romero et al. (2012) detected a general trend toward down-regulation of Th2 and Th17 responses in ileum mucosa of *S. typhimurium* infected pigs, validating the importance of processes carried out by PP in the development of immune response at mucosal level during non-typhoidal salmonellosis. To further confirm results from differential expression analysis, a bioinformatic algorithm was used to predict the modulation of some immunity mechanisms after infection, by combining results disclosed for the screened genes and relating them with the available literature. Processes such leukocytes recruitment, stimulation of DC and macrophages, DC maturation and influx of neutrophils were predicted to be activated as a consequence of infection. The same was detected for mechanisms of T lymphocytes proliferation, priming and differentiation (see Supplementary File 3).

Intriguingly, up-regulation of Th1 response was not observed by us in mesenteric lymph nodes (MLN) of *S. typhimurium* infected pigs. Furthermore, contrary to the clear induction of DC and T-cell activity uncovered by current results, DC-T-cells interaction was inferred to be compromised in these organs after infection (Martins et al., 2013). Therefore, it is tempting to speculate that, in spite of their similar functions as components of gut associated lymphoid tissue, PP trigger mechanisms distinct from those occurring in MLN upon oral infection

with *S. typhimurium*. Besides, it could be deduced that inhibition of T-cell activation by DCs, largely reported as an evasion mechanism evolved by *S. typhimurium* (Bueno et al., 2012), might not be induced in swine PP or is effectively counteracted by host response.

In short, combination of an in vivo infection model with LCM and gene expression analysis proved to be a promising strategy to clarify the role of specific cell populations during infectious processes. This approach enabled us to gain an insight into the immunity mechanisms carried out in PP during non-typhoidal salmonellosis. Results pointed to an effective induction of innate and adaptive immune responses in this organs, inferred to be different from those observed in MLN and closely related to the processes carried out at intestinal mucosa after infection. Data provided here could represent useful information for the establishment of control and therapeutic strategies focused on the enhancement of immunity against *Salmonella* at gut level.

Acknowledgements

Appendix A. Supplementary data

Supplementary data associated with this article can be found, in the online version, at http://dx.doi.org/10.1016/j.dci.2013.04.020.

References

1. Alvarez-Ordóñez, A., Begley, M., Prieto, M., Messens, W., López, M., Bernardo, A., Hill, C., 2011. *Salmonella* spp. survival strategies within the host gastrointestinal tract. Microbiology. 157, 3268-81.

2. Broz, P., Ohlson, M.B., Monack, D.M., 2012. Innate immune response to *Salmonella typhimurium*, a model enteric pathogen. Gut. Microbes. 3, 62-70.

3. Bueno, S.M., Riquelme, S., Riedel, C.A., Kalergis, A.M., 2012. Mechanisms used by virulent *Salmonella* to impair dendritic cell function and evade adaptive immunity. Immunology. 137, 28-36.

4. Centers for Disease Control and Prevention (CDC), 2011. Vital signs: incidence and trends of infection with pathogens transmitted commonly through food – foodborne diseases active surveillance network, 10 U.S. sites, 1996-2010. MMWR. Morb. Mortal. Wkly. Rep. 60, 749-55.

5. Cheng, L., Zhang, S., MacLennan, G.T., Williamson, S.R., Davidson, D.D., Wang, M., Jones, T.D., Lopez-Beltran, A., Montironi, R., 2013. Laser-assisted microdissection in translational research: theory, technical considerations, and future applications. Appl. Immunohistochem. Mol. Morphol. 21, 31-47.

6. Collado-Romero, M., Martins, R.P., Arce, C., Moreno, Á., Lucena, C., Carvajal, A., Garrido, J.J., 2012. An *in vivo* proteomic study of the interaction between *Salmonella* Typhimurium and porcine ileum mucosa. J. Proteomics.75, 2015-2026.

7. European Food Safety Authority (EFSA), 2012. The European Union summary report on trends and sources of zoonoses, zoonotic agents and food-borne outbreaks in 2010. EFSA. J. 9, 2597.

8. Gopinath, S., Carden, S., Monack, D., 2012. Shedding light on *Salmonella* carriers. Trends. Microbiol. 20, 320-327.

9. Livak, K.J., Schmittgen, T.D., 2001. Analysis of relative gene expression data using real-time quantitative PCR and the $2^{-\Delta\Delta CT}$ method. Methods. 25, 402-408.

10. Martins, R.P., Collado-Romero, M., Arce, C., Lucena, C., Carvajal, A., Garrido, J.J., 2012. Exploring the immune response of porcine mesenteric lymph nodes to *Salmonella enterica* serovar Typhimurium: an analysis of transcriptional changes, morphological alterations and pathogen burden. Comp. Immunol. Microbiol. Infect. Dis. In press. doi: 10.1016/j.cimid.2012.11.003.

11. Meurens, F., Berri, M., Auray, G., Melo, S., Levast, B., Virlogeux-Payant, I., Chevaleyre, C., Gerdts, V., Salmon, H., 2009. Early immune response following *Salmonella enterica* subspecies *enterica* serovar Typhimurium infection in porcine jejunal gut loops. Vet. Res. 40, 5.

12. Nunes, J.S., Lawhon, S.D., Rossetti, C.A., Khare, S., Figueiredo, J.F., Gull, T., Burghardt, R.C., Bäumler, A.J., Tsolis, R.M., Andrews-Polymenis, H.L., Adams, L.G., 2010. Morphologic and cytokine profile characterization of *Salmonella enterica* serovar Typhimurium infection in calves with bovine leukocyte adhesion deficiency. Vet. Pathol. 47, 322-333.

13. Raupach, B., Peuschel, S.K., Monack, D.M., Zychlinsky, A., 2006. Caspase-1-mediated activation of interleukin-1beta (IL-1beta) and IL-18 contributes to innate immune defenses against *Salmonella enterica* serovar Typhimurium infection. Infect. Immun. 74, 4922-4926.

14. Schauser, K., Olsen, J.E., Larsson, L.I., 2004. Immunocytochemical studies of *Salmonella Typhimurium* invasion of porcine jejunal epithelial cells. J. Med. Microbiol. 53, 691-695.

15. Tam, M.A., Rydström, A., Sundquist, M., Wick, M.J., 2008. Early cellular responses to *Salmonella* infection: dendritic cells, monocytes, and more. Immunol. Rev. 225, 140-162

.

3.5 Host activates both B-cell and CD8^{+} T cell-mediated mechanisms in Peyer's patches follicles to engender immunological memory during infections by non-typhoid *Salmonella*

Rodrigo Prado Martins[1], Carmen Aguilar[1], Valentina Lorenzi[1], Ana Carvajal[2], Rocío Bautista[3], M. Gonzalo Claros[3], Juan J. Garrido[1]

1 Grupo de Genómica y Mejora Animal, Departamento de Genética, Facultad de Veterinaria, Universidad de Córdoba, Campus de Rabanales, Edificio Gregor Mendel C5, 14071 Córdoba, Spain.

2 Departamento de Sanidad Animal, Facultad de Veterinaria, Universidad de León, 24071 León, Spain.

3 Plataforma Andaluza de Bioinformática, Universidad de Málaga, Parque Tecnológico de Andalucía, 29590 Málaga, Spain

Abstract

In the current study we coupled our swine model of non-typhoid salmonellosis to laser microdissection and microarrays analysis to dissect the mechanisms carried out in PP follicles in response to *Salmonella enterica* serovar Typhimurium. (*S.* Typhimurium). Infection resulted in the assembling of different immunity mediators in PP follicles, enabling host to mount multiple levels of the adaptive response against pathogen. Results indicated the induction of antibody responses and long-lived humoral immunity at a short time (2 days) after infection. Interestingly, several evidences of cross-presentation triggering were found out, suggesting that besides eliciting B-cell-mediated immune responses, PP follicles might mediate the generation of effector and memory CD8 T cells during infections by non-typhoid *Salmonella*. Our results reveal a novel function for PP follicles during *Salmonella* infections that should be considered for development of therapies and vaccine approaches against salmonellosis.

Keywords: *Salmonella enterica* serovar Typhimurium, laser microdissection, Peyer's patches follicles, germinal center, cross-presentation.

3.5.1 Introduction

Salmonella species are a leading bacterial cause of disease, exerting considerable impact on global human health. It is estimated that 93.8 million cases of gastroenteritis due *Salmonella* occur worldwide leading to 155,000 deaths each year (Majowicz et al., 2010). Data from the Centers for Disease Control (CDC) uncovered *Salmonella* as the main cause of hospitalization due to foodborne disease in the United States (CDC, 2013). Similarly, the European Food Safety Authority (EFSA) reported salmonellosis as the second most notified zoonotic disease in the European Union (EFSA, 2013).

Salmonella enterica serovar Typhimurium (herein *S.* Typhimurium), referred to as a non-typhoid *Salmonella* (NTS), is the second most commonly isolated serovar from human infections (Sanchez-Vargas et al 2011). Although the pathogenesis of infections caused by this pathogen has been extensively studied using the mouse model of systemic disease (Tsolis et al., 2011), one limitation of the murine typhoid model is that *S.* Typhimurium typically causes a self-limiting gastroenteritis rather than typhoid fever in humans (Majowicz et al., 2010). For this reason, the pathogenesis of NTS gastroenteritis remained largely unexplored until recently, when alternative animal models of infection became more widely used (Tsolis et al., 2011).

Accumulating evidences demonstrate the anatomic and physiological similarities between pig and human, highlighting swine as a valuable model for a number of infectious diseases relevant to human health (Meurens et al 2012). Indeed, pigs are ideal models for the study of salmonellosis by NTS, since upon infection with *S.* Typhimurium, swine undergo a self-limiting gastroenteritis which parallels the clinical manifestation observed in man (Boyen et al., 2008).

PP are the main portal of *Salmonella* host entry into host mucosa (Broz et al., 2012; Tam et al., 2008). These organs are clusters of organized lymphoid tissue located in the small intestine, which act as sites of antigen sampling and induction of mucosal immune responses (Makala et al., 2002). Upon infection, PP follicles undergo substantial changes that involve numerous cellular and cell surface components, giving rise to the formation of germinal centers (GC). These structures are intimately associated with the production of B cell humoral immune response and host cell interactions which consist in a fundamental aspect of adaptive immunity and generation of immunological memory (El Shikh and Pitzalis., 2012).

Recently, laser microdisssection coupled to qPCR technology was successfully used to provide a preliminary view of the immune response carried out by Peyer's patches (PP) follicles during oral infections with NTS (Martins et al 2013b). Thus, in the current study, laser microdissection followed by microarray analysis and bioinformatic data mining was applied to our swine model of gastroenteritis by *S.* Typhimurium to generate a broader view of the biological processes carried out by PP follicles upon infection.

3.5.2 Materials and methods

3.5.2.1 Experimental infection and tissue sampling

Eight crossbred weaned piglets of approximately four weeks of age and confirmed to be fecal-negative for *Salmonella* were randomly allocated to control or infected groups (four animals each). Control (0 day post-infection — dpi) pigs were necropsied 2 h before the experimental infection, whereas infected group was orally challenged with 10^8 cfu of *Salmonella* Typhimurium phagetype DT104 and subsequently necropsied at 2 dpi. Ileum samples were collected from all

experimental animals and immediately frozen in liquid nitrogen for RNA and protein isolation or fixed in 10% neutral buffered formalin for histological processing. Piglets were housed in experimental isolation facilities of the University of León (Spain). All procedures involving animals were performed in accordance with the European regulations regarding the protection of animals used for experimental and other scientific purposes, under the supervision of the Ethical and Animal Welfare Committee of the University of León (Spain).

3.5.2.2 Laser microdissection and RNA preparations

Frozen gut samples from all experimental animals were embedded in optimal cutting temperature compound (Sakura Finetek USA, Torrance, CA, USA) and cut into serial 20 μm sections. Before microdissection, eight cryostat sections from each pig were mounted on glass slides and treated with RNAlater-ICE (Ambion) according to manufacturer instructions. Afterwards, PP cells were laser-microdissected and captured from terminal ileum sections by Auto-Laser Pressure Catapulting (LPC) mode (Figure 1A and B) with a PALM MicroBeam device (Carl Zeiss MicroImaging GmbH, Jena, Germany). Catapulted tissue was soaked in 15 μl of RLT buffer (Qiagen, Valencia, CA, USA) poured in 200 μl microtubes caps and RNA purifications were carried out employing the RNeasy Mini Kit (Qiagen). Eluted RNA was digested with RNase-Free DNase Set (Qiagen) and RNA quality was checked by Experion RNA analysis (Bio-Rad, Hercules, CA, USA).

3.5.2.3 Microarray analysis

Gene expression analysis was carried out using the GeneChip Porcine Genome Array by Affymetrix platform (Affymetrix Inc., Santa Clara, CA, USA) at the Genomics Unit of CABIMER (Andalusian Center for Molecular Biology and

Regenerative Medicine, Seville, Spain). This chip contains 23,937 probe sets to interrogate 23,256 transcripts in pig, which represents 20,201 genes. The One-Cycle Eukaryotic Target Labeling Assay was used to obtain biotinylated cRNA to be used in the subsequent chip hybridization according to manufacturer instructions (Expression Analysis Technical Manual, Affymetrix). The biotinylated cRNA targets were then cleaned up, fragmented, and hybridized with the GeneChip Porcine Genome Array following Affymetrix recommended protocols. Chips were washed, stained with a GeneChip Fluidics Station 450 (Affymetrix) using the standard fluidics protocol and scanned with an Affymetrix GeneChip Scanner 3000 (Affymetrix). Probe signal intensities were captured and processed with the GeneChip Operating Software 1.4.0.036 (Affymetrix) and the resulting CEL files were reprocessed using robust multi-array average normalization (RMA) (Irizarry et al., 2003). Then, differentially expressed (DE) genes were accessed by the Rank Products (RP) method (Breitling et al., 2004), using default settings. A FDR adjusted p-value of 0.05 was used as cutoff to rank significantly regulated transcripts. Since the Affymetrix Porcine GeneChip is not fully annotated in all the features, it was re-annotated with Blast2GO (Conesa et al, 2005) with a minimum E-value of 10^{-10} and a minimum similarity of 50%.

3.5.2.4 Systems biology analysis

For bioinformatic analysis of microarray data, the list of genes found to be significantly regulated after infection was uploaded into Ingenuity Pathway Analysis (IPA, Ingenuity Systems, www.ingenuity.com). Gene interaction networks were automatically generated, ranked by score and depicted on IPA. Score estimated the probability that a collection of genes equal to or greater than the number in a network could be achieved by chance alone and values of 3 or higher were considered to have a 99.9% confidence of not being generated by

random chance alone. For statistical analysis of enriched functions/pathways, IPA Knowledge Base was used as a reference set and Fisher's exact test was employed to estimate the significance of association. P-values bellow 0.05 were considered statistically significant. The Activation z-score was employed to predict the activation state of enriched functions and upstream regulators. Predictions with z-score values higher or lower than 2 and a p-value ≤0.05 denoted a statistically increased or decreased activation state respectively. In pathways and networks diagrams, nodes represented a gene and its relationship with other molecules was represented by a line (solid and dashed lines represented direct and indirect associations respectively). Nodes with a red or green background were input genes found to be up or down-regulated respectively. Grey and white nodes were molecules inserted by IPA basing on the Ingenuity Knowledge Base to produce diagrams. Grey highlighted molecules without significant changes and white indicated genes not included in the analysis. In the canonical pathways bar graph, ratio indicated the percentage of genes taking part in a pathway that could be found in the uploaded data set and –log(p-value) meant the level of confidence of association. Threshold line represented a p-value of 0.05.

3.5.2.5 Real-time quantitative PCR (qPCR)

RNA from infected and control samples was reverse transcribed to cDNA using the qScript cDNA Synthesis kit (Quanta BioSciences, Gaithersburg, MD, USA) and real-time quantitative PCR (qPCR) assays were performed to access gene relative expression by the $2^{-\Delta\Delta Cq}$ method (Livak et al., 2001) as previously described (Martins et al., 2013b). Beta-actin was used as reference gene and fold change values higher or lower than 1 meant up-regulation or down-regulation respectively. Subsequently, data were analyzed by Student's t-test using the

software SPSS 15.0 for Windows® (SPSS, Inc) and a p-value bellow 0.05 was considered statistically significant. Primer pairs used for amplifications can be found as supporting information [see Supplementary File 1].

3.5.2.6 Western blot analysis

For protein extractions, catapulted tissue was homogenized with lysis buffer (150 mM sodium chloride, 1.0% NP-40, 50 mM Tris pH 8.00 and 5 mM PMSF) and incubated at room temperature for 30 min. Subsequently, samples were disrupted by vortexing for 30 sec and lysate concentration was determined using Bradford Protein Assay (Bio-Rad). Protein from individual replicates belonging to the same group was pooled (10 ug total), electrophoretically fractionated in 12% (w/v) SDS-PAGE gels and transferred onto a PVDF membrane (Millipore, Bedford, MA, USA). Western blot assays were carried out as described by Martins et al.(2012) employing the following primary antibodies: mouse anti-swine histocompatibility class I (SLA-I) 4B7/8 (Bullido et al., 1997), rabbit anti-NLRC5 antibody (ab105411, Abcam, Cambridge, UK) and mouse anti-porcine CD5 1H6/8 (Pescovitz et al., 1998). To confirm equal sample loading, membranes were reblotted with anti-GAPDH monoclonal antibody (GenScript, Picastaway, NJ, USA). Membranes were scanned in a FLA-5100 imager (Fujifilm, Tokyo, Japan) and signal intensity was determined using Multigauge software (Fujifilm, Tokyo,Japan) as previously described (Martins et al., 2012).

3.5.2.7 Histopathology, immunohistochemistry and confocal microscopy

Paraffin sections (5 μm) of formalin fixed samples were routinely processed for immunohistochemistry assays, as described elsewhere (Yubero et al., 2011). Mouse anti-porcine macrophage 4E9/11 (Bullido et al 1997), anti-swine histocompatibility class I (SLA-I) 4B7/8 (Bullido et al 1997) and anti-porcine

TLR2 1H11 (Alvarez et al., 2008) as well as rabbit anti-NLRC5 (ab105411, Abcam) and anti-Apolipoprotein AI (ab75922, Abcam) were employed as primary antibodies. Biotinylated anti-mouse and anti-rabbit Ig (Dako, Barcelona, Spain) were used to detect immune complexes. Immunofluorescence using confocal microscopy was performed employing anti-SLAI 4B7/8 (Bullido et al. 1997) and anti-porcine macrophage 4E9/11 (Bullido et al 1997) mouse antibodies, anti-NLRC5 polyclonal antibody (ab105411, Abcam) and a rabbit antiserum against *Salmonella* Typhimurium flagellin (Martins et al., 2013a). Fluorescein isothiocyanate (FITC)-conjugated goat anti-rabbit IgG (Sigma-Aldrich, St. Louis, MO, USA) and Alexa Fluor 594 anti-mouse IgG (Life Technologies, Carlsbad, CA, USA) were used as secondary antibodies. Immunostaining was performed as described by Robertson et al. (2008). Briefly, deparaffinized sections of formalin fixed MLN were blocked for 30 min with 1% bovine serum albumin and 2% foetal calf serum in PBS. Then, sections were overnight incubated with primary antibodies at 4°C, three times washed with PBS for 5 min and incubated for 1 h at 37°C with fluorescent secondary antibodies. For negative controls, primary antibody was omitted. Finally, sections were three times washed for 5 min in PBS containing 1.43 µM 4',6-diamidino-2-phenylindole (Life Technologies). Samples were subsequently evaluated and imaged using a LSM 5 Exciter confocal microscope (Carl Zeiss, Jena, Germany).

3.5.3 Results

3.5.3.1 Genes are mostly up-regulated in Peyer patches follicles after *S. Typhimurium* infection

Microarray technology coupled to Rank Products analysis (Breitling et al., 2004) was employed to explore the transcriptional response carried out in PP

follicles at 2 dpi with *S.* Typhimurium. A total of 164 transcripts, corresponding to 152 unique genes, were found to be differently expressed as a consequence of infection (FDR adjusted p<0.05). Among them, 37 genes were down-regulated whereas 115 were up-regulated. [see Supplementary File 2] To validate microarray data, qPCR assays were performed on a panel of 22 genes filtered by Rank Products analysis. As expected, all of them were confirmed to be significantly regulated (p<0.05) after infection and showed the same expression pattern observed by microarray analysis (Table 1).

Table 1 - Microarray data validation by qPCR

Gene	Microarrays		qPCR	
	Fold Change	**P-value**	**Fold Change**	**P-value**
B2M	1.9	0.039	3.3	0.008
CCL2	2.1	0.013	8.9	0.024
CCR5	2.1	0.018	18.2	0.001
CD163[a]	2.5	0.012	24.6	0.02
CD1A	1.8	0.038	3.1	0.001
CD44	2.3	0.006	7.1	0.002
CD80	2.3	0.004	7.0	0.006
CXCL2	2.3	0.003	5.8	0.002
DEFB1	14.4	0.000	3.1	0.002
HLA-A[a]	2.1	0.030	3.7	0.010
IL1RN	2.2	0.013	10.0	0.011
IL8	3.7	0.001	9.5	0.006
IRF1	3.3	0.001	44.4	0.001
LPCAT2	3.1	0.002	14.9	0.001
MAP3K8	2.3	0.010	18.9	0.001
NLRC5	3.6	<0.001	21.0	0.001
STAT1	2.1	0.026	15.7	0.001
SOD2	2.0	0.018	2.6	0.016
TAP1	2.3	0.008	4.3	0.005
TLR2	2.2	0.008	17.1	0.013
WARS[a]	2.2	0.010	4.6	<0.001
XIST[a]	0.2	0.004	0.01	<0.001

[a]Data from microarray analysis are mean values from more than one probe.

3.5.3.2 Processes related to cell movement and activation are primarily induced in *Salmonella* infected follicles

Bioinformatic tools were used to translate microarray data into biological information. It was revealed that infection mainly resulted in an enrichment of genes involved in cellular movement, followed by other host functions such as immune cell trafficking, inflammatory response and cell-to-cell signalling and interaction [see Supplementary File 3]. Subsequently, IPA z-score was employed to predict the effect of the uncovered gene expression changes on distinct biological processes. Results indicated that processes related to migration and activation of phagocytes and leukocytes were most significantly activated in *S.* Typhimurium infected PP follicles (Table 2). Besides, terms related to activation of lymphocytes, and especially T-lymphocytes, were uncovered to show the highest activation z-score values [see Supplementary File 3]. Thus, we carried out a series of assays to validate the predictions accessed by the bioinformatic engine. Firstly, hematoxylin-eosin staining disclosed a notably increase of phagocytes, mainly neutrophils, in PP upon infection (Figure 1C and D). This find could be further related to the presence of pathogen in tissue, being *S.* Typhimurium antigens detected mostly in the cytoplasm of polymorphonuclear cells (Figure 1E and F) found in areas of PP follicles where an accumulation of neutrophils was observed. Lastly, we checked the induction of lymphocytes activation in follicles by western blot assays, which uncovered higher levels of CD5 in infected samples (Figure 1G).

3.5.3.3 Adaptive immune responses are properly induced in Peyer's patches follicles during infections by NTS

Network analysis depicted direct and indirect relationships between genes involved in distinct processes of immune response [see Supplementary File
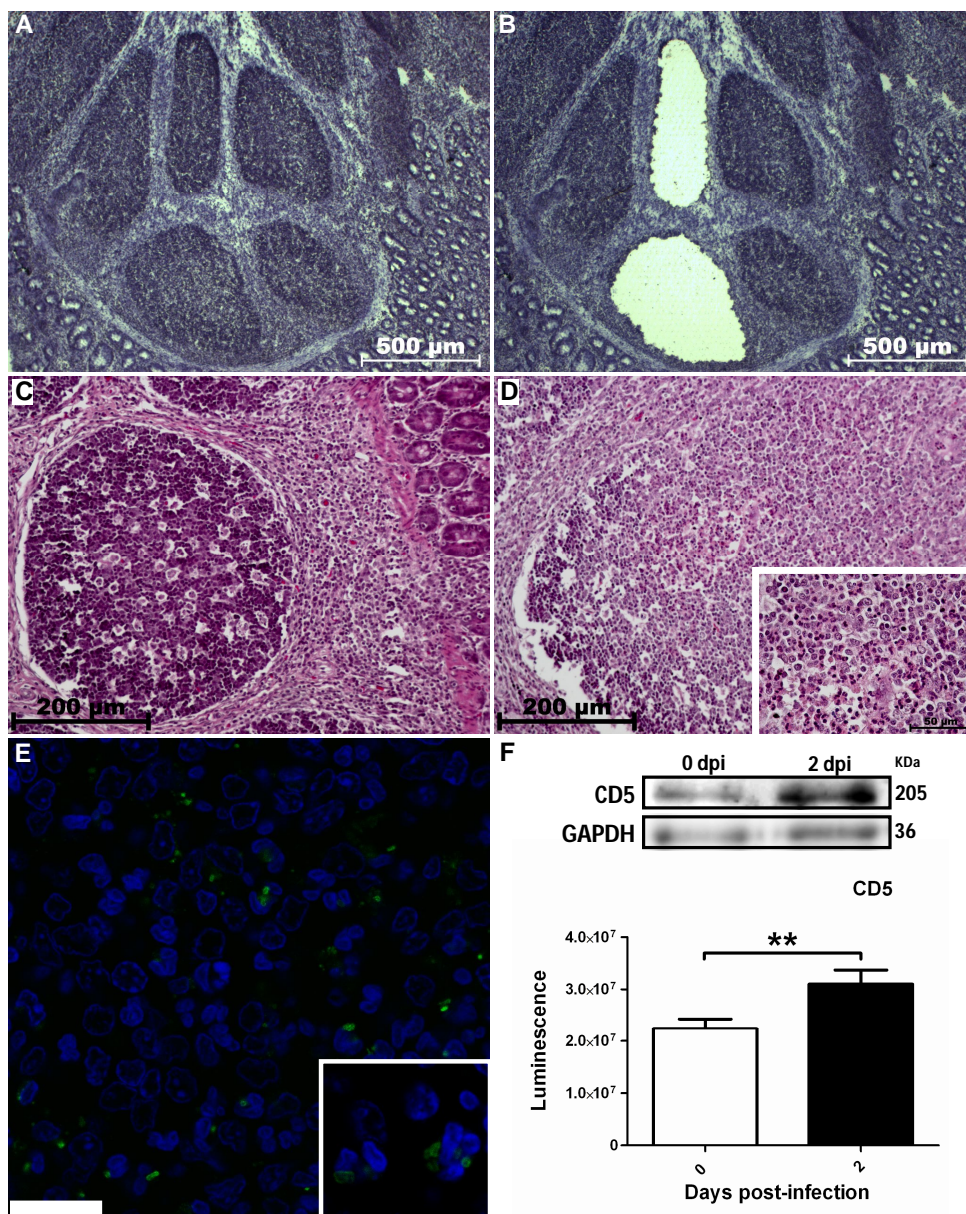
Figure 1 – Laser microdissection, histological analysis and CD5 quantification in PP follicles upon infection with *S.* Typhimurium. A-B: After their identification (A), PP follicles were microdissected by Auto-Laser Pressure Catapulting. C-D: H/E staining of ileum sections demonstrating PP follicles before (C) and after (D) the bacterial challenge. A highlighted in (D), infection resulted in a relevant infiltration of neutrophils. E: fluorescent labelling of *S.* Typhimurium in tissue. Pathogen was mainly detected in the perinuclear zone of polymorphonuclear cells. F: western blot assays uncovered increased levels of CD5 in infected tissue.

3]. The major generated network integrated genes involved in the communication between innate and adaptive immune cells and dendritic cell maturation (Figure 2A). Curiously, all genes involved in these processes were found to be up-regulated and were directly or indirectly related with I and type II interferon (IFN) genes. In light of the role of PP follicles in the establishment of immune response, we additionally verified the differential expression of a sort of genes involved in the formation of GC. This analysis revealed up-regulation of the main mediators of B-cell-T-cell interactions and cytokines involved in the triggering of B-cell mediated immunity (Figure 2B).

Table 2 - Predicted activation state of biological functions and upstream regulators enriched in PP follicles during infections by S. Typhimurium

| Category	Predicted Activation State	Activation z-score	p-value
Downstream effect			
Migration of phagocytes	Increased	2,930	6,33E-13
Cell movement of phagocytes	Increased	2,928	4,09E-11
Cell movement of leukocytes	Increased	2,342	4,54E-10
Cell movement of myeloid cells	Increased	3,012	9,53E-10
Leukocyte migration	Increased	2,498	3,35E-09
Activation of leukocytes	Increased	3,213	4,77E-09
Activation of blood cells	Increased	3,514	4,96E-09
Activation of cells	Increased	3,378	1,80E-08
Quantity of leukocytes	Increased	2,564	1,92E-08
Homing of leukocytes	Increased	2,604	2,64E-08
Upstream regulator			
IFNG	Activated	4,211	1,04E-26
lipopolysaccharide	Activated	4,918	6,03E-23
poly rI:rC-RNA	Activated	4,291	4,60E-22
Interferon alpha	Activated	2,541	5,35E-21
TNF	Activated	4,107	1,46E-18
IL1B	Activated	4,096	1,05E-17
STAT3	Activated	3,039	1,43E-17
STAT1	Activated	3,110	2,58E-17
IL6	Activated	2,861	4,18E-17
NFkB (complex)	Activated	4,092	6,77E-16

A

B
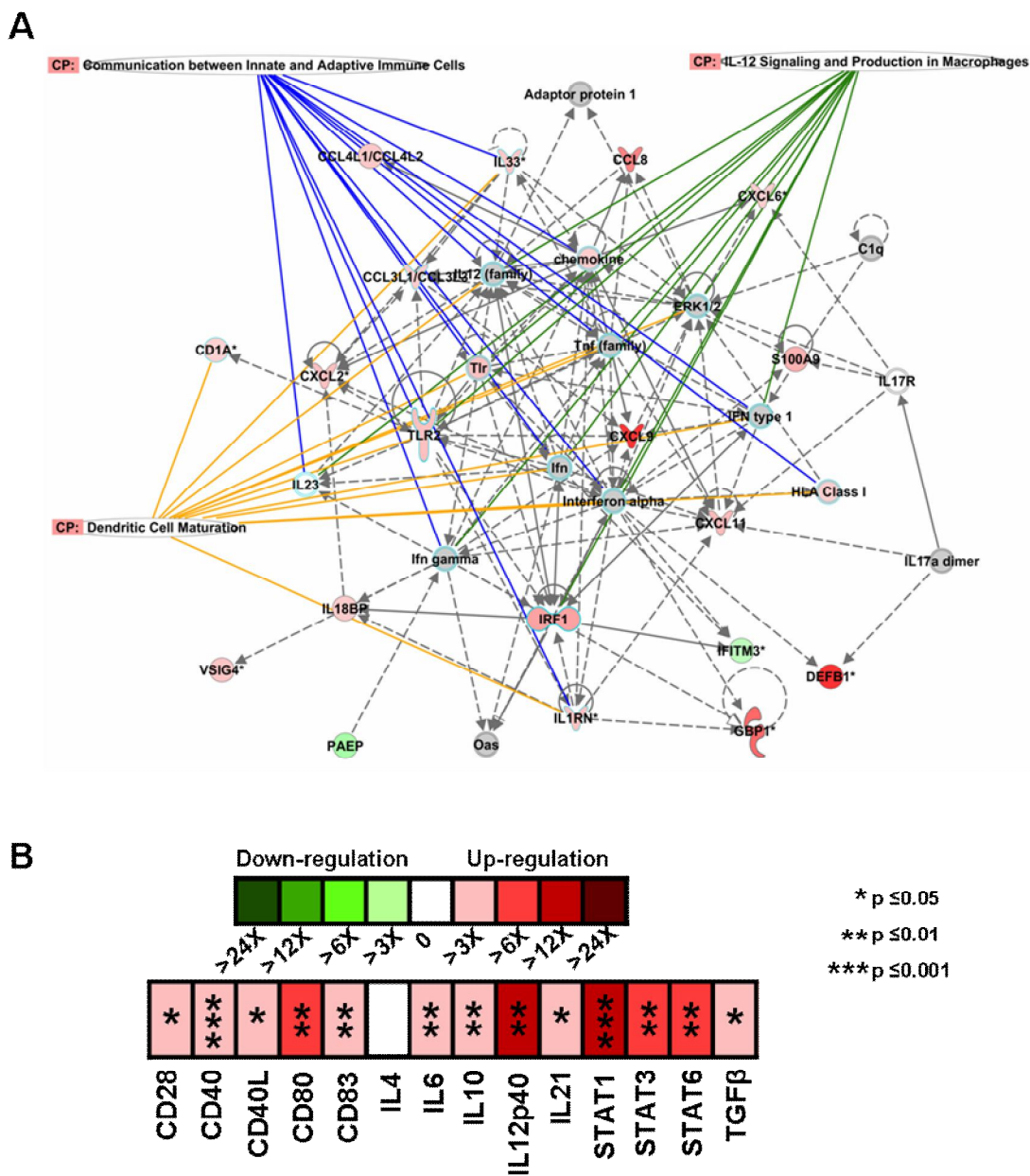
Figure 2 – Network analysis of microarray data and qPCR assays in *S.* Typhimurium infected PP follicles. A: major generated network depicted a common up-regulation of genes taking part in communication between innate and adaptive immune cells and dendritic cell maturation pathways. B: differential gene expression analysis by qPCR revealed an up-regulation of molecules involved in the formation of geminal centers in infected PP follicles.

3.5.3.4 IFNγ is the main upstream regulator of the transcriptional response carried out in Peyer's patches during non-typhoidal salmonellosis

IPA z-score tool was also employed to identify and predict the activation state of upstream regulators, aiming to explain gene expression changes observed in tissue after infection. In this analysis, IFNγ was found to be the main regulator of transcriptional changes observed in PP follicles in response to *S.* Typhimurium, affecting the expression of 53 (35%) out 152 molecules in dataset [see Supplementary File 3, worksheet 5]. Thus, network analysis displayed that IFNγ up-regulation mostly lead to the activation of connected genes (Figure 3A). Interestingly, functional analysis of only IFNγ-target molecules revealed an enrichment of biological processes including migration of phagocytes and antigen presenting cells, bacterial infection of mammalia and activation of leukocytes, similarly to results observed for the whole dataset [see Supplementary File 3, worksheet 6]. Although significant changes in IFNγ mRNA levels were not detected by microarray analysis, we observed by qPCR that this gene was 18 times more expressed in infected than control samples. Moreover, results of bioinformatic data mining could be further confirmed by the expression profile observed by qPCR for a panel of IFNγ-target genes (Figure 3B) and the uncovered abundance changes in tissue of two IFNγ-regulated molecules after infection (Figure 3C). Of note, STAT1 and STAT3, both transcriptional factors involved in interferon signalling, and IFNα were also detected among the upstream regulators most significantly implicated in tissue response to infection (Table 2).

3.5.3.5 NLRC5 activates different molecules of the antigen presentation via MHCI pathway in Peyer patches follicles of *S.* Typhimurium infected swine

NLRC5 was also disclosed as a relevant mediator of host response to NTS. Network analysis followed by the IPA Molecule Activity Predictor tool revealed
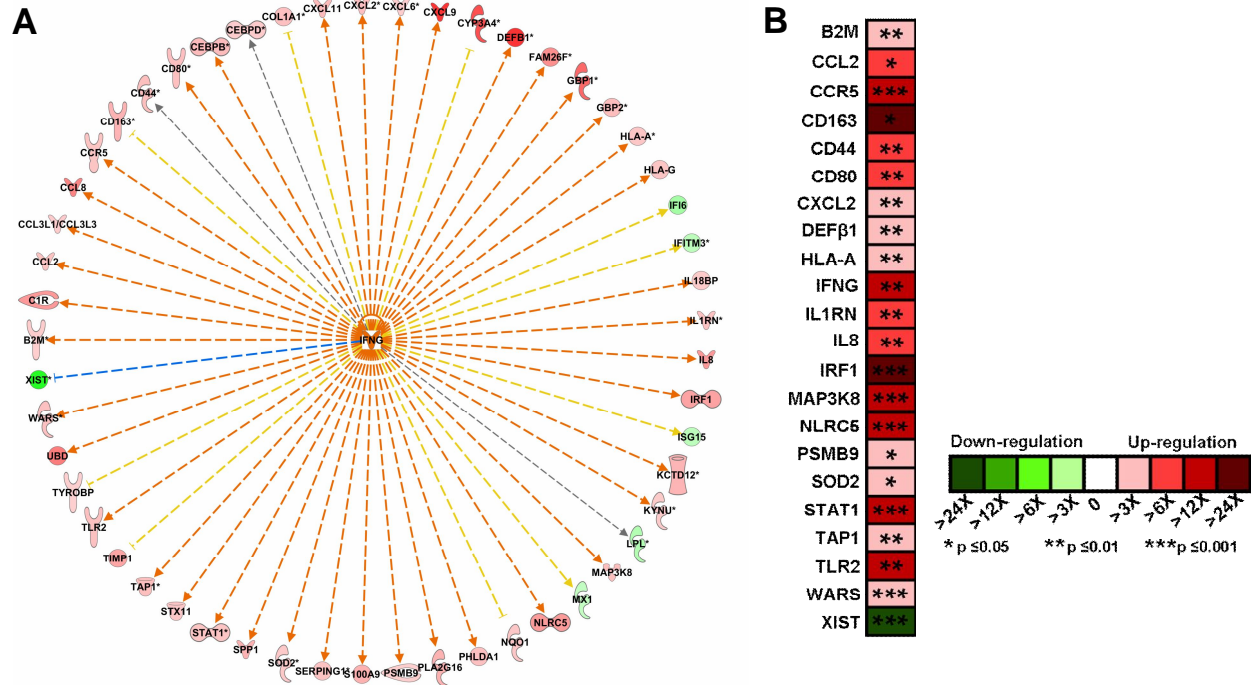
Figure 3 – IFNγ is the main regulator of transcriptional response of PP follicles to non-typhoid *Salmonella*. A: network analysis disclosed that IFNγ up-regulation resulted in the activation or inhibition (orange and blue lines respectively) of 53 genes differently expressed after infection. Data were inconsistent for genes liked with yellow lines and effect could not be predicted for those linked with grey lines. B: differential gene expression analysis of a sort of IFNγ-target genes by qPCR confirmed the effect of this gene in the expression of downstream molecules. C: immunohistochemistry assays further corroborated that up-regulation of IFNγ gene also resulted in increase or decrease of target molecules at protein level.
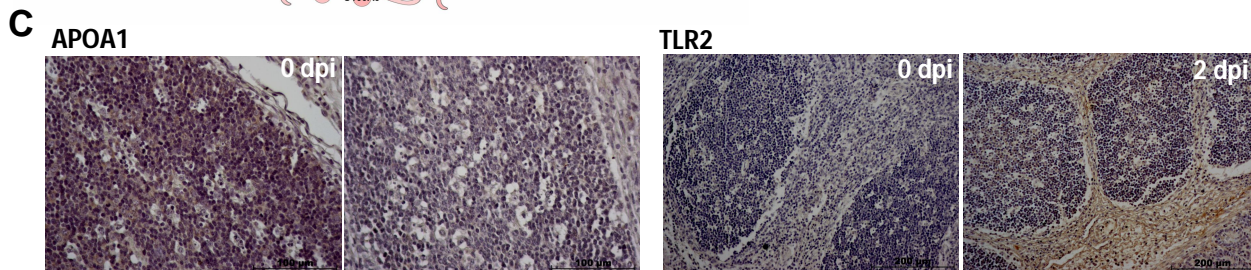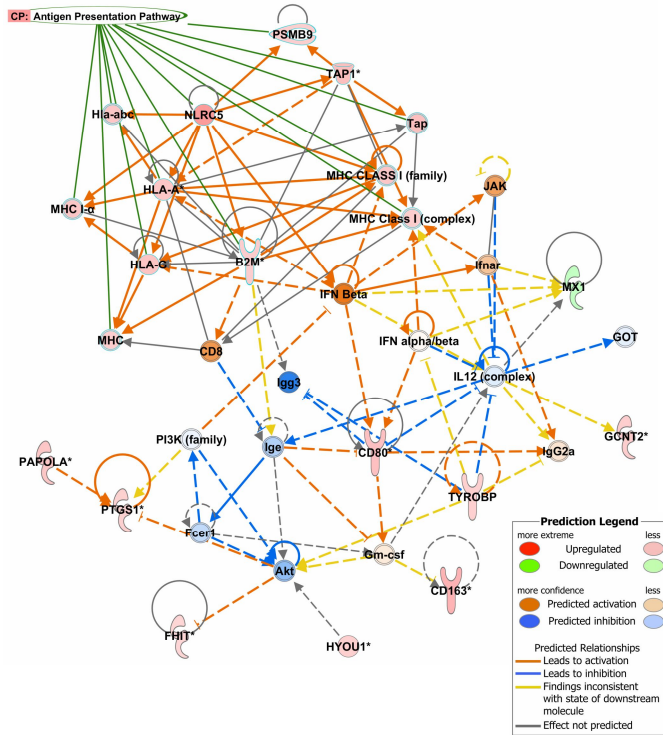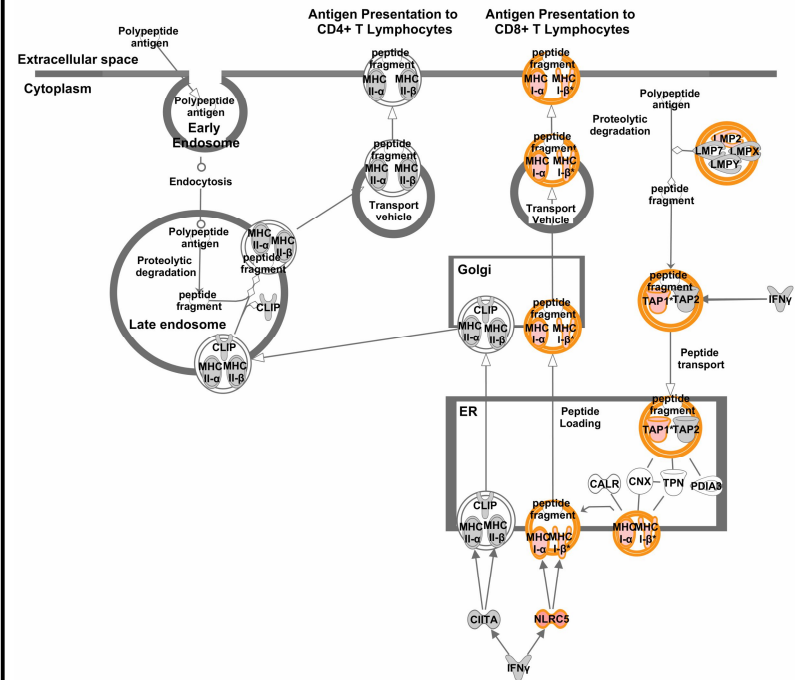
Figure 4 – NLRC5 activates the antigen presentation via MHCI pathway after infection with non-typhoid *Salmonella*. Network analysis (A) disclosed direct relationships between NLCR5 and distinct molecules involved in the antigen presentation via MHCI (B).

that NLRC5 up-regulation induces the activation of genes coding for molecules involved in different stages of the antigen presentation via MHCI pathway (Figure 4A) Notably, all these genes were up-regulated after infection (Figure 4B). In order to clarify these results, we initially checked changes in the abundance of NLRC5 and MHCI in tissue by western blot. In accordance with transcriptomic data (Table 1), bacterial challenge also resulted in an increase of both molecules in tissue at protein level (Figure 5). Then, immunohistochemistry assays were carried out to verify the distribution of NLRC5 and MHCI in tissue. Higher levels of NLRC5 were detected at 2 dpi and labelling was observed in the cytoplasm and nucleus of mononuclear and polymorphonuclear cells (Figure 6A and B). Similarly, MHCI was also more detected in infected PP follicles, being mainly localized in the cytoplasm of mononuclear phagocytes (Figure 6C and D). Finally, immunofluorescence followed by confocal was executed to deepen and sharpen the role of NLRC5 and MHCI in the context of NTS. In spite of the diffuse labelling observed for NLRC5 over the whole follicle, high levels of this molecule were uncovered in polymorphonuclear cells located in the periphery of infected PP follicles (Figure 6E). Regarding MHCI, we observed that *S.* Typhimurium infected cells showed high levels of MHCI (Figure 6F).
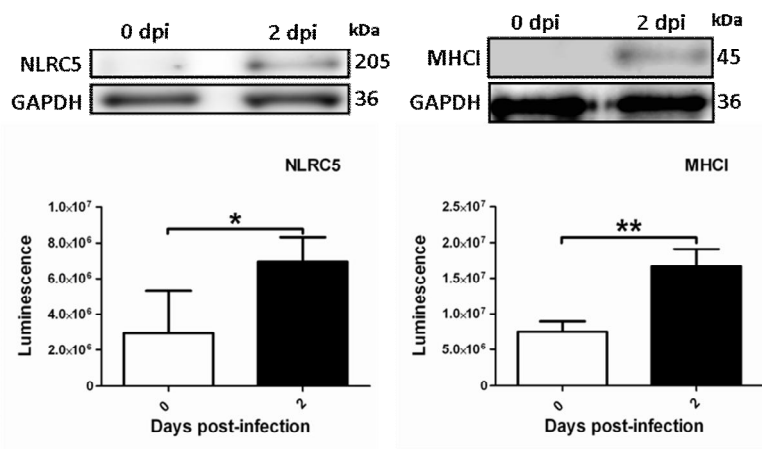

Figure 5 - Western blot assays of NLRC5 and MHCI in infected and control follicles.
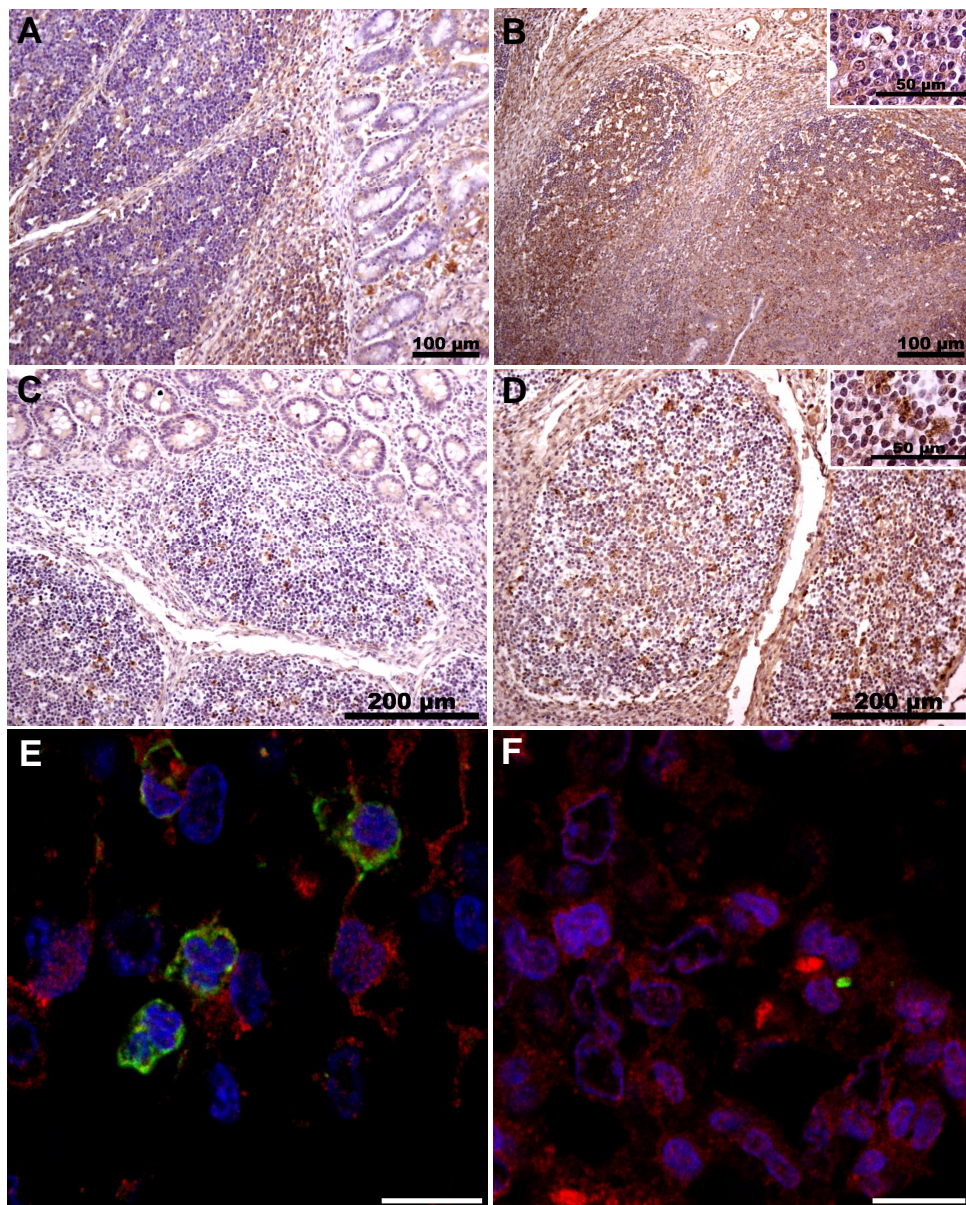
Figure 6 – *S.* **Typhimurium infected PP follicles showed increased levels of NLRC5 and MHCI at protein level. A**-D: Immunohistochemistry assays further detected increased levels of both NLRC5 (A-B) and MHCI (C-D) in follicles after infection. E: confocal microscopy analysis revealed high levels of NLRC5 in polymorphonuclear cells. Merge image: NLRC5-FITC, MHCI-Alexa Fluor® 594 and DAPI. F: *S.* Typhimurium was detected in cells showing high levels of MHCI. Merge image: *S.* Typhimurium-FITC, MHCI-Alexa Fluor® 594 and DAPI.

3.5.4 Discussion

Until recently, the pathogenesis of infections by NTS was largely overlooked due to the dominance of the murine model of typhoid fever and the lack of alternative models for the study of salmonellosis (Tsolis et al., 2011). Porcine immune system show a high level of resemblance with human (Meurens et al., 2012) and differently from rodents, human and swine PP share common anatomical and physiological peculiarities such as a predominant localization in the ileum and prenatal development (Makala et al., 2002). In light of this and the similarity of disease caused by *S.* Typhimurium in human and pig (Sanchez-Vargas et al 2011, Boyen et al., 2008), in the current study we coupled our swine model of non-typhoid salmonellosis to LM and microarrays analysis to dissect the mechanisms carried out in PP follicles upon infection with *S.* Typhimurium.

PP follicles are aggregations of B cells and follicular dendritic cells (FDC) that after antigenic stimulus form the germinal center (GC). These specialized structures contain large B lymphoblasts, follicular T cells, macrophages and a tight network of FDC, playing a relevant role in the generation of protective antibody production and memory B-cells (El Shikh and Pitzalis, 2012). We observed that infection triggered in PP follicles the migration and activation of lymphocytes as well as the up-regulation of distinct genes involved in the formation of GC. Thus, it could be suggested that antibody responses and long-lived humoral immunity are triggered at a short time (2dpi) in PP follicles during NTS infections.

During primary immune responses in PP, protein antigens are processed and presented by antigen presenting cells (APCs) which activate Ag-specific Th cells in the PP T-cell zones (Acheson and Luccioli.2004). These cells expand and differentiate into effector Th cells that move towards PP follicles to regulate the development of Ag primed B-cells and lead to the formation of a germinal center

Traditionally, T-cell help to B-cell has been attributed to the type-2 helper CD4^{+} T cells (Th2) (Coquerelle and Moser, 2010). However, T-follicular helper cells (Tfh) were recently described as CD4^{+} mature cells that are capable of providing help to B-cells during the GC reaction and switched Ag-specific antibody responses via IL21 (through STAT3 and STAT1), IL4 (through STAT6), IL10 and IFNγ (Cerutti et al., 2012, El Shikh and Pitzalis., 2012,Coquerelle and Moser, 2010). IL21 production by naïve CD4^{+} T cells is induced by IL6 and IL12 released by DC located out of the follicle (Ma et al. 2012). However, FDC also stimulates Tfh differentiation by producing IL6 upon type I interferon signaling (Coquerelle and Moser, 2010) and collaborate with B-cell activation by releasing large amounts of active TGF-β (Cerutti et al., 2012). Interestingly, all these cytokines were found to be up-regulated, indicating that the cytokine environment necessary for B cell differentiation was established in infected PP follicles.

Apart from this, the fate of a responding B cell is determined by the interaction between T-cell and B-cell through mediators also uncovered by us to be up-regulated. A cognate interaction between T cell receptor and peptide-MHCII on B cells must be assembled, as well as ligation of CD40 on B cells by CD40L and provision of CD80 and CD86 by B cells to ligate CD28 on T cells (Zotos and Tarlinton, 2012). B cells thereafter differentiate along the follicular pathway generating GC B cells that further differentiate into long-lived memory B cells and plasma cells producing high-affinity antibodies (Cerutti et al., 2012).

PP follicles underwent a marked infiltration of phagocytes upon infection, in line with the increased expression levels uncovered by microarray analysis for distinct chemokine encoding genes. Curiously, *S.* Typhimurium was predominantly labelled in the cytoplasm of polymorphonuclear cells (PMN) that were presumed to be neutrophils due to the notable presence of these cells in infected follicles. In spite of the accumulating evidences that the recruitment of neutrophils is crucial to prevent *Salmonella* dissemination (Broz et al., 2012), the

infiltration of inflammatory cells is usually observed in the PP subepithelial dome as well as interfollicular area during mice *Salmonella* infections (Tam et al., 2008). Therefore, the remarkable infiltration of neutrophils observed by us in PP follicles led us to speculate that apart from killing of bacteria, these cells could also take part in the induction of adaptive immune responses during infections by NTS.

Indeed, it has been reported that neutrophils may influence adaptive immunity by acting either directly on T cells or indirectly through DC modulation (Beauvillain et al., 2007). Thus, the first hypothesis considered by us was that infected neutrophils could carry *Salmonella* to follicles for further processing. Previously, Mengiovanni et al. (2006) and Morel et al. (2008) uncovered that physical interactions involving neutrophils, DC and T cells play a major role in the human immune response to *Candida* and *Mycobacterium* respectively, resulting in T cell activation following DC acquisition of antigens delivered by polymorphonuclear cells (PMN). More recently, Alfaro et al. (2011) found out that DC can uptake viable PMN and subsequently cross-present antigens previously internalized by these cells.

Cross-presentation defines the process by which professional APC present peptides from extracellular antigens via their own MHCI molecules to CD8$^+$ T cells (Houde et al., 2003). Notably, several evidences of the induction of cross-presentation were found out in this study. Firstly, bioinformatic mining of microarray data disclosed an up-regulation of genes encoding molecules involved in different steps of the antigen presentation pathway via MHCI. BATF3, a transcription factor required for development of DC subsets capable of priming CD8 T-cell responses (Tussiwand et al., 2012) was also found to be up-regulated and IFNγ, followed by IFNα and their signal transducers STAT1 and STAT3 were identified as the most relevant upstream regulators of the transcriptional response carried out in follicles upon infection. Types I and II IFN up-regulate multiple functions within the class I antigen presentation pathway to increase the

quantity and diversity of peptides presented in the context of MHCI (Schroder et al. 2004). Infected tissue also showed increased levels of CD5, a marker of T-cell activation (Soldevila et al., 2011) and over-expression of CXCL9 and CXCL11, both strong inducers of cytotoxic lymphocytes (CTL) and type-1 helper CD4+ T cells (Th1) activation and migration (Groom and Luster, 2011). Additionally, we confirmed by western blot analysis and immunohistochemistry assays that MHCI was more abundant in tissue after the bacterial challenge and demonstrated by confocal analysis that *S.* Typhimurium infected phagocytes expressed high levels of this molecule. Therefore, on the whole, our results suggested that *Salmonella* antigens are cross-presented in infected PP follicles, in line with our previous observations in *S.* Typhimurium infected mesenteric lymph nodes (Martins et al., 2012). These finds, supported by previous evidences (Alfaro et al., 2011, Morel et al., 2008, Mengiovanni et al., 2006), could highlight a relevant role for infected neutrophils in the response to *S.* Typhimurium, since these cells would be able to modulate DC function while transferring to them antigens to be employed in acquired immunity mechanisms.

However, the induction of cross-presentation in infected PP through other mechanisms/cells should not be dismissed. Interestingly, we observed that PMN cells located in the boundary of infected PP showed high levels of NLRC5, a NOD-like receptor newly identified as a key transcriptional regulator of genes involved in the MHCI antigen presentation pathway (Yao and Qian, 2013). Immunohistochemistry and western blot assays demonstrated that NLRC5 was increased at protein level in infected tissue and network analysis of microarray data also related the up-regulation of this gene with the activation of molecules involved in the Ag presentation via MHCI. Moreover, *S.* Typhimurium was found by us to induce up-regulation of NLRC5 and MHCI in porcine neutrophils infected *in vitro* (Data not shown). In light of this, we infer that infected neutrophils could directly cross-present *S.* Typhimurium antigens to CD8^{+} T cells. This presumption

can be further supported by a previous demonstration that neutrophils are able to cross-prime CD8^{+} T cells *in vivo* (Beauvillain et al., 2007).

Finally, we envisaged that cross-presentation in PP follicles could also be triggered by activated B cells. De Wit et al. (2010) reported that upon BCR-mediated phagocytosis of *Salmonella,* human B-cell boosts antibody production and in addition, cross-present bacterial antigens in a proteasome-dependent manner. Nevertheless, besides the direct interaction with CD8^{+} T-cells, the functionality of B cells as professional APC could also enable them to work in synergy with infected neutrophils, to initiate and/or amplify T cell cytotoxic response to exogenous antigens. As previously discussed, this hypothesis could also justify the notably presence of infiltrating neutrophils in an area of PP mostly composed of B-cells, but further research is necessary to elucidate it.

Although we have discussed the distinct mechanisms that could trigger cross-presentation separately, it is probable that all of them occur simultaneously during infections. If true, this redundancy in cross-presentation induction could enhance the potency and efficiency of host cell-mediated immunity against *Salmonella.* Indeed, suicide cross-presentation of *S.* Typhi by DC is reported to generate mostly CD8^{+} effector memory T cells (Salermo-Gonçalves and Sztein 2009), whereas infected B-cells are capable of activating both the central and effector memory CD8^{+} compartments (De Wit et al., 2010).

In summary, this study disclosed a prominent role for PP follicles in the establishment of immune responses against *S.* Typhimurium. It was demonstrated that infection resulted in the assembling of different mediators of immune response in PP follicles, aiming to induce early antibody responses and long-lived humoral immunity at a short time after infection. Interestingly, several evidences of cross-presentation triggering were found out by us, suggesting that besides eliciting B-cell-mediated immune responses, PP follicles might mediate the generation effector and memory CD8 T cells during infections by NTS.

Therefore, our results reveal a novel function for PP follicles during *Salmonella* infections that should be considered for development of therapies and vaccine approaches against salmonellosis.

Acknowledgements

Supplementary files

Supplementary File 1 - Primer pairs employed in host differential expression analysis by real-time qPCR.

Supplementary File 2 - Differently expressed transcripts

Supplementary File 3 Ingenuity Pathways Analysis annotations

References

1. Acheson DW, Luccioli S. Microbial-gut interactions in health and disease. Mucosal immune responses. Best Pract Res Clin Gastroenterol. 2004; 18:387-404.

2. Alfaro C, Suarez N, Oñate C, Perez-Gracia JL, Martinez-Forero I, Hervas-Stubbs S, Rodriguez I, Perez G, Bolaños E, Palazon A, Sanmamed MF, Morales-Kastresana

A, Gonzalez A, Melero I. Dendritic cells take up and present antigens from viable and apoptotic polymorphonuclear leukocytes. PLoS One. 2011; 6:e29300.

3. Alvarez B, Revilla C, Doménech N, Pérez C, Martínez P, Alonso F, Ezquerra A, Domíguez J. Expression of toll-like receptor 2 (TLR2) in porcine leukocyte subsets and tissues. Vet Res. 2008; 39:13.

4. Beauvillain C, Delneste Y, Scotet M, Peres A, Gascan H, Guermonprez P, Barnaba V, Jeannin P. Neutrophils efficiently cross-prime naive T cells *in vivo.* Blood. 2007; 110:2965-73.

5. Boyen F, Haesebrouck F, Maes D, Van Immerseel F, Ducatelle R, Pasmans F. Non-typhoidal *Salmonella* infections in pigs: a closer look at epidemiology, pathogenesis and control. Vet Microbiol. 2008; 130:1-19.

6. Breitling R, Armengaud P, Amtmann A, Herzyk P. Rank products: a simple, yet powerful, new method to detect differentially regulated genes in replicated microarray experiments. FEBS Lett. 2004; 573:83-92.

7. Broz P, Ohlson MB, Monack DM. Innate immune response to *Salmonella* typhimurium, a model enteric pathogen. Gut Microbes. 2012; 3:62-70.

8. Bullido R, Gomez del Moral M, Alonso F, Ezquerra A, Zapata A, Sánchez C, Ortuño E, Alvarez B, Domínguez J: Monoclonal antibodies specific for porcine monocytes/macrophages: macrophage heterogeneity in the pig evidenced by the expression of surface antigens.Tissue Antigens 1997, 49:403-413.

9. Centers for Disease Control and Prevention (CDC). Vital signs: incidence and trends of infection with pathogens transmitted commonly through food--foodborne diseases active surveillance network, 10 U.S. sites, 1996-2010. MMWR Morb Mortal Wkly Rep. 2011; 60:749-55.

10. Cerutti A, Puga I, Cols M. New helping friends for B cells. Eur J Immunol. 2012; 42:1956-68.

Conesa A, Götz S, García-Gómez JM, Terol J, Talón M, Robles M: Blast2GO: a universal tool for annotation, visualization and analysis in functional genomics research. Bioinformatics 2005, 21:3674-3676.

11. Coquerelle C, Moser M. DC subsets in positive and negative regulation of immunity. Immunol Rev. 2010 Mar;234(1):317-34.

12. European Food Safety Authority (EFSA). The European Union summary report on trends and sources of zoonoses, zoonotic agents and food-borne outbreaks in 2011. Euro Surveill. 2013; 18:20449.

13. El Shikh ME, Pitzalis C. Follicular dendritic cells in health and disease. Front Immunol. 2012;3:292.

14. Groom JR, Luster AD. CXCR3 in T cell function. Exp Cell Res. 2011 Mar 10;317(5):620-31.

15. Houde M, Bertholet S, Gagnon E, Brunet S, Goyette G, Laplante A, Princiotta MF, Thibault P, Sacks D, Desjardins M: Phagosomes are competent organelles for antigen cross-presentation. Nature 2003, 425:402-406.

16. Irizarry RA, Hobbs B, Collin F, Beazer-Barclay YD, Antonellis KJ, Scherf U, Speed TP: Exploration, normalization, and summaries of high density oligonucleotide array probe level data. Biostatistics 2003, 4:249-264.

17. Livak KJ, Schmittgen TD: Analysis of relative gene expression data using real-time quantitative PCR and the 2−ΔΔCT method. Methods 2001, 25:402-408.

18. Ma CS, Deenick EK, Batten M, Tangye SG. The origins, function, and regulation of T follicular helper cells. J Exp Med. 2012; 209:1241-53.

20. Majowicz SE, Musto J, Scallan E, Angulo FJ, Kirk M, O'Brien SJ, Jones TF, Fazil A, Hoekstra RM; International Collaboration on Enteric Disease 'Burden of Illness' Studies. The global burden of nontyphoidal *Salmonella* gastroenteritis. Clin Infect Dis. 2010; 50:882-9.

21. Makala LH, Suzuki N, Nagasawa H. Peyer's patches: organized lymphoid structures for the induction of mucosal immune responses in the intestine. Pathobiology. 2002-2003; 70:55-68.

22. Martins RP, Collado-Romero M, Martínez-Gomáriz M, Carvajal A, Gil C, Lucena C, Moreno A, Garrido JJ: Proteomic analysis of porcine mesenteric lymph-nodes alter *Salmonella typhimurium* infection. J Proteomics 2012, 75: 4457-4470.

23. Martins RP, Collado-Romero M, Arce C, Lucena C, Carvajal A, Garrido JJ: Exploring the immune response of porcine mesenteric lymph nodes to *Salmonella enterica* serovar Typhimurium: an analysis of transcriptional changes, morphological alterations and pathogen burden. Comp Immunol Microbiol Infect Dis 2013a,36: 149-160.

24. Martins RP, Lorenzi V, Arce C, Lucena C, Carvajal A, Garrido JJ. Innate and adaptive immune mechanisms are effectively induced in ileal Peyer's patches of *Salmonella typhimurium* infected pigs. Dev Comp Immunol. 2013b; 41:100-4.

25. Megiovanni AM, Sanchez F, Robledo-Sarmiento M, Morel C, Gluckman JC, Boudaly S.

Mengiovanni et al. (2006) Polymorphonuclear neutrophils deliver activation signals and antigenic molecules to dendritic cells: a new link between leukocytes upstream of T lymphocytes. J Leukoc Biol. 2006; 79:977-88.

26. Meurens F, Summerfield A, Nauwynck H, Saif L, Gerdts V. The pig: a model for human infectious diseases. Trends Microbiol. 2012; 20:50-7.

27. Morel C, Badell E, Abadie V, Robledo M, Setterblad N, Gluckman JC, Gicquel B, Boudaly S, Winter N. *Mycobacterium bovis* BCG-infected neutrophils and dendritic cells cooperate to induce specific T cell responses in humans and mice. Eur J Immunol. 2008 ; 38:437-47.

28. Pescovitz MD, Book BK, Aasted B, Dominguez J, Bullido R, Trebichavsky I, Novikov B, Valpotic I, Tomaskovic M, Nielsen J, Arn S, Sachs DH, Lunney JK, Boyd PC, Walker J, Lee R, Saalmüller A. Analyses of monoclonal antibodies reacting

with porcine CD5: results from the Second International Swine CD Workshop. Vet Immunol Immunopathol. 1998; 60:269-73.

29. Robertson D, Savage K, Reis-Filho JS, Isacke CM: Multiple immunofluorescence labelling of formalin-fixed paraffin-embedded (FFPE) tissue. BMC Cell Biol 2008, 9:13-22.

30. Salerno-Goncalves R, Sztein MB. Priming of *Salmonella enterica* serovar typhi-specific CD8(+) T cells by suicide dendritic cell cross-presentation in humans. PLoS One. 2009;4(6):e5879.

31. Sánchez-Vargas FM, Abu-El-Haija MA, Gómez-Duarte OG. *Salmonella* infections: an update on epidemiology, management, and prevention. Travel Med Infect Dis. 2011; 9:263-77.

32. Schroder K, Hertzog PJ, Ravasi T, Hume DA. Interferon-gamma: an overview of signals, mechanisms and functions. J Leukoc Biol. 2004; 75:163-89.

33. Soldevila G, Raman C, Lozano F. The immunomodulatory properties of the CD5 lymphocyte receptor in health and disease. Curr Opin Immunol. 2011; 23:310-8.

34. Tam MA, Rydström A, Sundquist M, Wick MJ. Early cellular responses to *Salmonella* infection: dendritic cells, monocytes, and more. Immunol Rev. 2008; 225:140-62.

35. Tsolis RM, Xavier MN, Santos RL, Bäumler AJ. How to become a top model: impact of animal experimentation on human *Salmonella* disease research. Infect Immun. 2011; 79:1806-14.

36. Tussiwand R, Lee WL, Murphy TL, Mashayekhi M, Wumesh KC, Albring JC, Satpathy AT, Rotondo JA, Edelson BT, Kretzer NM, Wu X, Weiss LA, Glasmacher E, Li P, Liao W, Behnke M, Lam SS, Aurthur CT, Leonard WJ, Singh H, Stallings CL, Sibley LD, Schreiber RD, Murphy KM. Compensatory dendritic cell development mediated by BATF-IRF interactions. Nature. 2012; 490:502-7.

37. de Wit J, Souwer Y, Jorritsma T, Klaasse Bos H, ten Brinke A, Neefjes J, van Ham SM. Antigen-specific B cells reactivate an effective cytotoxic T cell response against phagocytosed *Salmonella* through cross-presentation.

38. Yao Y, Qian Y. Expression regulation and function of NLRC5. Protein Cell. 2013; 4:168-75.

39. Yubero N, Jiménez-Marín A, Barbancho M, Garrido JJ: Two cDNAs coding for the porcine CD51 αV integrin subunit: cloning, expression analysis, adhesion assays and chromosomal localization. Gene 2011, 481:29-40.

40. Zotos D, Tarlinton DM. Determining germinal centre B cell fate. Trends Immunol. 2012; 33:281-8.

4. Conclusions

Conclusions

The conclusions of this thesis are:

1. Swine salmonellosis could be successfully reproduced under experimental conditions (Martins et al. Comp Immunol Microbiol Infect Dis. 2013. 36:149-160).

2. *Salmonella* burden in swine MLN fluctuated along the studied time course and picked at 2 dpi, when the most prominent transcriptomic and proteomic responses were observed (Martins et al. Comp Immunol Microbiol Infect Dis. 2013. 36:149-160; Martins et al. J Proteomics. 2012. 75:4457-4470);

3. *S.* Typhimurium triggered the induction of innate immunity mechanisms in porcine MLN, marked by a substantial infiltration of phagocytes and up-regulation of pro-inflammatory genes in tissue (Martins et al. Comp Immunol Microbiol Infect Dis. 2013. 36:149-160).

4. Swine innate immune response reduced substantially *S.* Typhimurium burden in MLN. However, pathogen was able to maintain itself in tissue despite host defence mechanisms (Martins et al. Comp Immunol Microbiol Infect Dis. 2013. 36:149-160).

5. Proteome analysis revealed that *S.* Typhimurium mediated GTPases activity in infected MLN to give rise to cytoskeleton rearrangements necessary for phagosome formation and pathogen replication (Martins et al. J Proteomics. 2012. 75:4457-4470)

6. The *S.* Typhimurium strain used in this work expressed both invasion and intracellular survival inducers in MLN during pig infections. Besides, genes coding for two different flagellar filament proteins were found to be expressed in MLN, suggesting that pathogen could employ flagellar phase variation to hinder pig immune response (Martins et al. Vet Res. Under review);

7. Swine might take advantage of flagellin and prgJ expression by *S.* Typhimurium to induce pyroptosis of infected cells in MLN and consequently promote clearance of pathogen by innate mechanisms in the extracellular milieu. This process, concurrent with the inhibition of apoptosis might consist in a host protective response that prevents pathogen spread beyond gut-associated lymph-nodes (Martins et al. Vet Res. Under review; Martins et al. J Proteomics. 2012. 75:4457-4470);

8. Transcriptomic and proteomic analysis conjunctively indicated that *S.* Typhimurium antigens are cross-presented via MHCI in a proteasome-dependent manner in MLN of infected pigs, which might enable host to trigger an early CD8 T cell mediated response to control infection (Martins et al. Vet Res. Under review; Martins et al. J Proteomics. 2012. 75:4457-4470);

9. Combination of an *in vivo* infection model with laser microdissection and gene expression analysis proved to be a promising strategy to clarify the role of specific cell populations during infectious processes (Martins et al. Dev Com Immunol. 2013. 41:100-104);

10. *S.* Typhimurium induced a remarkable infiltration of phagocytes, mainly neutrophils, in PP follicles of infected pigs. Additionally, these structures were found to assemble distinct immunity mediators upon infection, enabling host to

mount multiple levels of the adaptive response against pathogen (Martins et al. Dev Com Immunol. 2013. 41:100-104; Martins et al. J Infect Dis. Manuscript in preparation);

11. Swine PP follicles engendered the development of antibody responses and long-lived humoral immunity at a short time (2 days) after infection with non-typhoid *Salmonella* (Martins et al. J Infect Dis. Manuscript in preparation);
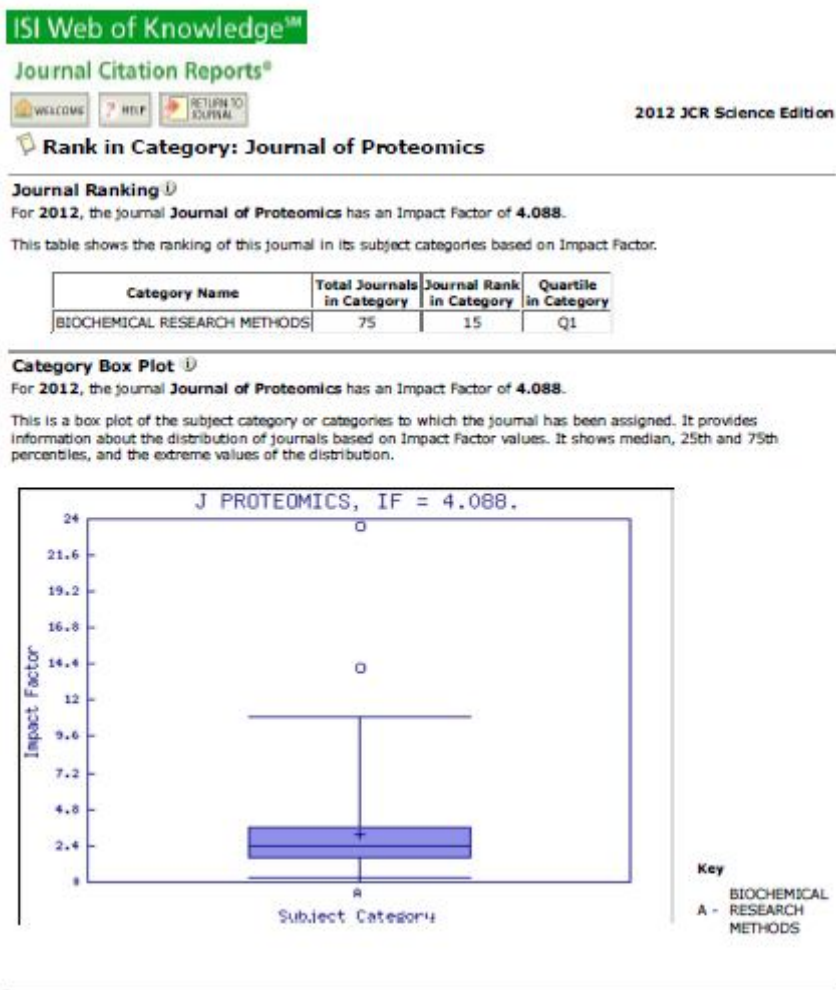
12. Besides eliciting B-cell-mediated immune responses, PP follicles mediate the generation of effector and memory CD8 T cells during infections by *S.* Typhimurium. Thus, this particularity should be considered for the development of therapies and vaccine approaches against salmonellosis (Martins et al. J Infect Dis. Manuscript in preparation);

13. Pyroptosis and cross-presentation appeared to be the core processes in the establishment of immune-response to *S.* Typhimurium in swine lymphoid organs. For this reason, this work highlight NLRC4 and NLRC5, the main mediators of each of these processes, as attractive targets for genetic variation screenings, focused on the genetic improvement of resistance to salmonellosis in porcine (Martins et al. J Proteomics. 2012. 75:4457-4470; Martins et al. Vet Res. Under review; Martins et al. J Infect Dis. Manuscript in preparation).

5. Appendix

5.1 Journal information

5.1.1 Journal of Proteomics

ISI Web of Knowledge℠

Journal Citation Reports®

[WELCOME] [? HELP] [RETURN TO JOURNAL]   **2012 JCR Science Edition**

📖 **Rank in Category: Journal of Proteomics**

Journal Ranking ⓘ

For **2012**, the journal **Journal of Proteomics** has an Impact Factor of **4.088**.

This table shows the ranking of this journal in its subject categories based on Impact Factor.

Category Name	Total Journals in Category	Journal Rank in Category	Quartile in Category
BIOCHEMICAL RESEARCH METHODS	75	15	Q1

Category Box Plot ⓘ

For **2012**, the journal **Journal of Proteomics** has an Impact Factor of **4.088**.

This is a box plot of the subject category or categories to which the journal has been assigned. It provides information about the distribution of journals based on Impact Factor values. It shows median, 25th and 75th percentiles, and the extreme values of the distribution.

5.1.2 Comparative Immunology, Microbiology and Infectious Diseases

ISI Web of Knowledge℠

Journal Citation Reports®

WELCOME | ? HELP | RETURN TO JOURNAL

2012 JCR Science Edition

Rank in Category: COMPARATIVE IMMUNOLOGY MICROBIOLOGY AND INFECTIOUS...

Journal Ranking ⓘ

For **2012**, the journal **COMPARATIVE IMMUNOLOGY MICROBIOLOGY AND INFECTIOUS...** has an Impact Factor of **1.808**.
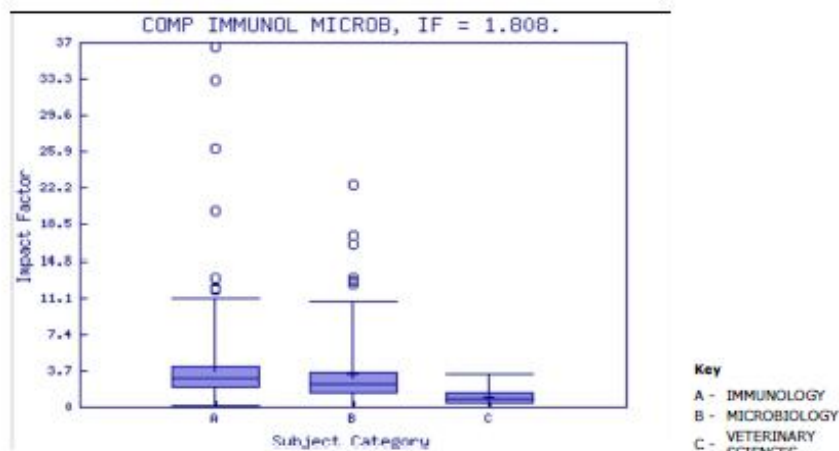
This table shows the ranking of this journal in its subject categories based on Impact Factor.

Category Name	Total Journals in Category	Journal Rank in Category	Quartile in Category
IMMUNOLOGY	135	110	Q4
MICROBIOLOGY	116	79	Q3
VETERINARY SCIENCES	142	20	Q1

Category Box Plot ⓘ

For **2012**, the journal **COMPARATIVE IMMUNOLOGY MICROBIOLOGY AND INFECTIOUS...** has an Impact Factor of **1.808**.

This is a box plot of the subject category or categories to which the journal has been assigned. It provides information about the distribution of journals based on Impact Factor values. It shows median, 25th and 75th percentiles, and the extreme values of the distribution.

COMP IMMUNOL MICROB, IF = 1.808.

Key
A - IMMUNOLOGY
B - MICROBIOLOGY
C - VETERINARY SCIENCES

5.1.3 Developmental and Comparative Immunology

ISI Web of Knowledge™

Journal Citation Reports®

WELCOME ? HELP RETURN TO JOURNAL

2012 JCR Science Edition

Rank in Category: DEVELOPMENTAL AND COMPARATIVE IMMUNOLOGY

Journal Ranking ⓘ

For **2012**, the journal **DEVELOPMENTAL AND COMPARATIVE IMMUNOLOGY** has an Impact Factor of **3.238**.
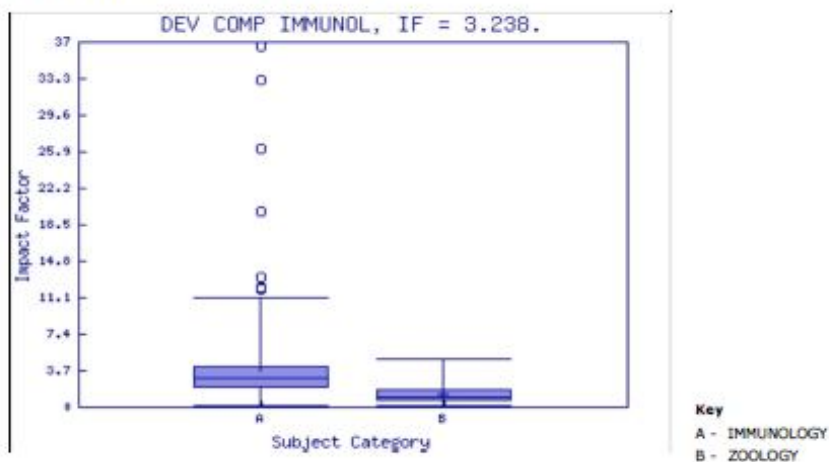
This table shows the ranking of this journal in its subject categories based on Impact Factor.

Category Name	Total Journals in Category	Journal Rank in Category	Quartile in Category
IMMUNOLOGY	135	59	Q2
ZOOLOGY	149	5	Q1

Category Box Plot ⓘ

For **2012**, the journal **DEVELOPMENTAL AND COMPARATIVE IMMUNOLOGY** has an Impact Factor of **3.238**.

This is a box plot of the subject category or categories to which the journal has been assigned. It provides information about the distribution of journals based on Impact Factor values. It shows median, 25th and 75th percentiles, and the extreme values of the distribution.

Key
A - IMMUNOLOGY
B - ZOOLOGY